# UC San Diego
## Research Theses and Dissertations

**Title**
Anticancer Compounds from Marine Invertebrates

**Permalink**
https://escholarship.org/uc/item/1xk3x815

**Author**
Sandler, Joel S.

**Publication Date**
2005

Peer reviewed

UNIVERSITY OF CALIFORNIA, SAN DIEGO

SCRIPPS INSTITUTION OF OCEANOGRAPHY


Anticancer Compounds from Marine Invertebrates


A dissertation submitted in partial satisfaction of the

requirements for the degree Doctor of Philosophy in

in Oceanography


by

Joel Stuart Sandler


Committee in charge

Professor William H. Fenical, Chair
Professor Lihini L. Aluwihare
Professor Douglas H. Bartlett
Professor Katherine A. Barbeau
Professor Emmanuel Theodorakis


2005

UMI Number: 3247792

INFORMATION TO USERS

The quality of this reproduction is dependent upon the quality of the copy submitted. Broken or indistinct print, colored or poor quality illustrations and photographs, print bleed-through, substandard margins, and improper alignment can adversely affect reproduction.

In the unlikely event that the author did not send a complete manuscript and there are missing pages, these will be noted. Also, if unauthorized copyright material had to be removed, a note will indicate the deletion.

# UMI®
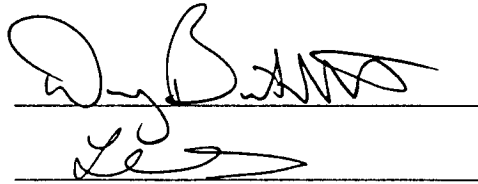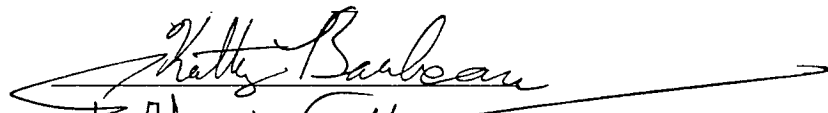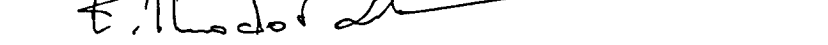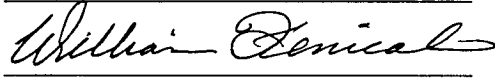
The dissertation of Joel Stuart

Sandler is approved, and it is

acceptable in quality and form for

publication on microfilm:

Chair

University of California, San Diego

2005

iii

To Mom and Dad,
for giving me the imagination to dream the impossible
and the means of attaining it.

# TABLE OF CONTENTS

# LIST OF ABBREVIATIONS

| | |
|---|---|
| $[\alpha]_D$ | optical rotation |
| $\delta/\delta_H/\delta_C$ | NMR chemical shift/ proton shift/ carbon shift |
| $\Delta$ | double bond or genetic deletion |
| $\Delta\delta_{S-R}$ | delta-delta value (Mosher's method) |
| $\varepsilon$ | epsilon value (indicates intensity of ultraviolet absorption) |
| $\lambda_{max}$ | ultraviolet wavelength maximum |
| $v_{max}$ | infrared wavelength maximum |
| $[\theta]$ | circular dichroism rotation |
| $^1H$ | proton |
| $^{13}C$ | carbon-13 |
| CD | circular dicrhroism |
| $CDCl_3$ | deuterated chloroform |
| COSY | correlation spectroscopy |
| DMSO-$d_6$ | deuterated dimethyl sulfoxide |
| DSB | double strand break |
| EIMS | electron ionization mass spectrometry |
| ESI | electrospray ionization mass spectrometry |
| EtOAc | ethyl acetate |
| FABMS | fast atom bombardment mass spectrometry |
| FACS | fluorescence activated cell sorting |

| | |
|---|---|
| FDA | Food and Drug Administration |
| HCl | hydrochloric acid |
| HCT-116 | human colon tumor cell line 116 |
| HMBC/gHMBC | heteronuclear multiple-bond correlation/ gradient HMBC |
| HPLC | high performance liquid chromatography |
| $IC_{50}$ | concentration at which 50% survival is observed |
| MALDI | matrix assisted laser desporption mass spectrometry |
| HR | high-resolution |
| HSQC/gHSQC | heteronuclear single-quantum correlation/ gradient HSQC |
| HSQMBC | heteronuclear single quantum multiple bond correlation |
| IR | infrared |
| $J$ | coupling constant |
| $[M+H]^+$ | protonated molecular ion |
| $m/z$ | mass to charge ratio |
| MeOH-$d_4$ | deuterated methanol |
| MTPA/MTPACl | methoxy trifluoromethyl phenyl acetate/ MTPA acid chloride |
| NCI | National Cancer Institute |
| NMR | nuclear magnetic resonance |
| NOE/NOESY | nuclear Overhauser effect/ NOE spectroscopy |
| $OD_{600}$ | optical density at 600 nm wavelength |
| ROESY | rotational NOE spectroscopy |

| | |
|---|---|
| TOCSY | total correlation spectroscopy |
| TOP1/topo I | topoisomerase 1 |
| TOP2/topo II | topoisomerase 2 |
| UV | ultraviolet |

# LIST OF TABLES AND FIGURES

ix

CHAPTER 3

CHAPTER 4

# ACKNOWLEDGEMENTS

I am extremely grateful to everyone who has touched my life in the past five years as a graduate student. My tenure here has been very interesting, and I have learned more in this small amount of time than I had in the previous twenty years, both about myself and the natural world around me.

I must first thank the late John Faulkner, who served as my mentor and friend for three years before his untimely passing. It's difficult to summarize the impact that John had and continues to have on me. I believe that he truly took a chance on me, and I would like to think that I have validated his decision. John was always patient with my capricious curiosities, to which he enjoyed responding "Let's see how you feel about this project next week, shall we?" He was a scientist in the truest sense of the word, and I miss him dearly.

In addition to John, I have been fortunate to have two wonderful co-advisors who have influenced my approach to science and life. Susan Forsburg is a brilliant cell biologist who took a genuine interest in my dream to find novel and selective inhibitors of cell-cycle processes in yeast. It was always difficult to keep up with her, and I feel that I have become a better scientist by learning how to do so. Susan selflessly donated her time and resources to my cause, and she adopted me into her lab for nothing in return. Members of the Forsburg lab taught me how to approach a biological system with patience and exactitude.

I need to thank Bill Fenical, my second co-advisor, for many things. When John passed away, Bill made sure that everyone in the Faulkner lab had a home to continue their research without any hindrances or distractions. Without Bill's support, I would not be writing this today. Aside from this, Bill has served as a mentor during the second half of my graduate career. He has forced me to ask myself difficult questions about where I want to go and how I can get there. Bill taught me how to how to continue driving straight when I hit a bump in the road and finish what I've started.

My committee members have been very generous with their time and insight. Lihini Aluwihare is an enthusiastic and sympathetic scientist, and she is a good friend. She provided help with GC studies that were not mentioned in this thesis. Doug Bartlett has a genuine interest in all different kinds of scientific problems. His questions are remarkably pertinent and I have always enjoyed our meetings. I would like to thank the late Murray Goodman for sitting on my committee. He was an accomplished and demanding chemist who will be greatly missed. I am grateful to Emmanuel Theodorakis for agreeing to sit on my committee and for providing feedback on some of my stereochemistry problems. His student, Fatima Rivas, provided help with ozonolysis studies that were not mentioned in this thesis. I also thank Kathy Barbeau for serving on my committee.

Catherine Sincich was instrumental in keeping the Faulkner lab together after John left us. She was tireless in her devotion to keeping everything running

xiii

flawlessly and I thank her for that. Above all, I thank her for saving my life (literally) in Palau. James Laclair has been an interesting collaborator and I have always enjoyed our discussions. We worked together on several fluorescence studies that are not mentioned in this thesis. Jim has shown me how to question everything, including conventional science and convention in general. Evelyn York has done a great job keeping the NMR instruments running, and she was always fun to talk with. Pat and Lori Colin at the Coral Reef Research Foundation have been very generous with accommodations and other resources in Palau.

Students and postdocs at SIO have been instrumental in teaching me how to be a scientist. Marcus Huebes and Lyndon West are two postdocs who first taught me how to purify and characterize marine natural products. Christine Blackburn is an excellent scientist who helped inspire me in my first year at SIO. It is because of Chris that I am currently interested in chemical biology. Christine Salomon is an extremely enthusiastic person who taught me to have fun with my research. Christian Ridley is a great chemist, and I am indebted to him for many of my good decisions as a scientist. I thank Wendy Strangman for her friendship and delectable desserts. In my latter years at SIO, postdocs Philip Williams, Chambers Hughs, John Macmillan, and Han Kwon have been very helpful in forcing me to challenge myself as a chemist. They are all amazing chemists that I have been fortunate to work with. I thank the rest of the Faulkner lab and Fenical

lab for working with me and providing great feedback at seminars and chalk-talks.

I would never have been able to complete this thesis without the love and support of my family. My dad taught me how to work hard and stay focused. His life is a model that I aspire towards, both in work and play. My mom taught me how to overcome adversity with a smile, and she raised me to be a mensch. My brother Ian always told me that whatever I choose to do, make sure I do it well. My brand new niece Riley has given me the impetus to finish this thing and go back to New York. Finally, I thank Michelle, my true love and friend forever. Michelle always knows how to make me laugh and take life less seriously. And her countless late night hours spent in the lab with me entitles her to a piece of this degree.

<p style="text-align:center">*    *    *</p>

Chapter 2 acknowledgements: Collection of the sponge material was made by Patrick Colin of the Coral Reef Research Foundation. The sponge was identified by John Hooper. Ralf Goericke allowed me to work on his Finnigan LCQ mass spectrometer. We thank the Republic of Palau for providing collection permits and the Coral Reef Research Foundation for logistical support.

<p style="text-align:center">*    *    *</p>

Chapter 3 acknowledgements: This work is the result of a collaboration with Susan Forsburg, who is a co-author. Collection of the sponge material was made by Grace Lim, Melissa Lerch, Christine Blackburn, and Christine Salomon.

Lou Barrows and Kathryn Marshall at the University of Utah performed the DNA

cleavage assays.

<center>*    *    *</center>

# VITA

| | |
|---|---|
| July 1, 1977 | Born, Dix Hills, NY |
| June, 1999 | B.A., Cornell University, Ithaca, NY |
| 2000-2005 | Graduate student researcher, University of California, San Diego |
| 2005 | Ph.D., University of California, San Diego |

# PUBLICATIONS

Sandler, J.S.; Colin, P.L.; Hooper, J.N.; Faulkner, D.J. (2002) Cytotoxic beta-carbolines and cyclic peroxides from the Palauan sponge Plakortis nigra. *J. Nat. Prod.* **65**(9), 1258-61.

Sandler, J. S., Forsburg, S. L., Faulkner, D. J. (2005) Bioactive steroidal glycosides from the marine sponge Erylus lendenfeldi. *Tetrahedron* **61**, 1199-1206.

Sandler, J. S., Fenical, W., Gulledge, B. M., Chamberlin, A. R., La Clair, J. J. (2005) Fluorescent profiling of natural product producers. *J. Am. Chem. Soc.* 127(26), 9320-9321.

# FIELDS OF STUDY

Major Field: Marine Chemistry

Studies in Marine Natural Products Chemistry
Professors D. John Faulkner and William H. Fenical
Scripps Institution of Oceanography

Studies in Cell Biology and Genetics
Professor Susan L. Forsburg, Salk Institute for Biological Studies

# ABSTRACT OF THE DISSERTATION

Anticancer Compounds from Marine Invertebrates

by

Joel Stuart Sandler

Doctor of Philosophy in Oceanography

University of California, San Diego, 2005

Professor William H. Fenical, Chair

For more than thirty years, marine natural products chemists have studied sponges, ascidians, and other marine invertebrates because of their ability to produce secondary metabolites with unique chemical structures and potent bioactivities. The remarkable abundance and diversity of bioactive small molecules that have been isolated from marine invertebrates have made these organisms an important source of new drug candidates for human diseases, particularly in the fight against cancer. As a result, there are now a number of marine natural products in clinical or preclinical trials for the treatment of different kinds of cancer.

The objective of this thesis is to describe the isolation and characterization of novel anticancer compounds from marine invertebrates. Each chapter discusses dramatically different types of molecules that have been identified in marine sponges, linked only by the fact that they all demonstrate activity on a cancer or cancer-related assay. The first chapter provides an overview of the various anticancer compounds that have been isolated from marine invertebrates, with particular emphasis on the specific bioactivities demonstrated by each compound. Chapter 2 provides a report of several interesting series of molecules isolated from a single Palauan sponge. The techniques used towards the isolation and structural elucidation of organic compounds, including HPLC, NMR, and mass spectrometry, are presented here before being elaborated upon in subsequent chapters. In chapter 3, a series of compounds are isolated from a Red Sea sponge based on their activity in an assay designed to identify novel cell-cycle inhibitors. In addition to a report of the isolation and structural elucidation of these compounds, this chapter also describes several studies aimed at further characterizing their bioactivity. Chapter 4 presents two completely novel compounds isolated from a new deep-water sponge. Several interesting techniques were employed to develop a model of the relative stereochemistry of neighboring chiral centers within each molecule. Ultimately, a story is told of the challenges and solutions involved in purifying and characterizing marine invertebrate natural products.

# CHAPTER 1

## INTRODUCTION: ANTICANCER COMPOUNDS

## FROM MARINE INVERTEBRATES

The oceans cover roughly three-quarters of Earth's surface, and some marine ecosystems, such as coral reefs and deep-sea hydrothermal vents, exhibit biological diversity that rivals that found in any of the other ecosystems in the known universe. Marine invertebrates comprise an important part of many of these ecosystems. These organisms are soft-bodied and, in some cases, sessile, making them physically vulnerable to predation, microbial fouling, and competition for resources. As a result, they have evolved the ability to synthesize toxic compounds as a means of defense. Upon being released into the water, these natural products are rapidly diluted and therefore need to be highly potent to be effective.

A large number of bioactive marine natural products have been discovered in the quest for new drugs to treat human diseases. Marine invertebrates have provided a large proportion of bioactive natural products reported in the past 30 years,[1] and an ever-expanding access to new marine habitats ensures that this resource has not yet been exhausted. In particular, many bioactive natural products have been isolated in the search for new drugs to treat various types of

1

cancer. This chapter reviews the role of marine invertebrate natural products with respect to the discovery and development of different forms of cancer treatment.

## A Brief History of Cancer Treatment

Cancer and its various remedies have been described since the earliest medical records were kept.[2-4] Ancient Egyptian papyri contain descriptions of surgery and pharmacological treatments of cancer dating from sources as early as 2500 B.C. During the Renaissance, cancer was considered incurable, although a wide variety of pastes containing arsenic were compounded to treat its manifestations. Surgical techniques progressed in the 17th century thanks to the work of renowned practitioners such as Fabricius Hildanus, Johann Scultetus, and Marco Severinus. It wasn't until the the 19th century, however, with the invention and use of the modern microscope, that scientific oncology truly began. Rudolf Virchow, often called the founder of cellular pathology, provided the scientific basis for the modern study of cancer.[5] It was Virchow who first correlated microscopic observations of cancer cells with the clinical course of illness. At the same time, surgeons such as William Stewart Halsted and W. Sampson Handley were pioneering radical mastectomy procedures.[6] Stephen Paget, an English surgeon, suggested that cancer cells spread by way of the bloodstream to all organs, thereby delineating the concept of metastasis almost 100 years before the hypothesis could be confirmed by modern cellular and molecular biology.[7]

In 1901, German physics professor Wilhelm Conrad Roentgen generated global excitement with his characterization of the X-ray.[8] Within 3 years of its discovery, radiation was used in the treatment of cancer. A major breakthrough took place in France when it was discovered that daily doses of radiation over several weeks would greatly improve therapeutic response. The methods and the machines for delivery of radiation therapy steadily improved, and it can now be delivered with great precision in order to destroy malignant tumors while minimizing damage to adjacent normal tissue.

While physical methods, such as surgery and radiation, are invaluable measures for slowing or reversing the effects of cancer, chemical intervention provides a potentially less invasive and more effective solution. During World War II, the U.S Army was studying a number of compounds related to mustard gas in order to develop more effective chemical warfare agents. In the course of that work, nitrogen mustard (**1**) was found to have substantial activity in lymphoma patients. This compound served as the model for a series of more effective analogs that killed rapidly proliferating cancer cells. Soon afterwards, Sidney Farber demonstrated that aminopterin (**2**), an analog of folic acid, produced remission in child leukemia patients. Aminopterin, which blocked a critical chemical reaction needed for DNA replication, was the predecessor of methotrexate (**3**), a cancer drug commonly used today. The first cure of metastatic cancer was reported in 1956 when methotrexate was used to treat a rare

**1**



**2**



**3**
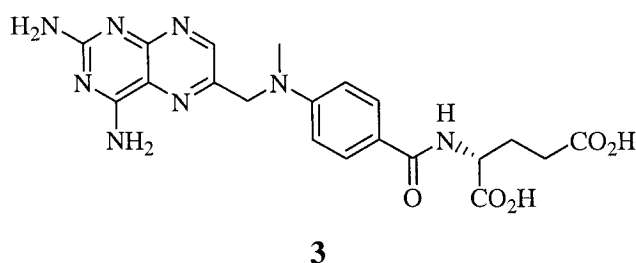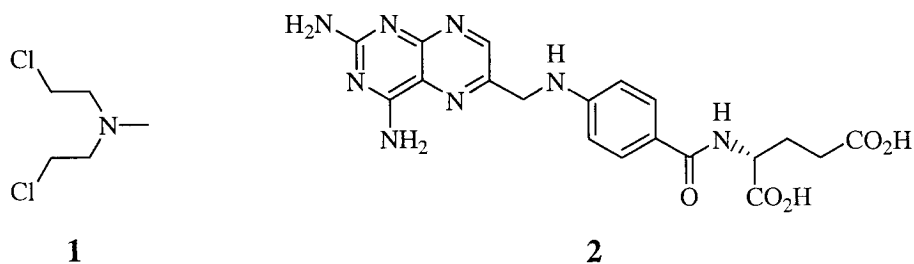
tumor called choriocarcinoma, thereby demonstrating the importance of chemotherapy in cancer treatment.

Since the discovery and implementation of these early drugs, researchers have uncovered numerous compounds that are used for cancer chemotherapy. While many of these compounds effectively inhibited cancer cell growth, they often displayed non-selective cytotoxicity in patients due to the molecular similarities between cancerous and healthy human cells. The discovery of selective anticancer drugs is now becoming more prevalent due to the advent of

molecular genetics combined with improved assay technology and remarkable

advances in organic chemistry.[9]

## Modern Drug Discovery

In 1953, James Watson and Francis Crick reported the chemical structure

of DNA, the building block of genetic material found in all living organisms.[10]

Researchers soon discovered that genes contained the information required for

cellular structure and function and that this information was passed down with

each cell division. Furthermore, genetic abnormalities did not always result in

cell death and could persist from one generation to the next, often in association

with cancer. Traditional genetic approaches combined with new genomics

technologies have subsequently revealed an abundance of "oncogenes" whose

aberrant function is implicated in different types of cancer.[11,12]

Most of the current strategies for finding new anticancer drugs rely on the

discovery of compounds that target the subtle molecular differences between

malignant and healthy human cells. Certain genetic defects render cancer cells

sensitive to particular compounds, and many pathways represent potential

chemotherapeutic targets to be exploited by drugs.[13] Countless assays are

currently employed to find compounds that inhibit almost all of the known

cancer-related proteins or pathways. When such assays are automated, it becomes

possible to screen huge libraries of compounds in a routine manner, thereby

increasing the likelihood of identifying specific inhibitors.

Large chemical libraries are typically generated from either combinatorial chemistry methods or natural product extracts. Combinatorial chemistry is a technology in which different chemical precursors are repeatedly pooled together and exposed to common synthetic conditions, thereby creating large numbers of diverse molecules *en mass.*[14] Rapid screening of the resulting libraries has the benefit of providing a large amount of data in a relatively short period of time. This method has several shortcomings, however, including the inability of existing chemical libraries to occupy diverse regions of biochemical space and the presence of nuisance compounds that generate false positives or non-specific hits in pure-protein assays.[15]

An alternative approach to generating large chemical libraries involves the collection and extraction of organisms that are known to produce bioactive secondary metabolites. Terrestrial plants, microbes, and invertebrates have provided man with countless natural remedies for thousands of years.[16] These organisms contain bioactive secondary metabolites that have enabled them to communicate, compete for resources, and defend against predators. Although secondary metabolites do not always exhibit biomedical activity, similarities between the biological targets (i.e. proteins, organelles, DNA) against which these compounds have evolved and the biomedical targets involved in human pathogenesis explain how certain natural products can be used to combat diseases.

Medicinal chemists have been interested in secondary metabolites for hundreds of years. Until recently, however, the purification and characterization

of complex natural products had been an arduous task. Dramatic improvements in analytical technologies, such as high-pressure liquid chromatography (HPLC), nuclear magnetic resonance (NMR), and mass spectroscopy, have greatly facilitated this process. The discovery and characterization of natural anticancer drugs such as vinblastine (4) and vincristine (5),[17] etoposide (6),[18] and Taxol (7)[19] from plants, and the bleomycins (8, bleomycin A),[20] mitomycin C (9),[21] doxorubicin (10),[22] and the epothilones (11, epothilone A)[23] from microbes, have illustrated the importance of bioactive secondary metabolites in the clinic.[24] In addition to terrestrial plants and microbes, marine organisms have recently become a fruitful resource for new anticancer compounds.

**Anticancer Compounds from Marine Invertebrates**

Until the mid-1960s, investigations of natural products from marine organisms was essentially non-existent. The modernization of scuba technology in the seventies and eighties resulted in accessibility to previously unexplored marine ecosystems. Since then, close to 20,000 new compounds have been reported from marine microbes, seaweeds, and invertebrates.[1, 25] Marine invertebrates have proven to be a particularly rich source of novel anticancer compounds. Despite the fact that no marine-derived compounds have been licensed for clinical use as anticancer drugs, at least ten compounds are in various stages of formal testing and many more are undergoing preclinical evaluation.[26]
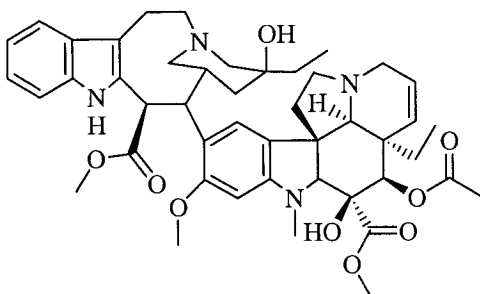
**4**
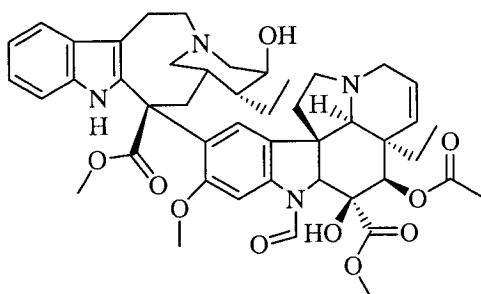


**5**
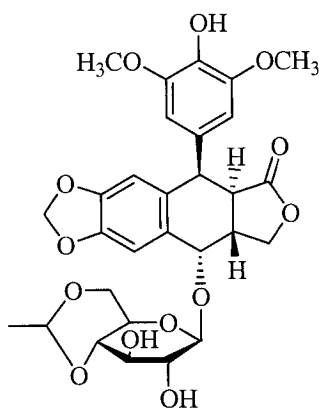


**6**
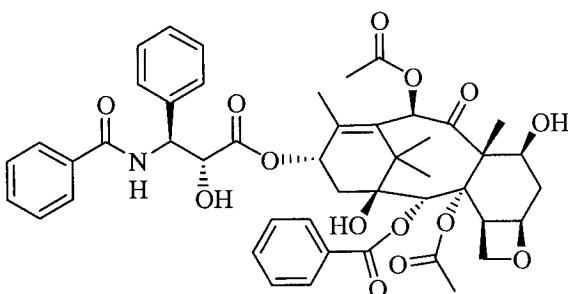


**7**
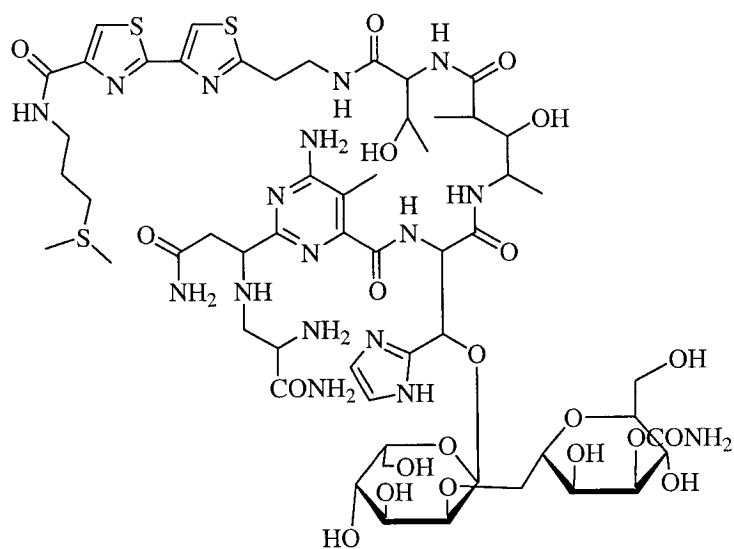
**8**
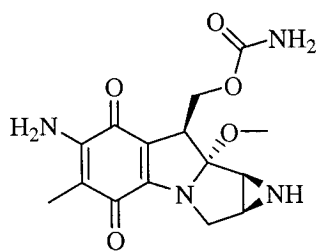
**9**
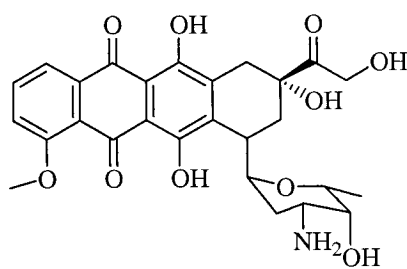
**10**
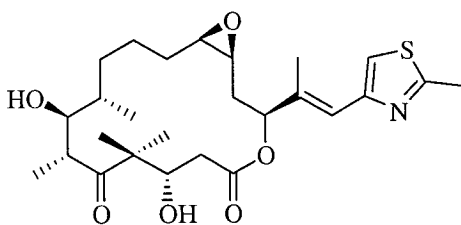
**11**

The following is a discussion of selected marine invertebrate natural products that have been investigated as potential anticancer drugs. Particular emphasis is placed on the biochemical pathways targeted by these compounds that result in their selective anticancer activity. By necessity, certain important examples are omitted, particularly in cases where a large number of molecules have been shown to inhibit the same target. Rather than providing a comprehensive review, the goal here is to emphasize the extraordinary range of cancer-related pathways targeted by marine natural products. The clinical activity of anticancer marine natural products has already been detailed in several excellent reviews,[27-29] and will therefore not be discussed here.

## I. Microtubule stabilization

Actively dividing cells undergo a process, known as mitosis, in which two identical copies of the cell's genetic material are equally distributed between the two nascent daughter cells. The chromosomes align along the central axis of the parent cell before each copy is pulled pole-ward by the spindle microtubules. Defects in microtubule regulation are implicated in the generation of chromosomal instability and aneuploidy, which are hallmarks of many types of cancers.[30] Paclitaxel (Taxol™)(**7**), one of the best-selling anticancer drugs and a standard against which many new drugs are evaluated,[31] acts by stabilizing microtubules during cell-division. As a result, it selectively targets actively dividing cancer cells.[32] Following the discovery of paclitaxel, several compounds

were isolated from marine invertebrates with similar bioactivity. Discodermolide (**12**), which was obtained from the Bahamian deep-water sponge *Discodermia dissoluta*,[33] was initially described as a cytotoxic immunosuppressive agent. Subsequent work showed that **12** stabilized microtubules with greater potency than paclitaxel.[34] Eleutherobin (**13**),[35] a diterpene glycoside, was isolated from a rare acyonacean soft coral in Western Australia. Eleutherobin and its analogs, such as sarcodictyin A (**14**)[36] were also shown to mimic the activity of paclitaxel by stabilizing microtubules.

## II. Tubulin depolymerization

In addition to microtubule stabilizing agents, there is a class of compounds that causes the depolymerization of microtubules. The first compounds that were shown to possess this kind of activity were the vinca alkaloids, such as vinblastine (**4**) and vincristine (**5**).[37] Since the discovery of these compounds, a handful of potent anticancer agents have been shown to bind to the "vinca" tubulin domain. The dolastatins, exemplified by dolastatin 10 (**15**), are linear peptides that were originally isolated in low yield from the sea hare *Dolabella auricularia*.[38, 39] Hemiasterlin (**16**) is a member of another series of linear peptides that have been isolated from several species of marine sponge.[40, 41] Both the dolastatins and the hemiasterlins were shown to inhibit tubulin polymerization, with dolastatin 10 exhibiting the most potent activity.[41] Spongistatin (**17**), a macrocyclic polyether lactone from an Eastern Indian Ocean *Spongia* species, was isolated based on its
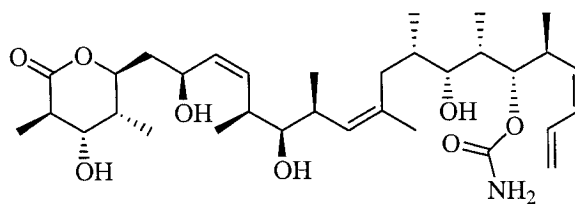
**12**
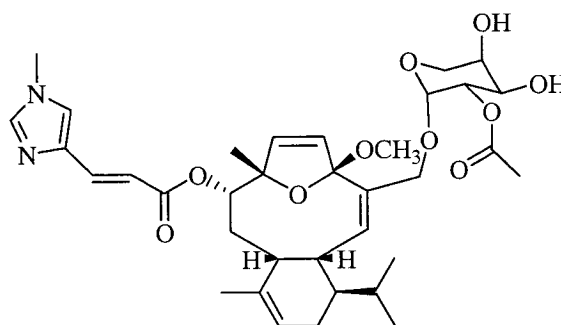
**13**
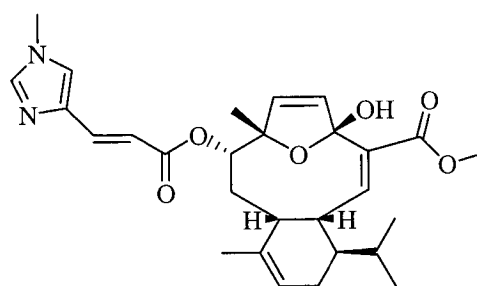
**14**
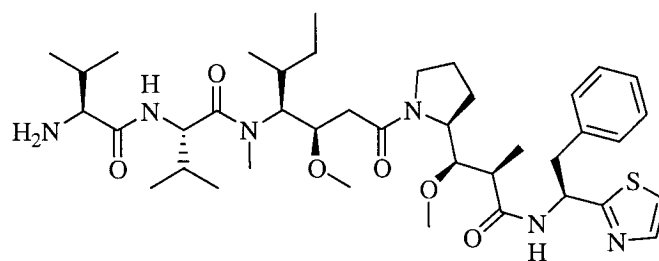
**15**
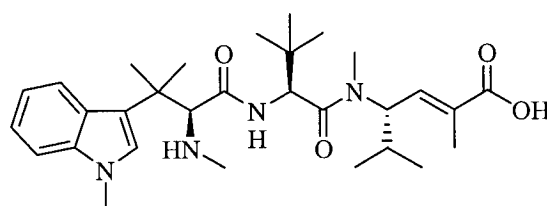
**16**
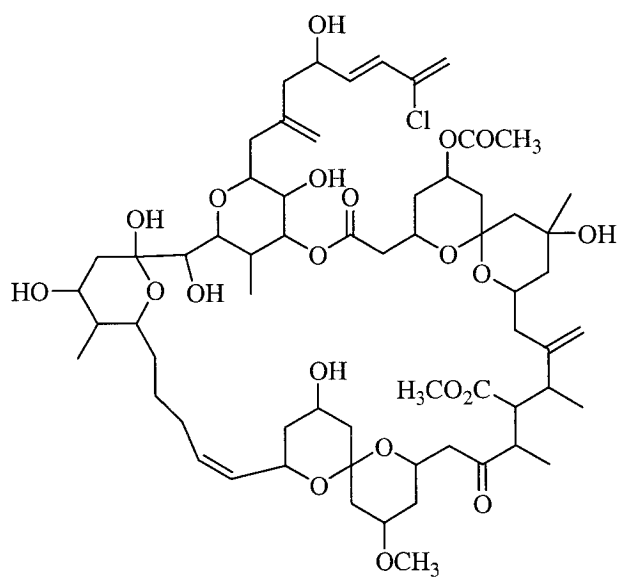
**17**

extremely potent antitumor activity.[42] Bai et al. showed that **17** was a non-competitive inhibitor of tubulin binding against radiolabeled vinblastine and radiolabeled dolastatin 10.[43] Since dolastatin 10 is also a non-competitive inhibitor, this finding implied the presence of at least three distinct binding sites in the vinca domain and helped to illustrate its complexity.

## III. Actin depolymerization

The actin cytoskeleton mediates a variety of essential biological functions in all eukaryotic cells. In addition to providing a structural framework around which cell shape and polarity are defined, the dynamic properties of actin provide the driving force for cells to move and to divide.[44] Like microtubules, the different forms of actin play important roles in mitosis, cell signaling, and motility, making them the target of a growing number of anticancer drugs.[45] Several marine natural products target the various forms of actin, and these compounds are important both as potential anticancer drugs and as biological tools to learn more about actin function. In 1999, Cuadros et al. reported the discovery of spisulosine (**18**), a hydroxyamino alkane from the marine clam *Spisula polynyma*.[46] Cells treated with **18** exhibited a decreased capacity for cellular adhesion, indicating that the compound prevented the formation of actin stress fibers. These fibers are controlled by the presence and activation of the small GTP-binding Rho proteins.[47] Spisulosine somewhat resembles the

endogenous Rho-modulating compound lysophosphatidic acid (LPA) and may act

by competitively binding to and inhibiting the LPA receptor. Latrunculins A (**19**)

and B (**20**), potent cytotoxins isolated from the Red Sea sponge *Latrunculia*

*magnifica*, induced striking changes in cell morphology that were shown by

immunofluorescence to be caused by an alteration in the organization of actin

microfilaments.[48, 49] Coue *et al.* demonstrated that latrunculin A inhibits the

polymerization of actin *in vitro*,[50] and the latrunculins have since been used as

molecular probes to investigate the biochemical roles of actin. Several other

cytotoxic marine macrolides, such as swinholide A, scytophycin C, and

mycalolide A, selectively inhibit actin and have been used as molecular probes.[51]

## IV. DNA alkylation

Since the introduction of the nitrogen mustard (**1**) over fifty years ago,

DNA alkylating agents have played a major role in cancer chemotherapy. These

compounds tend to possess a reactive functional group that allows them to bind to

DNA, resulting in damage and cell death.[52] The ecteinascidins are a series of

amino acid-derived alkaloids isolated from the Caribbean ascidian *Ecteinascidia*

*turbinata*.[53] The dominant metabolite, ecteinascidin 743 (**21**), exhibited potent

activity against a variety of tumor cells. Pommier *et al.* directly showed that **21**

was a DNA-alkylating agent.[54] Specifically, the carbinolamine center at the N2

position of **21** formed a Schiff base upon elimination of the adjacent alcohol,

which was subject to nucleophilic attack by nitrogen from guanine residues in the

DNA minor-groove. The resulting ecteinascidin-DNA linkage was irreversible

and caused the DNA helix to bend.


## V. DNA cleavage

Topoisomerases I and II are enzymes that bind to double-stranded DNA

and cause transient single-stranded (type I) or double-stranded (type II) breaks

that are essential for uncoiling of the DNA helix during replication and

transcription.[55] Both types of topoisomerases are overexpressed in cancer cells,

making them important chemotherapeutic targets. A class of anticancer

compounds, known as topoisomerase inhibitors, are capable of cleaving DNA by

covalently binding the DNA-topoisomerase complex and preventing resealing of

DNA after it has been cleaved by the enzyme.[55, 56] Ascididemin (**22**), a

pyridoacridine alkaloid from the Okinawan tunicate *Didemnum* sp., was shown to

exhibit potent DNA cleavage activity.[57, 58] Further studies have linked this

activity with the inhibition of topoisomerase II.[59] In addition, work by Ireland's

group showed that other pyridoacridines also cleaved DNA, and that this activity

was due to an ability to inhibit topoisomerase II catalytic activity.[60]


## VI. Protein kinase C activation

Protein kinases mediate the majority of signal transduction in eukaryotic

cells. In doing so, they control many cellular processes, such as transcription,

apoptosis, and cell cycle progression. Many types of cancers feature abnormal protein kinase activity, making these enzymes attractive targets for anticancer drug development.[61] The molecular heterogeneity of protein kinase C (PKC) isozymes and their functional divergence have drawn a lot of attention by medicinal chemists as potential drug targets.[62] PKC can also influence the sensitivity of tumor tissue to conventional cytotoxic drugs.[63] Bryostatin 1 (**23**) is a macrocyclic lactone from the bryozoan *Bugula neritina*.[64] Compound **23** showed potent *in vivo* antitumor activity and is being investigated as an anticancer drug. Mechanistic studies have shown that **23** was able to outcompete the tumor-promoting phorbol esters for binding to calcium phospholipid-dependent PKC.[65] In the absence of bryostatin 1, the phorbol esters bind to and activate PKC, resulting in the differentiation and proliferation of certain types of cancers. Compound **23** also activates PKC upon binding, but it does not promote tumor-cell proliferation. Bryostatin 1 is currently being tested in combination with other cancer drugs.[66]

## VII. Methionine Aminopeptidase inhibition

Methionine aminopeptidases (MetAPs) catalyze the removal of the initiator methionine residue in newly synthesized proteins. Inhibitors of MetAPs have been shown to exhibit selective activity against endothelial cells, despite a lack of differential expression or upregulation of MetAP in these cell types.[67] The
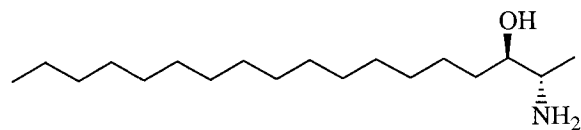
**18**
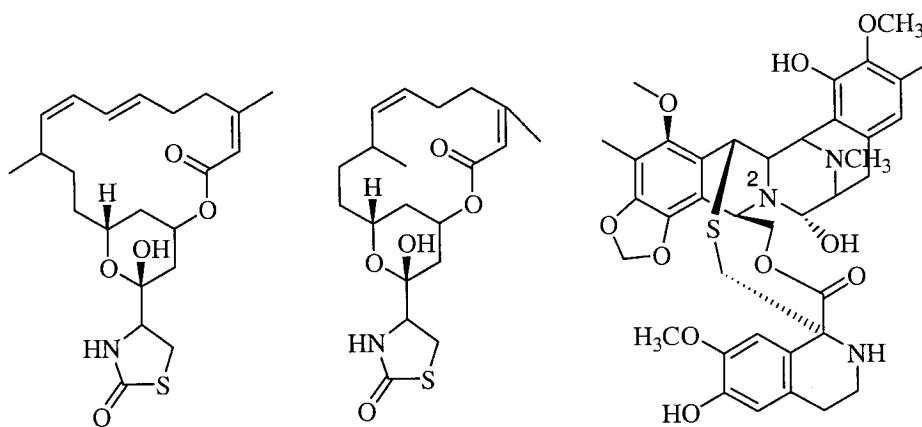
**19**

**20**

**21**
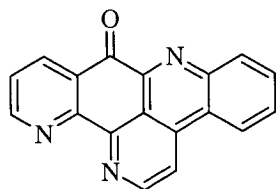
**22**
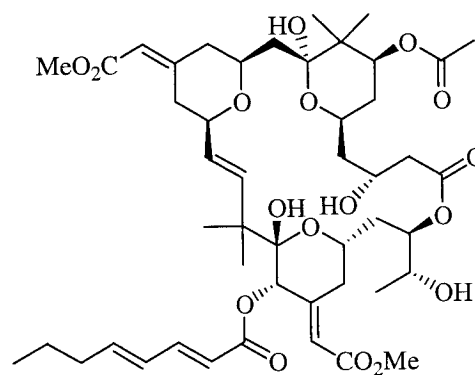
**23**

ability of fumagillin (**24**), a fungal metabolite, to selectively target MetAP2 leads

to an inhibition of angiogenesis (formation of blood vessels), which is necessary

for the survival of tumor cells.[68] Bengamides A (**25**) and B (**26**) were originally

isolated from a marine sponge *Jaspis* sp.[69] Bengamide B, which caused inhibition

of human tumor cells at low nanomolar concentrations, was one of the most

potent members of the class. Although **26** was an attractive drug candidate, its

limited availability from natural sources and poor solubility prevented further

development of the therapeutic agent. LAF389 (**27**), a synthetic bengamide

analog, showed *in vitro* activity equivalent to **26** against a broad panel of human

tumor cell lines and improved activity in human tumor xenograft models.[70] After

many failed attempts to identify the molecular target of the bengamides, including

tests in a number of enzymatic assays and the National Cancer Institute 60-cell

line panel, a proteomics approach was undertaken to show that the bengamides

inhibited MetAPs.[71] Unlike previously reported MetAP inhibitors, however, the

bengamides were non-selective against various cell lines and did not block

angiogenesis.


VIII. ATPase inhibition

ATPase enzymes are responsible for generating electrochemical gradients

in eukaryotic cells by pumping ions across cellular or organelle membranes. The

differential regulation of ATPases in various cell types suggests that their

inhibition could be therapeutically advantageous.[72] Vacuolar-ATPase (V-
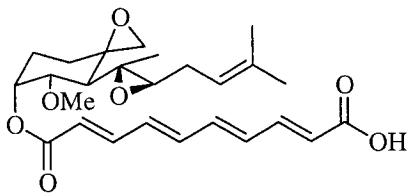
**24**
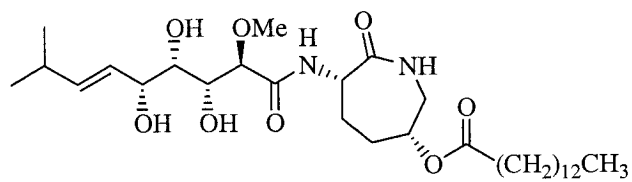


**25**
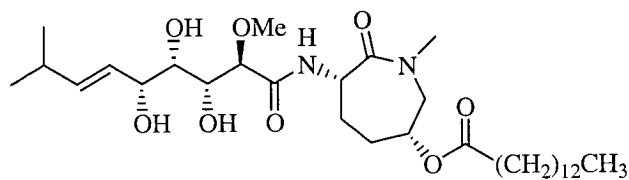


**26**
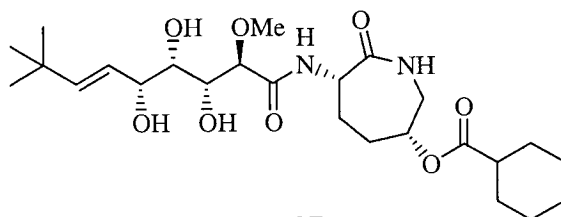


**27**

ATPase) has been proposed as a drug target in osteoporosis due to its involvement in bone resorption, and as a target in cancer due to potential involvement in tumor invasion and metastasis. Many of the known selective inhibitors of V-ATPase, however, have proven to be too toxic for therapeutic use.[73] Salicylihalamides A (**28**) and B (**29**) are potent macrolides that were isolated from a Western Australian sponge *Haliclona* sp.[74] The compounds were screened in the the NCI 60-cell line human tumor assay and showed similar activity profiles with known V-ATPase inhibitors. Subsequent work resulted in the isolation of several more bioactive analogs that were directly shown to inhibit V-ATPase function.[73]

IX. Telomerase inhibition

Telomeres, the structure at the ends of linear chromosomes, have long been recognized as critical for the maintenance of chromosomal integrity. Telomerase is a ribonucleoprotein enzyme that adds telomeres onto the 3'-ends of chromosomes.[75] While telomerase activity is found in about 90% of human tumors, the enzyme is somewhat quiescent in normal cells, suggesting that telomerase inhibitors might display good selectivity against tumor cells.[76] The validity of telomerase as a drug target has been shown by several telomerase inhibitors that have been successful in clinical trials.[77] In an effort to find anti-telomerase marine natural products, Warabi *et al.* investigated the Japanese marine sponge *Dictyodendrilla verongiformis*.[78] Bioassay-guided fractionation led to the isolation of the dictyodendrins (**30**, dictyodendrin C), which displayed

complete inhibition of human telomerase at 50 µg/ml. The desulfated analog **31**, which was obtained by acid hydrolysis of **30**, exhibited no telomerase inhibitory activity, demonstrating the necessity of a sulfate ester moiety for activity.

X. Cyclin-dependent kinase inhibition

The cyclin-dependent kinases (CDKs) are responsible for phosphorylating various substrates that are critical to cell-cycle progression. The levels of CDKs are invariant throughout the cell cycle, but their activities are modulated by interactions with cyclins, whose levels fluctuate with the cell cycle. The presence of a CDK-cyclin complex allows the cell cycle to progress. However, endogenous CDK inhibitors can bind to the complex and cause cell-cycle arrest,[79] suggesting the presence of binding sites that can be exploited by selective inhibitors. Cancer cells are generally characterized by a loss of cell-cycle regulation, aberrant expression of CDKs or cyclins, and the loss or mutation of native CDK inhibitors. Because cyclin levels can vary dramatically between normal and cancerous cells, compounds that target specific CDKs or CDK-cyclin complexes are highly sought after as anticancer drugs.[80] Indeed, selective CDK-inhibitors have shown promise in cancer clinical trials.[81, 82] Fascaplysin (**32**), an indole-containing pigment from the Fijian sponge *Fascaplysinopsis* sp., was originally reported with antimicrobial and cytotoxic properties.[83] In a subsequent search for CDK inhibitors, Soni *et al.* observed that **32** inhibited CDK4 activity

with an $IC_{50} = 0.35$ $\mu M$.[84] Molecular modeling showed that the compound, which caused $G_1$ arrest in several types of cancer cells, occupied the ATP binding pocket of CDK4. Variolins A (**33**) and B (**34**), cytotoxic pyridopyrrolopyrimidine alkaloids isolated from the Antarctic sponge *Kirkpatrickia variolosa*,[85, 86] exhibited nanomolar activity against a variety of cancer cell lines. These compounds were also shown to block the *in vitro* kinase activity of at least three different CDK-cyclin complexes.[87]


XI. Lysosome inhibition

Two major pathways for the degradation of proteins have been described: cytosolic degradation by the proteasome and autophagic degradation of proteins and organelles within the lysosome. The proteasome is responsible for the regulated degradation of short-lived proteins involved in cell cycle control as well as proteins that participate in stress responses such as DNA damage-induced cell cycle arrest or adaptation to hypoxia.[88] Autophagic degradation of cellular proteins by the lysosome has been demonstrated to be important in developmental/differentiative remodeling of cells, and is also required for the cellular adaptation to nutrient deprivation and the elimination of damaged organelles.[89] A number of examples linking alterations in proteasomal protein degradation to the pathogenesis of cancer exist,[90] and several proteasome inhibitors are being clinically evaluated.[91] In contrast, alterations in the lysosome
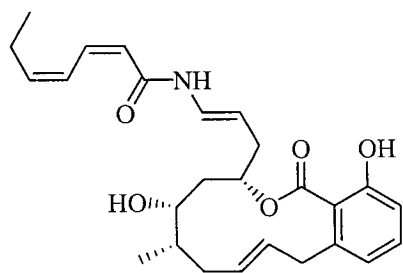
**28**
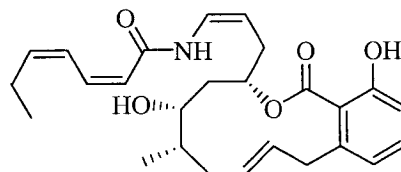
**29**
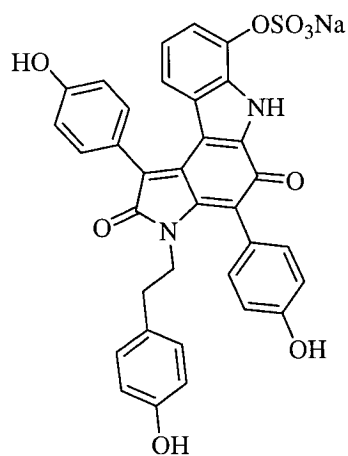
**30**
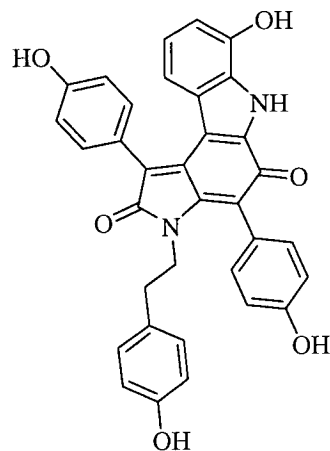
**31**
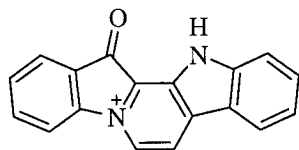
**32**
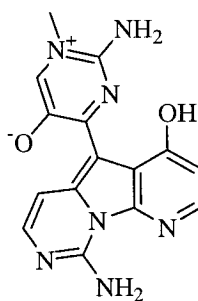
**33**
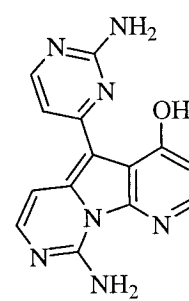
**34**

have only recently been linked to the causation of cancer,[92] and it has now become an attractive drug target. Kahalalide F (35) is a cyclic depsipeptide that was isolated from the ascoglossan mollusk *Elysia refuscens*.[93] In the presence of 35, HeLa cells became swollen with enlarged vacuoles. The formation of these vacuoles was shown to be the consequence of changes in lysosomal membranes, suggesting that the anticancer activity of kahalalide F is linked to its ability to selectively target the vacuoles.[94] The compound is currently being evaluated in clinical trials.


XII. Protein synthesis inhibition

In most eukaryotes, two distinct GTP-dependent elongation factors (eEF1 and eEF2) are required for protein translation. eEF1 mediates the binding of aminoacylated tRNA to the A-site of the ribosome and its subsequent release, whereas eEF2 catalyzes the translocation of peptidyl-tRNA from the A-site to the P-site. Protein elongation factors have been implicated in various types of cancers,[95, 96] making them attractive anticancer targets. Didemnins A (36) and B (37) belong to a class of highly cytotoxic cyclic depsipeptides that were originally isolated by Rinehart *et al.* from the Caribbean ascidian *Trididemnum solidum*.[97] Didemnin B (37) was the first marine natural product to enter clinical trials as an anticancer drug, but the compound was ultimately determined to be too toxic for use. Compound 37 rapidly induces apoptosis[98] and causes irreversible inhibition of protein biosynthesis.[99] Mechanistically, didemnin B was shown to bind and

inhibit the human elongation factor eEF1A, blocking protein biosynthesis at the elongation stage.[100, 101] Although this compound was not successful in clinical trials, the closely related dehydrodidemnin B (**38**, Aplidine) is currently being tested.[102]

Marine invertebrates have provided a large diversity of novel bioactive compounds. Within the context of treating cancer, marine natural products represent one of the latest burgeoning frontiers that promise to provide new cures or treatments that can complement existing remedies. The availability of secondary metabolites that selectively target such a wide array of molecular pathways (Table 1.1) suggests that the marine environment has imposed a unique set of constraints on its inhabitants, forcing them to adapt in order to protect themselves and survive. The sequencing of an ever-expanding number of different genomes has revealed an extraordinary level of conservation among proteins and cellular machinery, providing a link between the biological targets against which these compounds were originally designed and the biomedical targets that scientists hope to inhibit. Although many of the known species of marine invertebrates have already been analyzed for novel anticancer compounds, there remain a large number of organisms that have not been sampled, particularly those in the less accessible deeper waters. Clearly, there are many discoveries yet to be made.
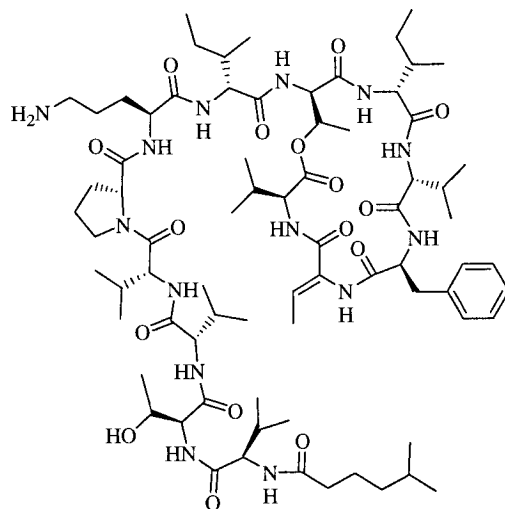
**35**
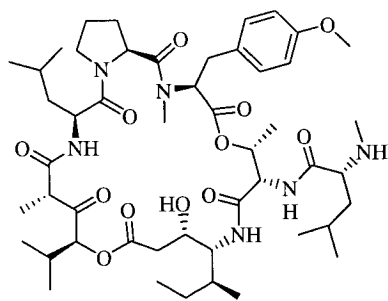


**36**
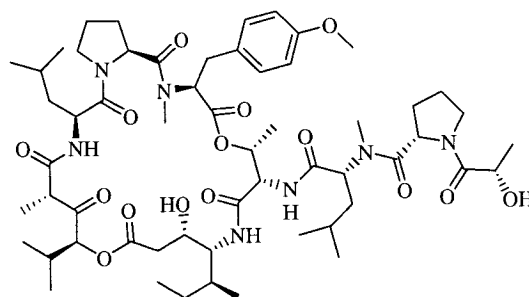


**37**
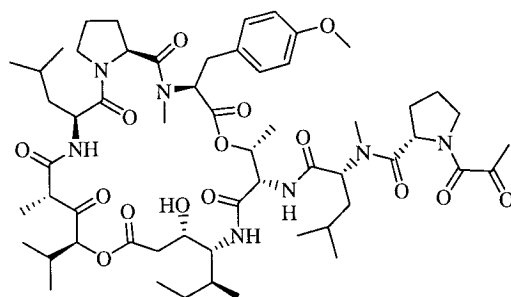


**38**

**Table 1.1** Biological activity of anticancer marine natural products.

| Target | Mechanism of action | Compound | Reference |
|---|---|---|---|
| Cytoskeleton | | | |
| | Microtubule stabilization | Discodermolide (12) | 33, 34 |
| | | Eleutherobin (13) | 35 |
| | Tubulin depolymerization | Dolastatin 10 (15) | 39 |
| | | Hemiasterlin (16) | 41 |
| | | Spongistatin (17) | 42, 43 |
| | Actin depolymerization | Spisulosin (18) | 46 |
| | | Latrunculins (19, 20) | 48, 49 |
| DNA | | | |
| | DNA alkylation | Ecteinascidin 743 (21) | 53, 54 |
| | DNA cleavage | Ascididemin (22) | 57-60 |
| Enzymes | | | |
| | Protein kinase activation | Bryostatin 1 (23) | 64, 65 |
| | MetAP inhibition | Bengamides (25,26) | 69, 71 |
| | ATPase inhibition | Salicylihalimides (28, 29) | 74 |
| | Telomerase inhibition | Dictyodendrins (30) | 78 |
| | Cyclin dependent kinase inhibition | Fascaplysin (32) | 83, 84 |
| | | Variolins (33, 34) | 85, 86 |
| Cellular Processes | | | |
| | Lysosome inhibition | Kahalalide F (35) | 93, 94 |
| | Protein synthesis inhibition | Didemnins (36, 37) | 97, 101 |

## References

1.    Faulkner, D. J. (2002). Marine Natural Products. *Nat. Prod. Rep.* **19**, 1-48, and previous reports in this series.

2.    Kardinal, C. G., Yarbro J. W. (1979). A conceptual history of cancer. *Semin. Oncol.* **6**, 396-408.

3.    Diamandopoulus, G. T. (1996). Cancer: An historical perspective. *Anticancer Res.* **16**, 1595-1602.

4.    Gallucci, B. B. (1985). Selected concepts of cancer as a disease: From the Greeks to 1900. *Oncol. Nurs. Forum* **12**, 67-71.

5.    Rubin, M. A. (2002). Understanding disease cell by cell. *Science* **296**, 1329-1330.

6.    Harvey, A. M. (1974). Early contributions to the surgery of cancer: William S. Halsted, Hugh H. Young and John G. Clark. *Johns Hopkins Med. J.* **135**, 399-417.

7.    Poste, G., Paruch, L. (1989). Stephen Paget, M.D., F.R.C.S., (1855-1926). A retrospective. *Cancer Metastasis Rev.* **8**, 93-7.

8.    Roentgen, W. C., Stanton, A. (1896). On a new kind of rays. *Nature* **53**, 274-276.

9.    Kleyn, P. W., Vesell, E. S. (1998). Pharmacogenomics: genetic variation as a guide to drug development. *Science* **281**, 1820-1821.

10.   Watson, J. D., Crick, F. H. (1953). Molecular structure of nucleic acids; a structure for deoxyribose nucleic acid. *Nature* **171**, 737-738.

11.   Cooper, G. M., *Oncogenes*. 2nd ed. 1995, Boston: Jones and Bartlett.

12.   Jones, D. A., Fitzpatrick, F. A. (1999). Genomics and the discovery of new drug targets. *Curr. Opin. Chem. Biol.* **3**, 71-76.

13.   Hartwell, L. H., Szankasi, P., Roberts, C. J., Murray, A. W., Friend, S. H. (1997). Integrating genetic approaches into the discovery of anticancer drugs. *Science* **278**, 1064-1068.

14.   Floyd, C. D., Leblanc, C., Whittaker, M. (1999). Combinatorial chemistry as a tool for drug discovery. *Prog. Med. Chem.* **36**, 91-168.

15.    Lyttle, M. H. (2004). Combinatorial chemistry: a conservative perspective. *Drug Dev. Res.* **35**, 230-6.

16.    Romanucci-Ross, L., Moerman, D. E., Tancredi, L. R., *The Anthropology of medicine : from culture to method.* 2nd ed. 1991, New York: Bergin & Garvey.

17.    Johnson, I. S., Armstrong, J. G., Gorman, M., Burnett, J. P. Jr. (1963). The Vinca alkaloids: a new class of oncolytic agents. *Cancer Res.* **23**, 1390-1397.

18.    Stahelin, H. (1973). Activity of a new glycosidic lignan derivative (VP 16-213) related to podophyllotoxin in experimental tumors. *Eur. J. Cancer.* **9**, 215-21.

19.    Wani, M. C., Taylor, H.L., Wall, M.E., Coggon, P., McPhail, A.T. (1971). Plant antitumor agents. VI. The isolation and structure of taxol, a novel antileukemic and antitumor agent from *Taxus brevifolia. J Am Chem Soc.* **93**, 2325-7.

20.    Umezawa, H., Suhara, Y., Takita, T., Maeda, K. (1966). Purification of bleomycins. *J. Antibiot.* **19**, 210-5.

21.    Hata, T., Hoshi, T., Kanamori, K., Matsumae, A., Sano, Y., Shima, T., Sugawara, R. (1956). Mitomycin, a new antibiotic from *Streptomyces.* I. *J Antibiot.* **9**, 141-6.

22.    Di Marco, A., Gaetani, M., Scarpinato, B. (1969). Adriamycin (NSC-123,127): a new antibiotic with antitumor activity. *Cancer Chemother. Rep.* **53**, 33-7.

23.    Gerth, K., Bedorf, N., Hofle, G., Irschik, H., Reichenbach, H. (1996). Epothilones A and B: antifungal and cytotoxic compounds from *Sorangium cellulosum* (Myxobacteria). Production, physico-chemical and biological properties. *J. Antibiot.* **49**, 560-3.

24.    Mann, J. (2002). Natural products in cancer chemotherapy: past, present and future. *Nature Rev.* **2**, 143-148.

25.    Faulkner, D. J. (2000). Highlights of marine natural products chemistry (1972–1999). *Nat. Prod. Rep.* **17**.

26.    Nuijen, B. (2000). Pharmaceutical developments of anticancer agents derived from marine sources. *Anti-Cancer Drugs* **11**, 793–811.

27.     Faulkner, D. J. (2000). Marine pharmacology. *Antonie van Leeuwenhoek* **77**, 135-145.

28.     Mayer, A. M. S., Gustafson, K. R. (2003). Marine pharmacology in 2000: Antitumor and cytotoxic compounds. *Int. J. Cancer* **105**, 291-299.

29.     Newman, D. J., Cragg, G. M. (2004). Marine natural products and related compounds in clinical and advanced preclinical trials. *J. Nat. Prod.* **67**, 1216 -1238.

30.     Vermeulen, K., Van Bockstaele, D. R., Berneman, Z. N. (2003). The cell cycle: a review of regulation, deregulation and therapeutic targets in cancer. *Cell Proliferation* **36**, 131-49.

31.     Goodman, J., Walsh, V., *The story of Taxol.* 2001, Cambridge, UK: Cambridge University Press.

32.     Schiff, P. B., Fant, J., Horwitz, S. (1979). Promotion of microtubule assembly *in vitro* by Taxol. *Nature* **277**, 665–667.

33.     Gunasekera, S. P., Gunasekera, M., Longley, R. E., Schulte, G. K. (1991). Discodermolide: a new bioactive polyhydroxylated lactone from the marine sponge *Discodermia dissoluta. J. Org. Chem.* **55**, 4912-4915.

34.     ter Haar, E., Kowalski, R. J., Hamel, E., Lin, C. M., Longley, R. E.,Gunasekera, S. P., Rosenkranz, H. S., Day, B. W. (1996). Discodermolide, a cytotoxic marine agent that stabilizes microtubules more potently than taxol. *Biochemistry* **35**, 243-250.

35.     Lindel, T., Jensen, P. R., Fenical, W., Long, B. H., Casazza, A. M., Carboni, J., Fairchild, C. R. (1997). Eleutherobin, a new cytotoxin that mimics paclitaxel (Taxol) by stabilizing microtubules. *J. Am. Chem. Soc.* **119**, 8744-45.

36.     D' Ambrosio, M., Guerriero, A., Pietra, F. (1987). Sarcodictyin A and sarcodictyin B, novel diterpenoidic alcohols  esterified by (E)-N(1)-methylurocanic acid. Isolation from the Mediterranean stolonifer *Sarcodictyon roseum. Helv. Chim. Acta* **70**, 2019-27.

37.     Noble, R. L. (1990). The discovery of the vinca alkaloids--chemotherapeutic agents against cancer. *Biochem. Cell. Biol.* **68**, 1344-51.

38.     Pettit, G. R., Kamano, Y., Herald, C. L., Tuinman, A. A., Boettner, F. E., Kizu, H., Schmidt, J. M., Baczynskyj, L., Tomer, K. B., Bontems, R. J.

(1987). The isolation and structure of a remarkable marine animal antineoplastic constituent: dolastatin 10. *J. Am. Chem. Soc.* **109**, 6883 - 6885.

39.     Pettit, G. R., Kamano, Y., Herald, C. L., Fujii, Y., Kizu, H., Boyd, M. R., Boettner, F. E., Doubek, D. L., Schmidt, J. M. (1993). Isolation of dolastatins 10-15 from the marine mollusc. *Tetrahedron* **49**, 9151-9170.

40.     Talpir, R., Benayahu, Y., Kashman, Y., Pannell, L., Scheyer, M. (1994). Hemiasterlin and geodiamolide TA; two new cytotoxic peptides from the marine sponge *Hemiasterella minor* (Kirkpatrick). *Tetrahedron Lett.* **35**, 4453-4456.

41.     Gamble, W. R., Durso, N. A., Fuller, R. W., Westergaard, C. K., Johnson, T. R., Sackett, D. L., Hamel, E., Cardellina, J. H. (1999). Cytotoxic and tubulin-interactive hemiasterlins from *Auletta* sp. and *Siphonochalina* sp. sponges. *Bioorg. Med. Chem.* **7**, 1611-1615.

42.     Pettit, G. R., Chicacz, Z. A., Gao, F., Herald, C. L., Boyd, M. R., Schmidt, J. M., Hooper, J. N. A. (1993). Antineoplastic agents. 257. Isolation and structure of spongistatin 1. *J. Org. Chem.* **58**, 1302-1304.

43.     Bai, R., Taylor, G. F., Cichacz, Z. A., Herald, C. L., Kepler, J. A., Pettit, G. R., Hamel, E. (1995). The spongistatins, potently cytotoxic inhibitors of tubulin polymerization, bind in a distinct region of the vinca domain. *Biochemistry* **34**, 9714 - 9721.

44.     Hall, A. (1998). Rho GTPases and the actin cytoskeleton. *Science* **279**, 509-514.

45.     Jordan, M. A., Wilson, L. (1998). Microtubules and actin filaments: dynamic targets for cancer chemotherapy. *Curr. Opin. Cell Biol.* 123-30.

46.     Cuadros, R., Montejo de Garinci, E., Wandosell, F., Faircloth, G., Fernandez-Sousa, J. M., Avilla, J. (2000). The marine compound spisulosine, an inhibitor of cell proliferation, promotes the disassembly of actin stress fibers. *Cancer Lett.* **152**, 23-29.

47.     Hall, A. (1994). Small GTP-binding proteins and the regulation of the actin cytoskeleton. *Annu. Rev. Cell Biol.* **10**, 31–54.

48.     Kashman, Y., Growiess, A., Shmueli, U. (1980). Latrunculin, a new 2-thiazolidinone macrolide from the marine sponge *Latruncula magnifica*. *Tetrahedron Lett.* **21**, 3629-32.

49. Spector, I., Shochet, N. R., Kashman, Y., Groweiss, A. (1983). Latrunculins: novel marine toxins that disrupt microfilament organization in cultured cells. *Science* 493-5.

50. Coue, M., Brenner, S. L., Spector, I., Korn, E. D. (1987). Inhibition of actin polymerization by latrunculin A. *FEBS Lett.* **213**, 316-8.

51. Yeung, K.-S., Paterson, I. Actin-binding marine macrolides: total synthesis and biological importance. *Angew. Chem. Int. Ed.* **41**, 4632-53.

52. Denny, W. A. (2001). DNA minor groove alkylating agents. *Curr. Med. Chem.* **8**, 533-544.

53. Rinehart, K. L., Holt, T. G., Fregeau, N. L., Stroh, J. G., Kiefer, P. A., Sun, F., Li, L. H., Martin, D. G. (1990). Ecteinascidins 729, 743, 745, 759A, 759B, and 770: potent antitumor agents from the Caribbean tunicate *Ecteinascidia turbinata. J. Org. Chem.* **55**, 4512-4515.

54. Pommier, Y., Kohlhagen, G., Bailly, C., Waring, M., Mazumder, A., Kohn, K. W. (1996). DNA sequence- and structure-selective alkylation of guanine N2 in the DNA minor groove by ecteinascidin 743, a potent antitumor compound from the caribbean tunicate *Ecteinascidia turbinata. Biochemistry* **35**, 13303 - 13309.

55. Wang, H.-K., Morris-Natschke, S.L., Lee, K.-H. (1997). Recent advances in the discovery and development of topoisomerase inhibitors as antitumor agents. *Med. Res. Rev.* **17**, 367-425.

56. Kaufmann, S. H. (1989). Induction of endonucleolytic DNA cleavage in human acute myelogenous leukemia cells by etoposide, camptothecin, and other cytotoxic anticancer drugs: a cautionary note. *Cancer Res.* **49**, 5870-5878.

57. Kobayashi, J., Cheng, J.-F., Nakamura, H., Ohizumi, Y., Hirata, Y., Sasaki, T., Ohta, T., Nozoe, S. (1988). Ascididemin, a novel pentacyclic aromatic alkaloid with potent antileukemic activity from the okinawan tunicate *Didemnum* sp. *Tetrahedron Lett.* **29**, 1177-1180.

58. Matsumoto, S. S., Sidford, M. H., Holden, J. A. (2000). Mechanism of action studies of cytotoxic marine alkaloids: ascididemin exhibits thiol-dependent oxidative DNA cleavage. *Tetrahedron Lett.* **41**, 1667-70.

59. Dassonneville, L., Wattez, N., Baldeyrou, B., Mahieu, C., Lansiaux, A., Banaigs, B., Bonnard, I., Bailly, C. (2000). Inhibition of topoisomerase II

by the marine alkaloid ascididemin and induction of apoptosis in leukemia cells. *Biochemical Pharmacology* **60**, 527-537.

60.   McDonald, L. A., Eldredge, G. S., Barrows, L. R., Ireland, C. M. (1994). Inhibition of topoisomerase II catalytic activity by pyridoacridine alkaloids from a *Cystodytes* sp. ascidian: a mechanism for the apparent intercalator-induced inhibition of topoisomerase II. *J. Med. Chem.* **37**, 3819 - 3827.

61.   Noble, M. E. M., Endicott, J. A. and Johnson, L. N. (2004). Protein kinase inhbitors: Insights into drug design from structure. *Science* **303**, 1800-1805.

62.   Nishizuka, Y. (1984). The role of protein kinase C in cell surface signal transduction and tumour promotion. *Nature* **308**, 693-698.

63.   Basu, A. (1993). The potential of protein kinase C as a target for anticancer treatment. *Pharmacol. Ther.* **59**, 257-80.

64.   Pettit, G. R., Herald, C. L., Doubek, D. L., Herald, D. L., Arnold, E., Clardy, J. (1982). Isolation and structure of bryostatin 1. *J. Am. Chem. Soc.* **104**, 6846-48.

65.   Kraft, A. S., Smith, J. B., Berkow, R. L. (1986). Bryostatin, an activator of the calcium phospholipid-dependent protein kinase, blocks phorbol ester-induced differentiation of human promyelocytic leukemia cells HL-60. *Proc. Nat. Acad. Sci.* **83**, 1334-1338.

66.   For a review, see Clamp, A., Jayson, G. C. (2002). The clinical development of the bryostatins. *Anti-Cancer Drugs* **13**, 673-683.

67.   Wang , J., Lou, P., Henkin, J. (2000). Selective inhibition of endothelial cell proliferation by fumagillin is not due to differential expression of methionine aminopeptidases. *J. Cell. Biol.* **77**, 465-473.

68.   Liu, S., Widom, J., Kemp, C. W., Crews, C. M., Clardy, J. (1998). Structure of human methionine aminopeptidase-2 complexed with fumagillin. *Science* **282**, 1324–1327.

69.   Quinoa, E., Adamczeski, M., Crews, P., Bakus, G. J. (1986). Bengamides, heterocyclic anthelmintics from a *Jaspidae* marine sponge. *J. Org. Chem.* **51**, 4494 - 4497.

70. Kinder Jr., F. R., Versace, R. W., Bair, K. W., Bontempo, J. M., Cesarz, D., Chen, S., Crews, P., Czuchta, A. M., Jagoe, C. T., Mou, Y., Nemzek, R., Phillips, P. E., Tran, L. D., Wang, R., Weltchek, S., Zabludoff, S. (2001). Synthesis and antitumor activity of ester-modified analogues of bengamide B. *J. Med. Chem.* **44**, 3692 - 3699.

71. Towbin, H., Bair, K. W., DeCaprio, J. A., Eck, M. J., Kim, S., Kinder, F. R., Morollo, A., Mueller, D. R., Schindler, P., Song, H. K., van Oostrum, J., Versace, R. W., Voshol, H., Wood, J., Zabludoff, S., Phillips, P. E. (2003). Proteomics-based target identification: bengamides as a new class of methionine aminopeptidase inhibitors. *J. Biol. Chem.* **278**, 52964-52971.

72. Hu, T., Sage, H., Hsieh, T.-S. (2002). ATPase domain of eukaryotic DNA topoisomerase II. Inhibition of ATPase activity by the anti-cancer drug bisdioxopiperazine and ATP/ADP-induced dimerization. *J. Biol. Chem.* **277**, 5944-5951.

73. Beutler J. A., M. T. C. (2003). Novel marine and microbial natural product inhibitors of vacuolar ATPase. *Curr. Med. Chem.* **10**, 787-796.

74. Erickson, K. L., Beutler, J. A., Cardellina, J. H., Boyd, M. R. (1997). Salicylihalamides A and B, novel cytotoxic macrolides from the marine sponge *Haliclona* sp. *J. Org. Chem.* **62**, 8188-8192.

75. Maser, R. S., DePinho, R. A. (2002). Connecting chromosomes, crisis, and cancer. *Science* **297**, 565-569.

76. Lavelle, F., Riou, J.-F., Laoui, A., Mailliet, P. (2000). Telomerase: a therapeutic target for the third millennium? *Crit. Rev. Oncol. Hematol.* **34**, 111-126.

77. Corey, D. R. (2002). Title Telomerase inhibition, oligonucleotides, and clinical trials. *Oncogene* **21**, 631-5.

78. Warabi, K., Matsunaga, S., van Soest, R. W. M., Fusetani, N. (2003). Dictyodendrins A-E, the first telomerase-inhibitory marine natural products from the sponge *Dictyodendrilla verongiformis. J. Org. Chem.* **68**, 2765-2770.

79. Hung, D. T., Jamison, T. F., Schreiber, S. L. (1996). Understanding and controlling the cell cycle with natural products. *Chem. Biol.* **3**, 623-39.

80. Mani, S., Wang, C., Wu, K., Francis, R., Pestell, R. (2000). Cyclin-dependent kinase inhibitors: novel anticancer agents. *Expert. Opin. Investig. Drugs* **9**, 1849-70.

81. Senderowicz, A. M. (1999). Flavopiridol: the first cyclin-dependent kinase inhibitor in human clinical trials. *Invest. New Drugs* **17**, 313-320.

82. Akinaga, S., Sugiyama, K., Akiyama, T. (2000). UCN-01 (7-hydroxystaurosporine) and other indolocarbazole compounds: a new generation of anti-cancer agents for the new century? *Anti-Cancer Drug Design* **1**, 43-52.

83. Roll, D. M., Ireland, C. M., Lu, H. S., Clardy, J. (1988). Fascaplysin, an unusual antimicrobial pigment from the marine sponge *Fascaplysinopsis* sp. *J. Org. Chem.* **53**, 3276-3278.

84. Soni, R., Muller, L., Furet, P. (2000). Inhibition of cyclin-dependent kinase 4 (Cdk4) by fascaplysin, a marine natural product. *Biochem. Biophys. Res. Commun.* **275**, 877-84.

85. Perry, N. B., Ettouati, L., Litaudon, M., Blunt, J. W., Munro, M. H. G. (1994). Alkaloids from the antarctic sponge *Kirkpatrickia varialosa.* : Part 1: variolin B, a new antitumour and antiviral compound. *Tetrahedron* **50**, 3987-92.

86. Trimurtulu, G., Faulkner, D. J., Perry, N. B., Ettouati, L., Litaudon, M., Blunt, J. W., Munro, M. H. G., Jameson, G. B. (1994). Alkaloids from the antarctic sponge *Kirkpatrickia variolosa.* Part 2: variolin A and N(3')-methyl tetrahydrovariolin B. *Tetrahedron* **50**, 3993-4000.

87. Erba, E., Simone, M., Damia, G., Vikhanskaya, F., Di Fransesco, A., Jimeno, J., Cuevas, C., Faircloth, G., D'Incalci, M. (2003). *Clin. Canc. Res.* **9**, C78 (supplemental).

88. Ciechanover, A. (1998). The ubiquitin-proteasome pathway: on protein death and cell life. *EMBO* **17**, 7151-60.

89. Klionsky, D. J., Emr, S. D. (2000). Autophagy as a regulated pathway of cellular degradation. *Science* **290**, 1717-1721.

90. Pagano, M., Benmaamar, R. (2003). When protein destruction runs amok, malignancy is on the loose. *Cancer Cell* **4**, 251-256.

91.   Lenz, H.-J. (2003). Clinical update: proteasome inhibitors in solid tumors. *Cancer Treat. Rev.* **29**, 41-48.

92.   Edinger, A. L., Thompson, C. B. (2003). Defective autophagy leads to cancer. *Cancer Cell* **4**, 422-424.

93.   Hamann, M. T., Scheuer, P. J. (1993). Kahalalide F: a bioactive depsipeptide from the sacoglossan mollusk *Elysia rufescens* and the green alga *Bryopsis* sp. *J. Am. Chem. Soc.* **115**, 5825 - 5826.

94.   Garcia-Rocha, M., Bonay, P., Avila, J. (1996). The antitumoral compound Kahalalide F acts on cell lysosomes. *Cancer Lett.* **99**, 43-50.

95.   Anand, N., Murthy, S., Amann, G., Wernick, M., Porter, L. A., Cukier, I. H., Collins, C., Gray, J. W., Diebold, J., Demetrick, D. J., Lee, J. M. (2002). Protein elongation factor eEF1A2 is a putative oncogene in ovarian cancer. *Nat. Genet.* **31**, 301-305.

96.   Lew, Y., Jones, D. V., Mars, W. M., Evans, D., Byrd, D., Frazier, M. L. (1992). Expression of elongation factor-1 gamma-related sequence in human pancreatic cancer. *Pancreas* **7**, 144-52.

97.   Rinehart, K. L. J., Gloer, J. B., Hughes, R. G, Jr., Renis, H. E., McGovren, J. P., Swynenberg, E. B., Stringfellow, D. A., Kuentzel, S. L., Li, L. H. (1981). Didemnins: antiviral and antitumor depsipeptides from a caribbean tunicate. *Science* **212**, 933-5.

98.   Grubb, D. R., Wolvetang, E. J., Lawen, A. (1995). Didemnin B induces cell death by apoptosis: the fastest induction of apoptosis ever described. *Biochem. Biophys. Res. Commun.* **215**, 1130-36.

99.   Li, L. H., Timmins, L. G., Wallace, T. L., Krueger, W. C., Prairie, M. D., Im, W. B. (1984). Mechanism of action of didemnin B, a depsipeptide from the sea. *Cancer Letters* **23**, 279-288.

100.   SirDashpande, B. V., Toogood, P. L. (1995). Mechanism of protein synthesis inhibition by didemnin B in vitro. *Biochemistry* **34**, 9177-84.

101.   Marco, E., Martín-Santamaría, S., Cuevas, C., Gago, F. (2004). Structural basis for the binding of didemnins to human elongation factor eEF1A and rationale for the potent antitumor activity of these marine natural products. *J. Med. Chem.* **47**, 4439 -4452.

102. Reviewed in: Rinehart, K. L. (2000). Antitumor compounds from tunicates. *Med. Res. Rev.* **20**, 1-27.

# CHAPTER 2

## CYTOTOXIC β-CARBOLINES AND CYCLIC PEROXIDES

## FROM THE PALAUAN SPONGE *PLAKORTIS NIGRA*[*]

Four β-carbolines, plakortamines A-D (**1-4**), two cyclic peroxides, epiplakinic acids G and H (**5-6**), and two related γ-lactones, (2*S*\*,4*R*\*)- and (2*R*\*,4*R*\*)-2,4-dimethyl-4-hydroxy-16-phenylhexadecanoic acid 1,4-lactones (**7-8**), were isolated from the deep-water sponge *Plakortis nigra* from Palau. The structures were established based mainly on 1D and 2D NMR data. Most of the metabolites inhibited the HCT-116 human colon tumor cell line, and the biological activity of several compounds is being investigated further using the NCI 60-cell line assay.

This work originally appeared in the *Journal of Natural Products* **2002**, 65, 1258-61 with co-authors Patrick L. Colin, John N.A. Hooper, and D. John Faulkner. It has been rewritten here for continuity and so that my contribution be clarified.

---

1



2



3



4



5



6



7



8
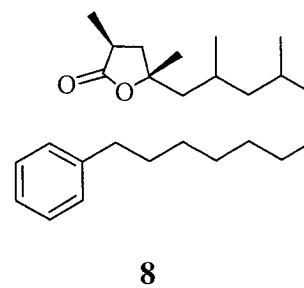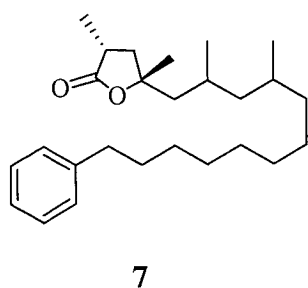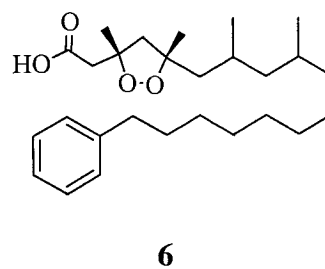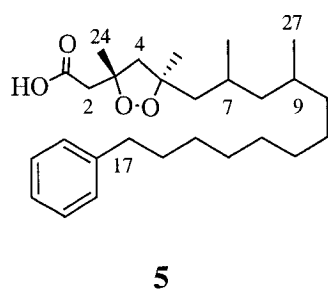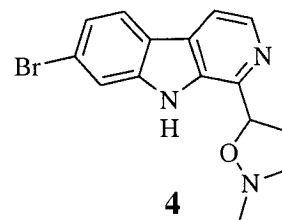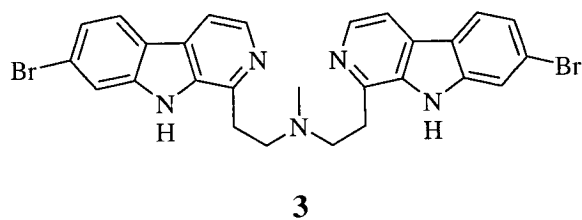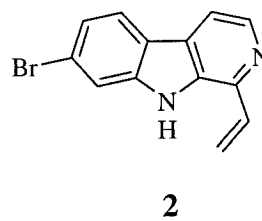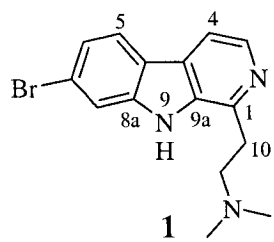
## Introduction

Bioactive indole alkaloids have been known for a long time and account for some of the earliest examples of natural products characterization by chemists.[1] In particular, many compounds possessing a β-carboline skeleton (9) have been isolated, some of which with potent and/or selective anticancer activity. Simple β-carbolines, such as harmane (10), harmaline (11), and harmine (12), were originally isolated from the medicinal plant *Peganum harmala*,[2] and have been shown to inhibit the human topoisomerase enzymes, which are important targets for anticancer chemotherapy.[3] More recently, harmine derivatives were shown to be potent inducers of apoptosis in certain tumors.[4] Extracts from the root of *Eurycoma harmandiana* have been used in Thai traditional medicine as an anticancer and antimalarial curative. Bioassay-guided fractionation of the root extract led to the isolation of the bioactive β-carboline alkaloids 13 and 14 that were responsible for the observed anticancer activity.[5] Similarly, the β-carboline-benzoquinolizidine alkaloid deoxytubulosine (15) was isolated as the active component from the flowers of the Indian medicinal plant *Alangium lamarckii*.[6] Several elegant studies conducted by Rao *et al.* showed that 15 inhibits the enzymatic activity of thymidylate synthase[7] and dihydrofolate reductase,[8] two attractive targets for the development of anticancer chemotherapeutic agents.

Simple marine-derived β-carbolines, such as those described in this chapter, are normally associated with ascidians[9] and are exemplified by the

antiviral eudistomins from the Caribbean tunicate *Eudistoma olivaceum*.[10] The

majority of β-carbolines found in sponges belong to a more complex group of

anticancer antibiotics known as the manzamines, such as manzamine A (**16**) and

hydroxymanzamine A (**17**).[11] More than thirty manzamine analogs have been

isolated from several different sponge species, and the ubiquity of these

compounds has led some to speculate that they may be produced by symbiotic

microorganisms.[12] In addition to the manzamines, a few simpler β-carboline

analogs have been isolated from sponges.[13, 14]

Naturally-occuring cyclic peroxides account for the potent anticancer and

antimalarial activity found in many species of medicinal plants and marine

sponges.[15,16] While the majority of sponge-derived peroxides contain six-

membered rings, a few five-membered 1,2-dioxolane carboxylates have also been

reported. The first example of a five-membered peroxide among marine natural

products was reported in 1983 when Phillipson and Rinehart isolated plakinic acid

A (**18**) from a sponge.[17] Additional examples include plakinic acids C (**19**) and D

(**20**) and epiplakinic acids C (**21**) and D (**22**),[18] epiplakinic acid E methyl ester

(**23**),[19] (3*R*\*,5*S*\*,12*E*,-14*E*,17*Z*)-3,5-dimethyl-3,5-peroxydodeca-12,14,17-trienoic

acid (**24**) and its methyl ester (**25**),[20] and other related analogues.[21-23] Many of the

cyclic peroxides have been reported with submicromolar anticancer activity and

were therefore further investigated as potential chemotherapeutic agents. In most
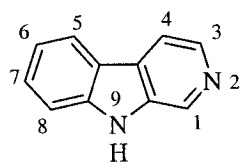
**9**
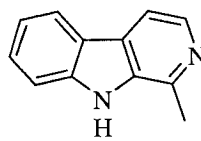
**10**
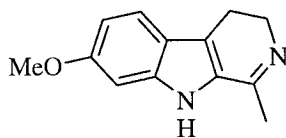
**11**
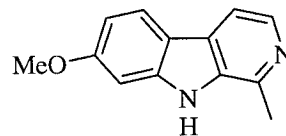
**12**
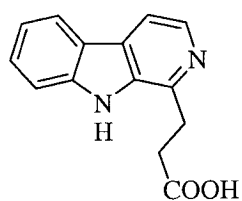
**13**
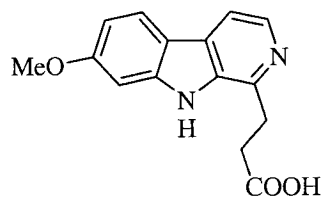
**14**
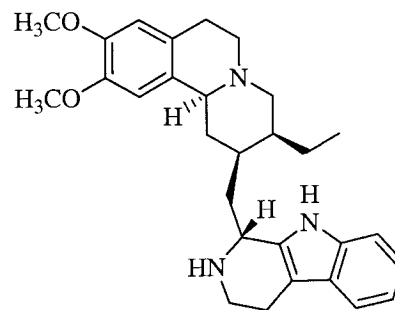
**15**
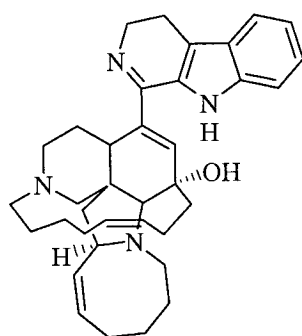
**16**
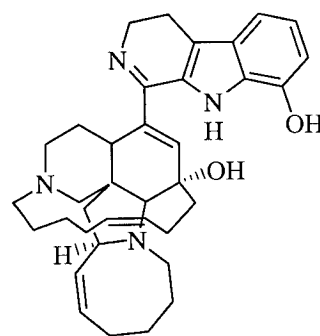
**17**
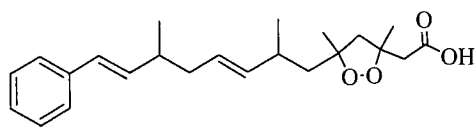
18
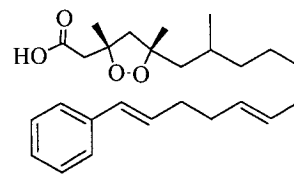
19
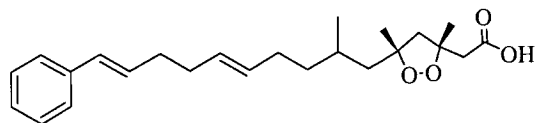
20
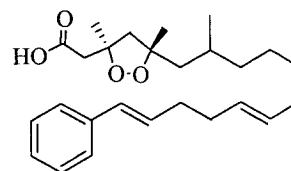
21
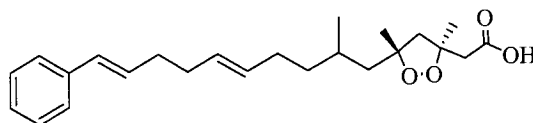
22
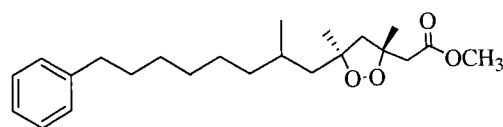
23
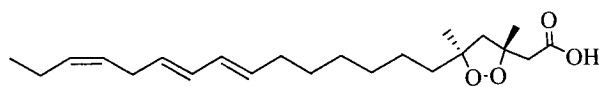
24
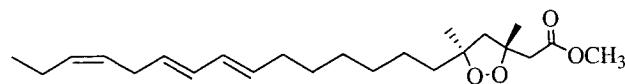
25

cases, however, the broad cytotoxicity profiles of these compounds rendered them unsuitable as anticancer drug candidates. Regardless, many of the cyclic peroxides are potently selective antiplasmodic agents that may be useful in fighting malaria.[15]

Described below is the first example of cytotoxic β-carbolines coexisting with cytotoxic cyclic peroxides and related lipids in a marine sponge. The structures of eight new metabolites were elucidated by interpretation of spectroscopic data, and an analysis of the structural elucidation and bioactivity of these compounds is presented below.

## Isolation and structural elucidation

The dark brown sponge *P. nigra* was collected by Pat Colin in Palau at a depth of 380 ft using a mixed gas rebreathing apparatus. The lyophilized sponge was extracted with methanol, and after removal of the solvent, the resulting material was partitioned between ethyl acetate and water. The aqueous extract was made basic with sodium hydroxide solution and again extracted with ethyl acetate (peroxy acids may have inadvertently been discarded or destroyed during this step). The ethyl acetate extracts, which exhibited activity against the HCT-116 human colon tumor cell line, were combined and fractionated on Sephadex LH-20 using methanol as an eluent to obtain plakortamines A (1, 144.4 mg, 0.61% dry wt), B (2, 15.0 mg, 0.063% dry wt), and C (3, 4.9 mg, 0.021% dry wt)

and several fractions that required further purification. One of these fractions was subjected to reversed-phase medium-pressure liquid chromatography on a Diaion HP-20SS column to obtain plakortamine D (**4**, 6.5 mg, 0.027% dry wt). Some of the fractions from the Sephadex column appeared by $^1$H NMR spectroscopy to consist of salts of the alkaloids and organic acids. After experiencing great difficulty in separating the acids from the plakortamines, and then suffering further losses while purifying the acids, I eventually succeeded in purifying epiplakinic acids G (**5**) and H (**6**) and two γ-lactones, **7** and **8**. Owing to the difficulty that I experienced in separating the acids from the bases, the yields reported for compounds **1-8** do not reflect their true concentrations in the crude extract as judged by its $^1$H NMR spectrum, which indicated that the ratio of plakortamines to epiplakinic acids was about 1:1.

Plakortamine A (**1**) was isolated as an optically inactive pale yellow oil. The mass spectrum contained equal intensity peaks at 318/320, indicating the presence of bromine, and the high-resolution mass measurement (*m/z* 318.0596, [M + H]$^+$) indicated a molecular formula of $C_{15}H_{16}{}^{79}BrN_3$, with 9 unsaturation equivalents. The UV spectrum contained absorptions at 243 nm and 295 nm (Figure 2.1), which, together with the presence of 11 signals in the aromatic region of the $^{13}$C NMR spectrum, suggested a heteroaromatic ring system. The $^1$H NMR data, with signals at δ12.52 (br s, NH), 8.28 (d, 1 H, *J* = 5.5 Hz, H-3), 7.78 (d, 1 H, *J* = 5.5 Hz, H-4), 7.95 (d, 1 H, *J* = 8.0 Hz, H-5), 7.34 (dd, 1 H, *J* =
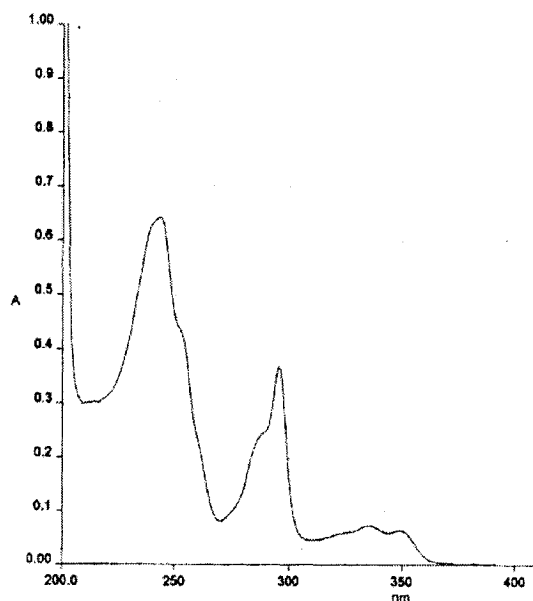
**Figure 2.1** UV spectrum for plakortamine A (**1**).

8.0, 1.5 Hz, H-6), and 7.67 (d, 1 H, $J$ = 1.5 Hz, H-8), suggested that the

heteroaromatic ring system was a 1-substituted 7-bromo-β-carboline, which

satisfies the requirement for 9 unsaturation equivalents. The $^{13}C$ NMR spectrum,

which was assigned using HSQC and HMBC data, confirmed the presence of a 1-

substituted 7-bromo-β-carboline moiety. The remaining signals in the $^1H$ NMR

spectrum at δ2.47 (s, 6 H, NMe$_2$), 2.82 (t, 2 H, $J$ = 5.5 Hz, H$_2$-11), and 3.36 (t, 2

H, $J$ = 5.5 Hz, H$_2$-10) were assigned to a $N,N$-dimethylethylamine side chain, the

position of which was determined by the HMBC correlations from the signals at
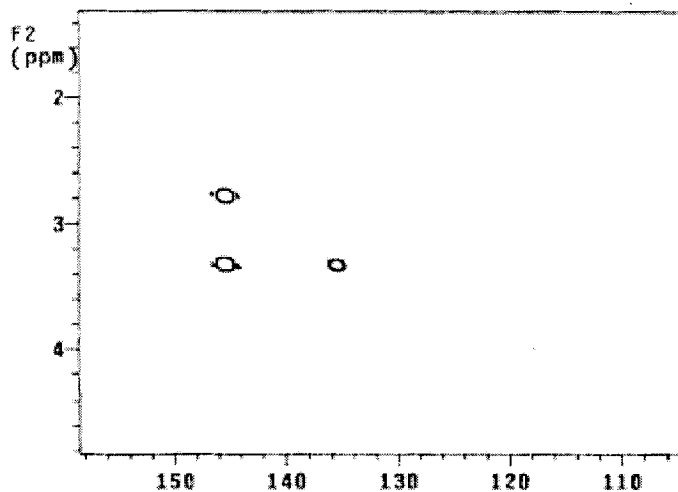
**Figure 2.2** Enlargement of the HMBC spectrum for plakortamine A (**1**), which was used to assign the position of the *N,N*-dimethylethylamine side chain.

2.28 and 3.36 to a carbon signal at 144.0 (C-1) and from 3.36 to only one

additional carbon signal at 135.9 (C-9a) (Figure 2.2). Thus plakortamine A (**1**) is

7-bromo-1-(*N,N*-dimethylethylamino)-β-carboline.

Plakortamine B (**2**), the most bioactive of the alkaloids, was isolated as an

optically inactive yellow oil. The mass spectrum contained $[M + H]^+$ peaks of

equal intensity at 273/275, indicating the presence of bromine (Figure 2.3), and

the high-resolution mass measurement indicated a molecular formula of

$C_{13}H_9{}^{81}BrN_2$ ($m/z$ 275.0008, $[M + H]^+$). The $^{13}C$ NMR spectra contained 13

signals in the aromatic/olefinic region, suggesting a heteroaromatic ring system

(Figure 2.4). The $^1H$ NMR spectrum contained signals assignable to a terminal

vinyl group at $\delta_H$ 5.72 (d, 1 H, $J = 11$ Hz), 6.40 (d, 1 H, $J = 17$ Hz), and 7.18 (dd,

1 H, $J = 17$, 11 Hz). In addition, signals at $\delta_H$ 8.61 (br s, 1 H, -NH), 8.48 (d, 1 H,

$J = 5.5$ Hz, H-3), 7.97 (d, 1 H, $J = 8$ Hz, H-5), 7.84 (d, 1 H, $J = 5.5$ Hz, H-4), 7.69

(d, 1 H, $J = 1.5$ Hz, H-8), and 7.41 (dd, 1 H, $J = 8$, 1.5 Hz, H-6), suggested that

the heteroaromatic ring system was a 1-substituted 7-bromo-$\beta$-carboline (Figure

2.5), which, along with the terminal olefin, satisfies the requirement for 10

unsaturation equivalents suggested by the molecular formula. An analysis of the

HMBC spectrum confirmed the presence of a 1-substituted 7-bromo-$\beta$-carboline

moiety. HMBC data was also used to assign the attachment site of the terminal

olefin at C-1. Plakortamine B was therefore assigned the structure 7-bromo-1-

vinyl-$\beta$-carboline (2).

Plakortamine C (3) was isolated as an optically inactive pale yellow gum.

The molecular formula, $C_{27}H_{23}N_5{}^{81}Br_2$ ($m/z$ 578.0372, [M + H]$^+$), coupled with

the presence of only 14 signals in the $^{13}C$ NMR spectrum, suggested that

plakortamine C contained two 1-substituted 7-bromo-$\beta$-carboline groups.

Assuming that each of the aromatic signals was due to 2 protons, the remaining

signals in the $^1H$ NMR spectrum at $\delta_H$ 3.31 (t, 4 H, $J = 5.5$ Hz), 3.09 (t, 4 H, $J =$

5.5 Hz), and 2.58 (s, 3 H) were assigned to a -CH$_2$-CH$_2$-N(Me)-CH$_2$-CH$_2$- chain

joining the two 7-bromo-$\beta$-carboline entities.

Plakortamine D (4), [$\alpha$]$_D$ -2.1° ($c$ 0.6, MeOH), was obtained as a yellow

oil. The molecular formula, $C_{15}H_{14}{}^{79}BrN_3O$ ($m/z$ 332.0385, [M + H]$^+$), required

10 unsaturation equivalents, nine of which were associated with a 7-bromo-β-

carboline moiety. The $^1$H NMR spectrum contained an *N*-methyl signal at $\delta_H$ 2.99

(s, 3 H) and signals at 5.90 (dd, 1 H, $J$ = 8.5, 7 Hz), 3.61 (t, 1 H, $J$ = 8 Hz), 3.08

(m, 1 H), 2.80 (m, 1 H), and 2.53 (m, 1 H), which were shown by the COSY

spectrum to be due to a O-CH-CH$_2$-CH$_2$-N unit. To account for the remaining

unsaturation equivalent, there must be an N-O bond to form a ring, which is

attached at C-1 to the carbon bearing oxygen (C-10). Further support for this

structure came from the HMBC experiment that showed correlations from the *N*-

methyl signal to C-12, from H-10 to C-1, C-9a, and C-11, and from H-11 (2.56) to

C-1, C-10, and C-12. There was insufficient material to determine the absolute

configuration at C-1.
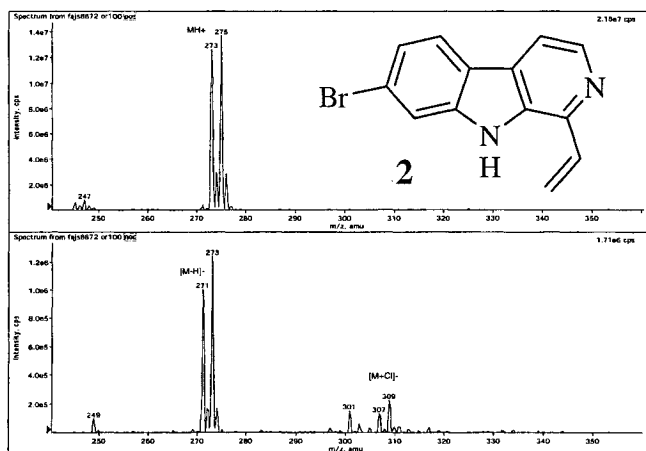


**Figure 2.3** Positive (top) and negative (bottom) electrospray ionization
mass spectra for plakortamine B (2).
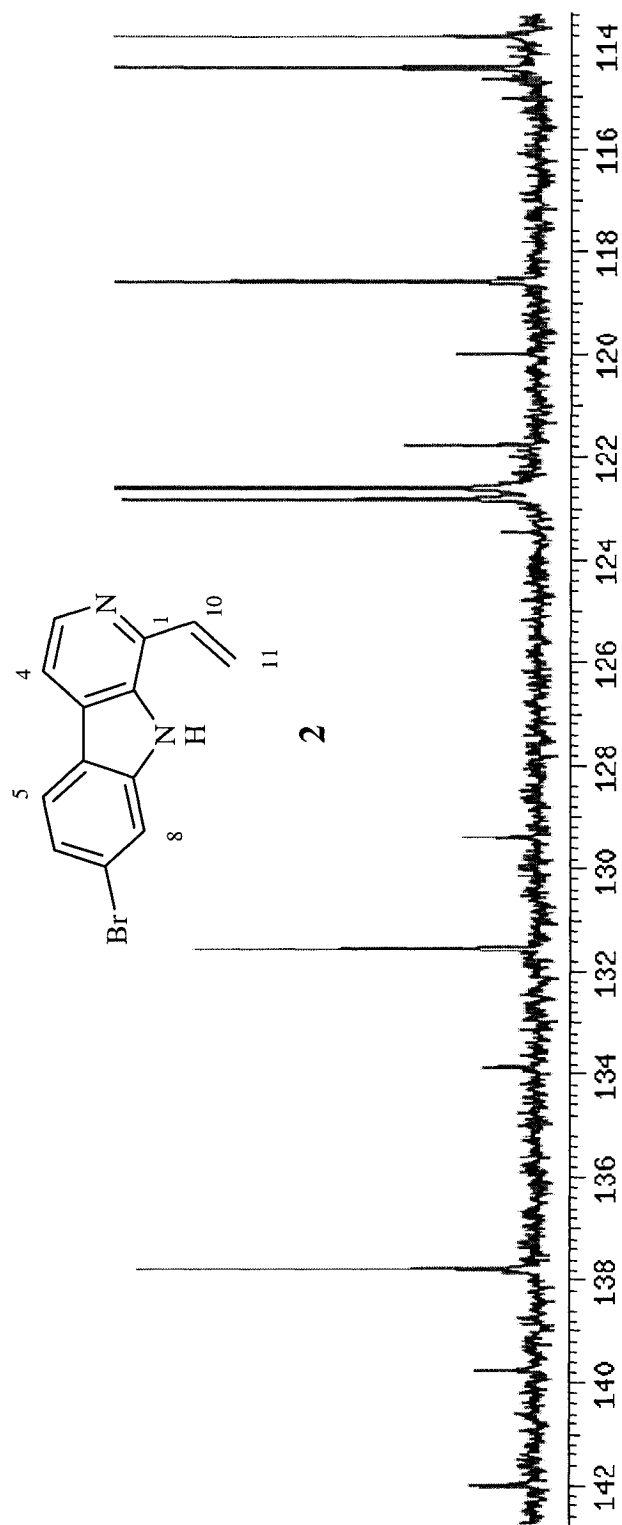
**Figure 2.4** $^{13}$C NMR spectrum for plakortamine B (**2**) in MeOH-$d_4$.
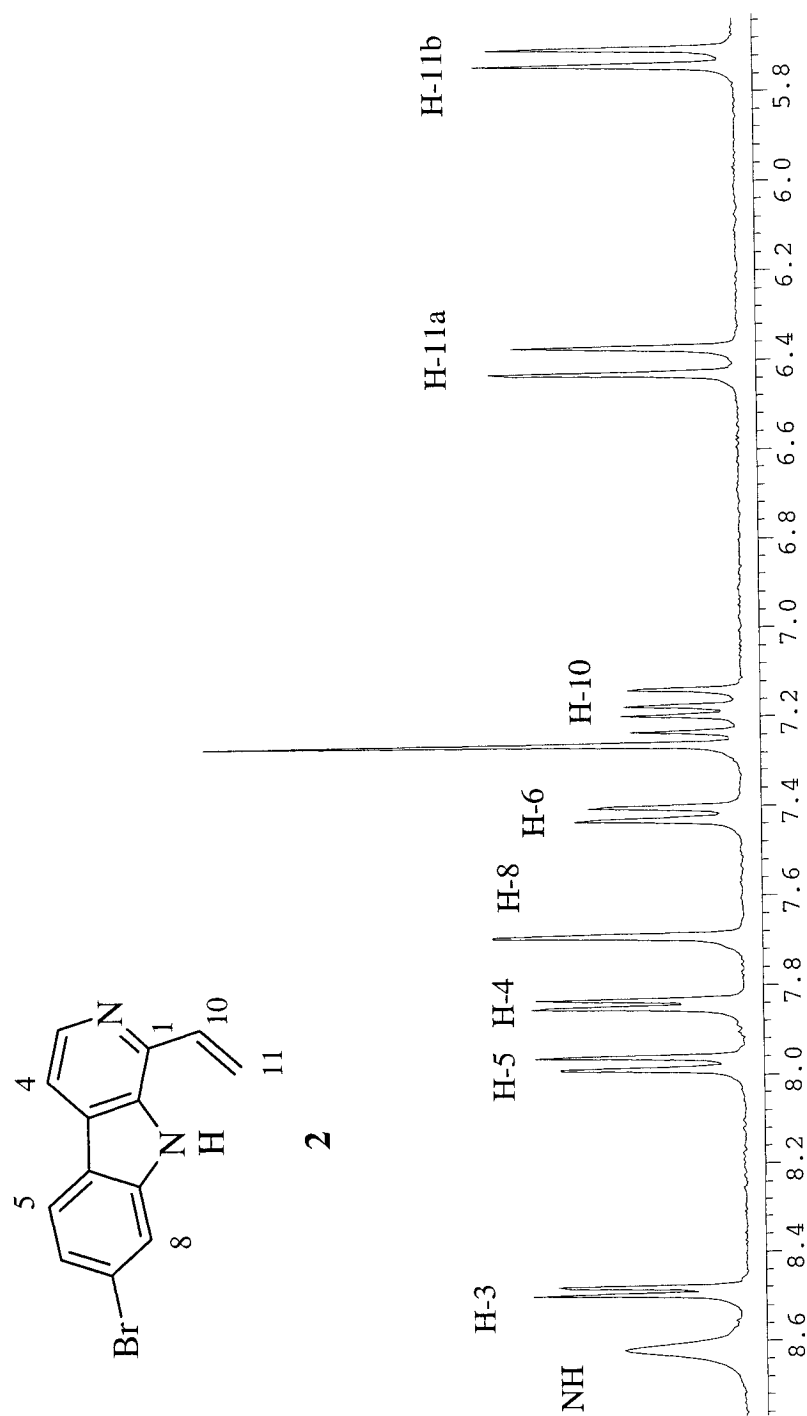
**Figure 2.5** Annotated $^1$H NMR spectrum for plakortamine B (**2**) in $CDCl_3$.

A general mechanism for the formation of brominated β-carbolines such

as 1-4 is illustrated in Figure 2.6. A nucleophilic addition of tryptamine to an

aldehyde results in the formation of a Schiff base. Position 2 of the indole system

is also nucleophilic due to the adjacent nitrogen and can now participate in an

intramolecular Pictet-Spengler condensation,[24] attacking the reactive iminium

carbon to close the ring. The resulting tricyclic intermediate is then oxidized and

brominated to give the β-carboline skeleton seen in the plakortamines.
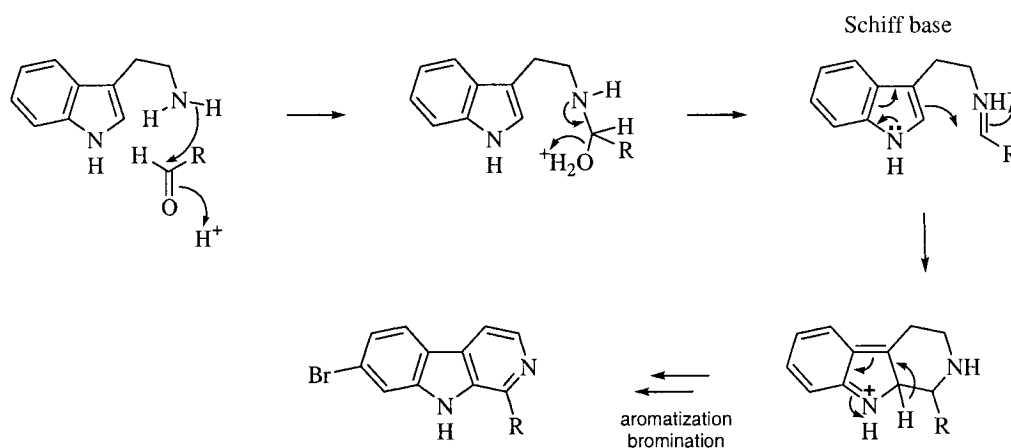


**Figure 2.6** Biosynthetic mechanism for the formation of the β-carboline skeleton of the plakortamines.

Epiplakinic acid G (**5**), [α]$_D$ -17.2° (*c* 0.3, MeOH), was isolated as a

colorless gum. The molecular formula, $C_{27}H_{44}O_4$, was initially inferred from the

high-resolution mass measurement of the [M + Na]$^+$ ion at *m/z* 455.3127. The $^{13}$C

NMR spectrum contained four signals at δ$_C$ 143.8, 129.2 (2C), 129.0 (2C), and

126.4 that were assigned to a terminal phenyl group, a signal at 174.3 due to the

carboxylic acid, two signals at δ$_C$ 87.8 and 84.9 due to fully substituted carbon

atoms bearing oxygen, and four methyl signals at δ$_C$ 24.8, 24.1, 22.2, and 20.7

(Figure 2.7). The $^1$H NMR spectrum confirmed the presence of the phenyl group

and the four methyl groups that gave rise to signals at δ$_H$ 1.46 (s, 3 H), 1.33 (s, 3

H), 0.95 (d, 3 H, *J* = 6.5 Hz), and 0.83 (d, 3 H, *J* = 7 Hz) (Figure 2.8). The signals

at δ$_H$ 1.46 and 1.33 were assigned to methyl groups on carbons bearing oxygen.

Interpretation of the HSQC and HMBC spectra suggested the presence of a five-

membered cyclic peroxide moiety. The C-2 methylene signals at δ$_H$ 2.77 (d, 1 H,

*J* = 16 Hz) and 2.73 (d, 1 H, *J* = 16 Hz) showed HMBC correlations to the

carboxylic acid signal at δ$_C$ 174.3 (C-1) and to signals at 84.9 (C-3), 58.3 (C-4),

and 24.8 (C-24, δ$_H$ 1.46). The Me-24 signal at δ$_H$ 1.46 showed HMBC

correlations to C-2, C-3, and C-4, while the Me-25 signal at 1.33 showed

correlations to C-4, C-5 (87.8), and C-6 (47.5). Since C-3 and C-5 are the only

carbon atoms bearing oxygen, there must be a peroxide bridge linking the two

carbons in order to satisfy both the number of oxygens and the number of

unsaturation equivalents in the molecule. The Me-26 signal at δ$_H$ 0.95 (d, 3 H, *J*
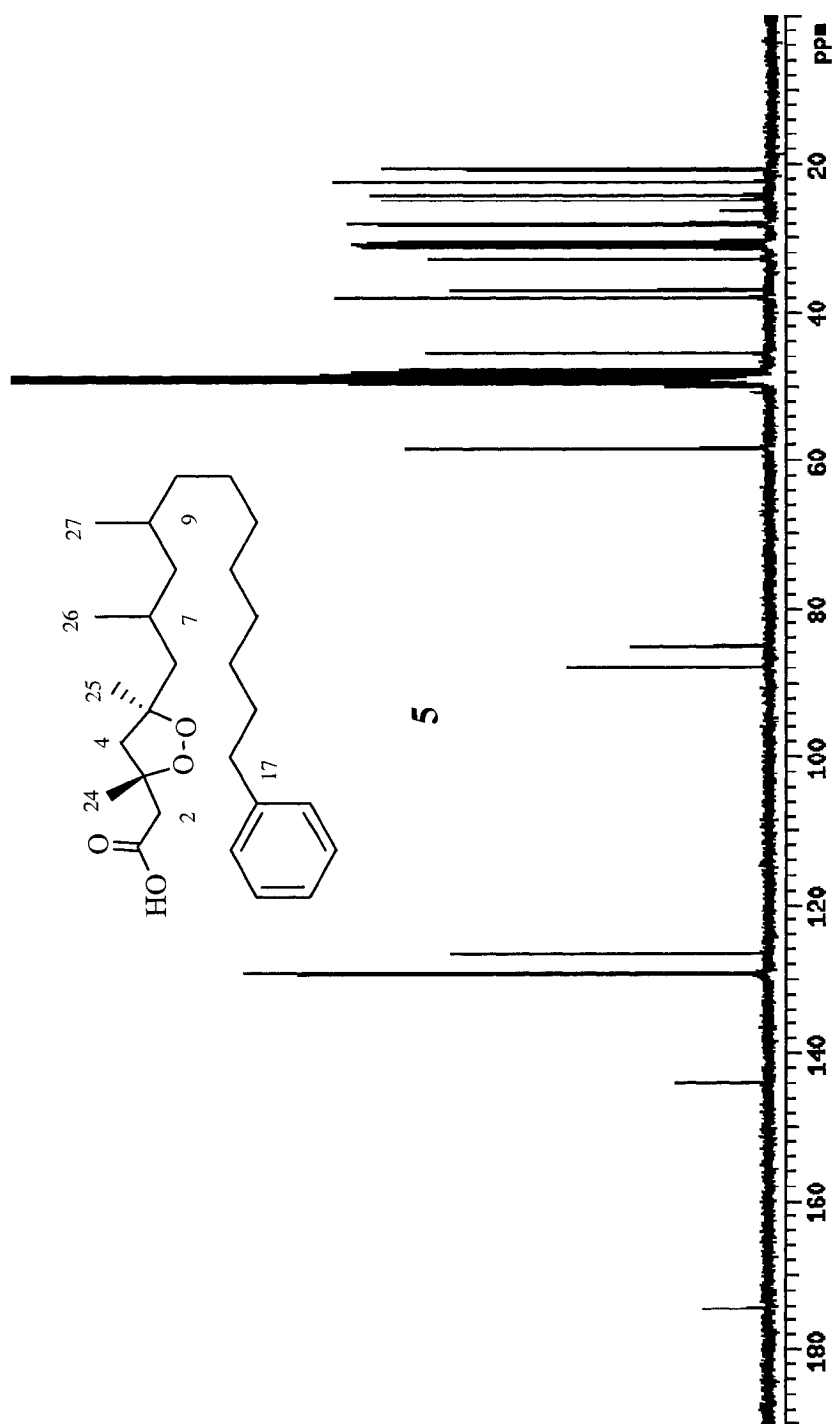
**Figure 2.7** $^{13}$C NMR spectrum for epiplakinic acid G (**5**) in MeOH-$d_4$.
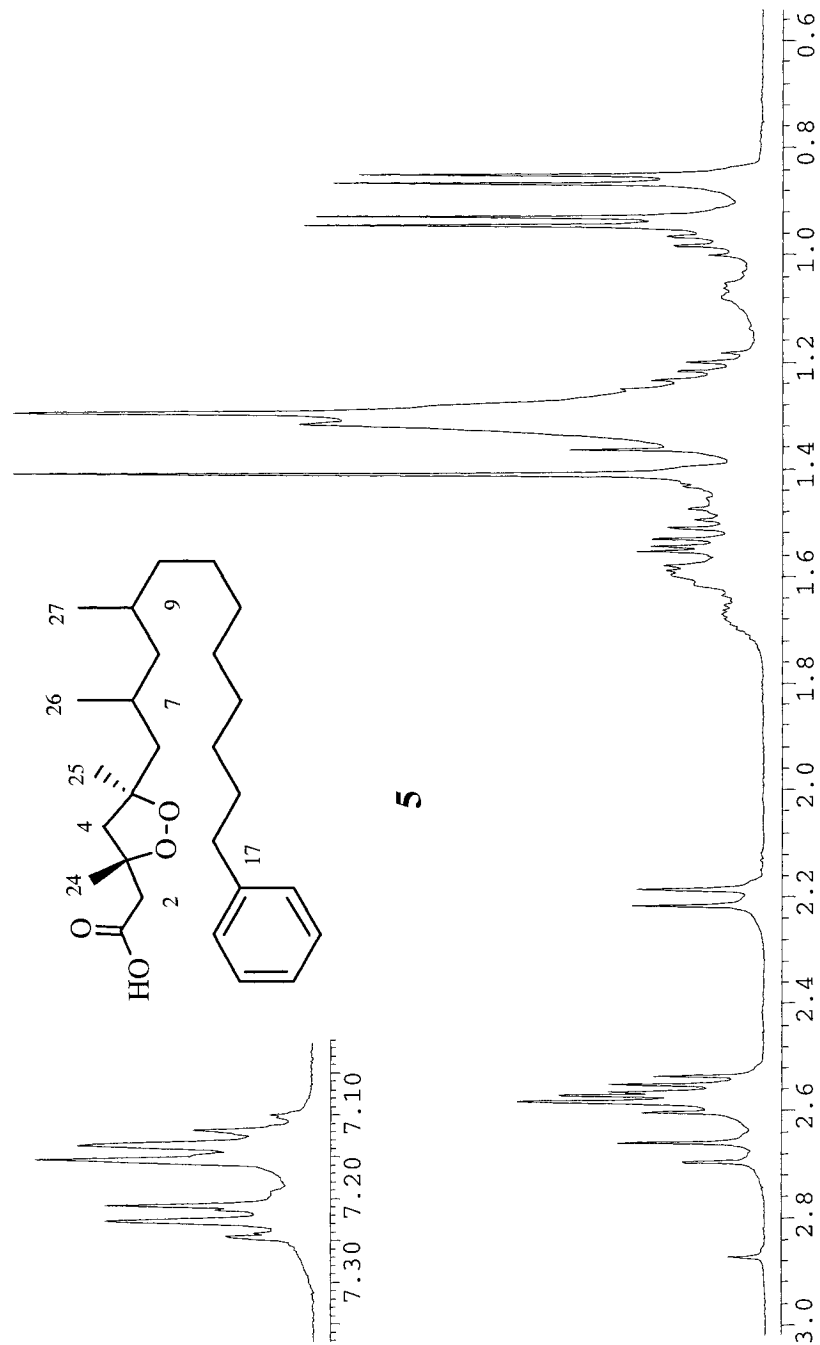
**Figure 2.8** $^1$H NMR spectrum for epiplakinic acid G (**5**) in CDCl$_3$. Inset shows downfield portion of the spectrum.

= 6.5 Hz) showed HMBC correlations to signals at 47.5 (C-6), 28.1 (C-7), and

47.9 (C-8), while the Me-27 signal at 0.83 (d, 3 H, $J$ = 7 Hz) was correlated to

signals at 47.9 (C-8), 30.7 (C-9), and 37.9 (C-10). These correlations established

the structure of the C-1 to C-10 portion of the molecule. The $H_2$-17 signal at

$\delta_H$ 2.59 (t, 2 H, $J$ = 8 Hz) showed HMBC correlations to signals at 143.8 (C-18),

129.0 (C-19, 23), and 32.7 (C-15). The remaining methylene signals must be due

to a linear chain between C-10 and C-15.

The relative stereochemistry about the peroxide ring was established by

the observation of NOEs between Me-24 and the H-4β signal at $\delta_H$ 2.22 (d, 1 H, $J$

= 13 Hz) and between Me-25 and the H-4α signal at 2.49 (d, 1 H, $J$ = 13 Hz)

(Figure 2.9). Unfortunately no useful NOEs were observed that could be used to

assign the relative stereochemistry at C-26 or C-27.

Epiplakinic acid H (6), [α]$_D$ +33° ($c$ 0.07, MeOH), was isolated as a

colorless gum. The molecular formula, $C_{27}H_{44}O_4$, which is the same as that of

epiplakinic acid G (5), was defined from the high-resolution mass measurement of

the [M + Na]$^+$ ion at $m/z$ 455.3128. The $^1$H and $^{13}$C NMR spectra were so similar

to those of 5 that it was apparent that epiplakinic acid H (6) was an epimer of

epiplakinic acid G (5) at either C-3 or C-5. This was confirmed by the

observation of NOE correlations from both the Me-24 signal at $\delta_H$ 1.48 and the

Me-25 signal at 1.37 to the H-4β signal at 2.22 in the ROESY spectrum. The H-

4α signal at $\delta_H$ 2.47 showed correlations to the C-2 signal at 2.73 and a signal at
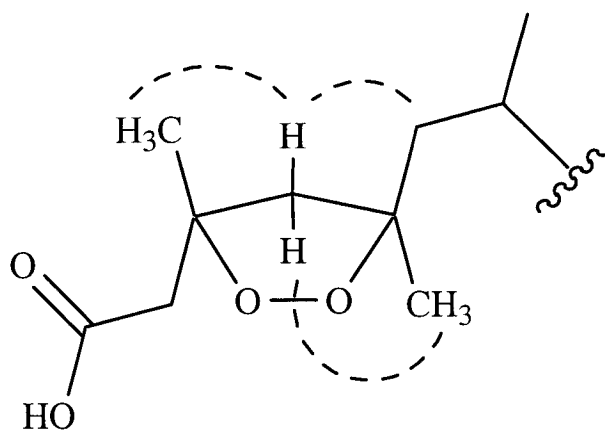
**Figure 2.9** 1D-NOESY correlations (dashed arcs) for cyclic peroxide portion of epiplakinic acid G (**5**).

1.64 that was assigned to H-7. Since the $^{13}C$ NMR signals of Me-26 and Me-27 are nearly identical in both compounds, I consider it preferable to assign the same stereochemistry at C-5, C-7, and C-9, implying that **5** and **6** are epimeric at C-3.

Both (2S\*,4R\*)- and (2R\*,4R\*)-2,4-dimethyl-4-hydroxy-16-phenylhexadecanoic acid 1,4-lactones (**7** and **8**) were isolated as colorless oils. They had the same molecular formula, $C_{24}H_{38}O_2$, which was determined by high-resolution mass measurement of the [M + Na]$^+$ ions at $m/z$ 381.2763 and 381.2770, respectively. The IR bands at 1765 cm$^{-1}$ indicated that both compounds contained a γ-lactone ring, which, together with a phenyl ring, accounted for the six degrees of unsaturation required by the molecular formula. The $^1H$ and $^{13}C$ NMR spectra of **7** and **8** were remarkably similar, especially the signals due to the monosubstituted phenyl ring and the attached linear alkyl chain, with the only notable differences being associated with the substituents about the γ-lactone ring (Figure 2.10). In the case of lactone **7**, the COSY spectrum revealed coupling from the methyl doublet at $\delta_H$ 1.21 ($J$ = 7 Hz, Me-23) to the H-2 methine signal at 2.91, which must be adjacent to the lactone carbonyl and which was in turn coupled to the H-3 signals at 2.27 and 1.72. The methyl singlet at $\delta_H$ 1.34 must be adjacent to the only remaining fully substituted carbon at 86.1, which must also be attached to the lactone oxygen, the alkyl chain, and the methylene group at C-3. The HMBC data confirmed the presence of the γ-lactone ring and its substituents. The Me-23 signal showed correlations to C-1 ($\delta_C$ 181.6),
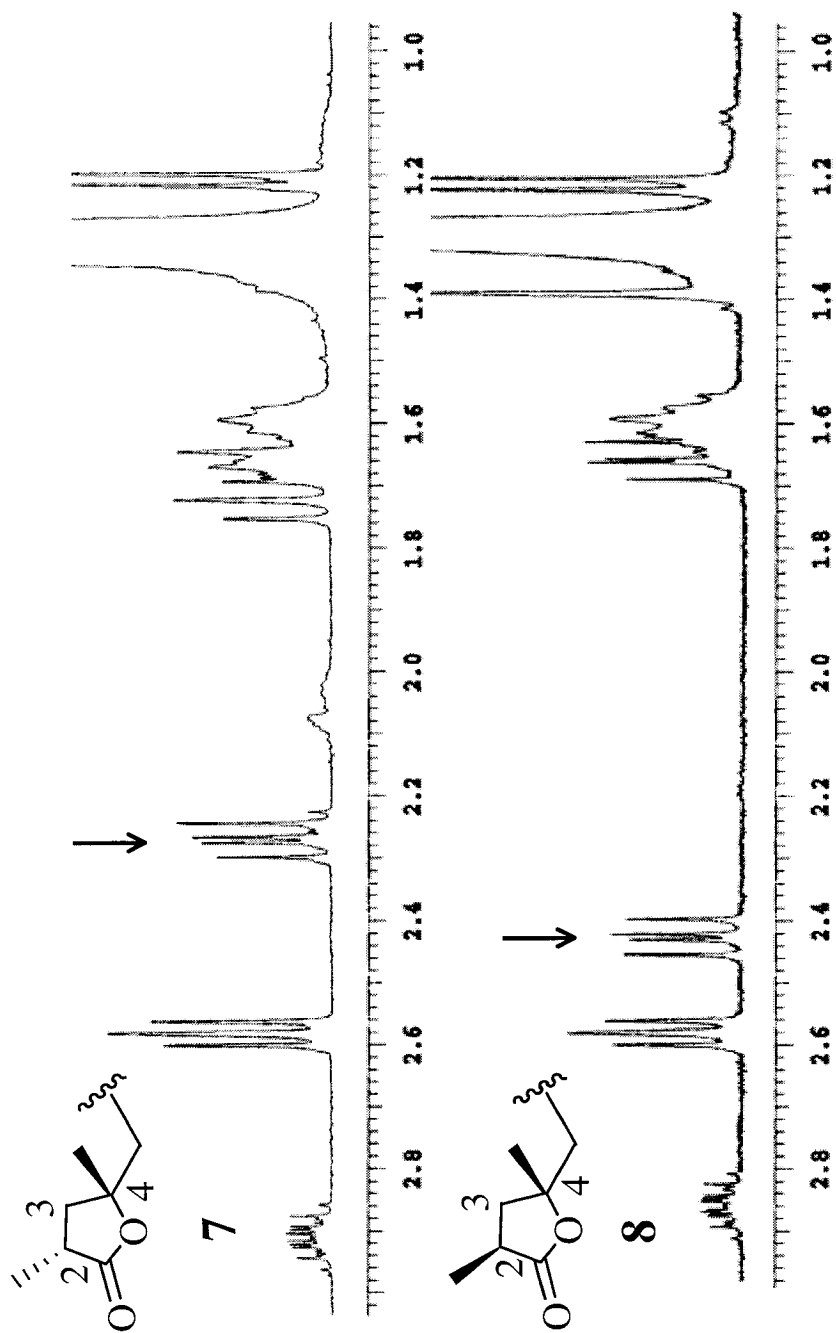
**Figure 2.10** Comparison of the upfield region of the $^1$H NMR spectra for **7** (top) and **8** (bottom). Arrows indicate the chemical shift of H-3α, which changes due to the relative stereochemistry of C-2 and C-4. Truncated portion of the molecules shown for clarity.

C-2 (36.3), and C-3 (42.5), while the Me-24 signal showed correlations to C-3, C-4 (86.1), and C-5 (42.8). The ROESY spectrum showed weak correlations between the Me-23 signal and the H-3α signal at $\delta_H$ 1.72 and between the Me-24 signal and the H-3β signal at 2.27, while the H-2 signal showed a stronger correlation to the H-3β signal than to the H-3α signal, all of which supported the $2S^*,4R^*$ stereochemistry. A similar analysis of the NMR data for lactone **8** revealed that its planar structure was the same as that of lactone **7**. The ROESY spectrum of **8** did not show strong correlations from the Me-23 and Me-24 signals to either of the H-3 signals, but since there are only two chiral centers in the compound, lactone **8** must have the $2R^*,4R^*$ stereochemistry.

All of the metabolites tested exhibited activity against the HCT-116 human colon tumor cell line. The most active alkaloid was plakortamine B (**2**, $IC_{50}$ 0.62 μM), followed by plakortamine A (**1**, $IC_{50}$ 3.2 μM) and plakortamine D (**4**, $IC_{50}$ 15 μM) (Figure 2.11). Epiplakinic acids G (**5**, $IC_{50}$ 0.16 μM) and H (**6**, $IC_{50}$ 0.39 μM) were also moderately active, and even lactone **7** ($IC_{50}$ 14.5 μM), but not lactone **8**, showed mild activity.

The text of this chapter is, in part, a reprint of the material as it appears in the Journal of Natural Products 2002, 65, 1258-61 with co-authors Patrick L. Colin, John N.A. Hooper, and D. John Faulkner. I was the primary researcher and author, and the co-authors listed in this publication helped direct and supervise the research, which forms the basis of this chapter.
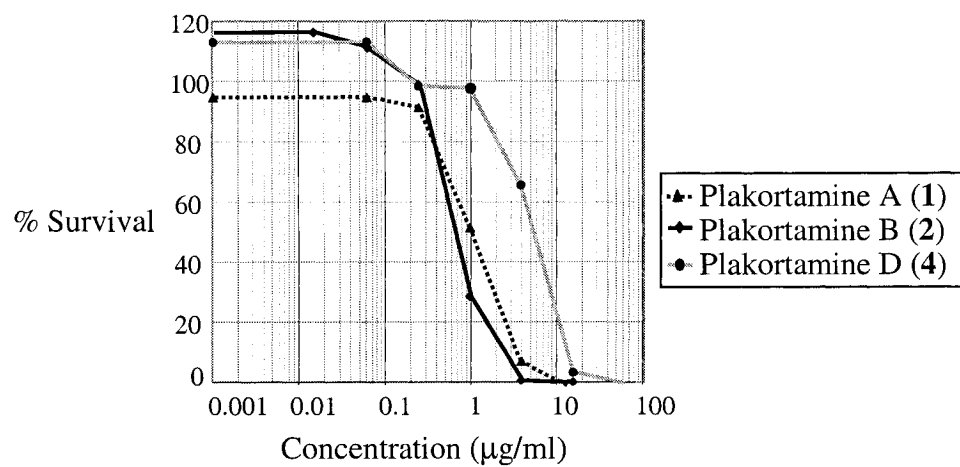
**Figure 2.11** Dose-response curve of human cancer cells (HCT-116) exposed to compounds **1**, **2**, and **4**.

## Experimental

**General Methods.** Optical rotations were measured on a Rudolf Autopol III polarimeter ($c$ g/100 mL) at 589 nm. IR spectra were recorded on a Perkin-Elmer 1600 FT-IR spectrophotometer. UV spectra were obtained using a Perkin-Elmer Lambda Bio-20 spectrophotometer. $^1$H, COSY, HMBC, HMQC, and ROESY NMR spectra were measured on a Varian Inova 300 MHz spectrometer. $^{13}$C and DEPT spectra were measured on a Varian Gemini 400 MHz spectrometer. ESIMS spectra were recorded using a Finnigan LCQ mass spectrometer. High-resolution FABMS data were obtained on a VG ZAB mass spectrometer at the U. C. Riverside Regional Facility. All solvents were distilled prior to use.

**Extraction and Purification.** The dark brown sponge, identified by Dr. John Hooper as *Plakortis nigra* Levi, 1959 (Plakinidae, Homosclerophida), was hand-collected by Pat Colin from a depth of 380 ft at Palau using a mixed gas rebreathing apparatus. A voucher specimen has been deposited in the SIO Benthic Invertebrate Collection (# P1181). The diced, lyophilized sponge (61.4 g dry wt) was repeatedly extracted with MeOH at room temperature to obtain a dark brown oil (8.1 g). After the extract had been partitioned between EtOAc and $H_2O$, the aqueous extract was basified with dilute sodium hydroxide to pH 10 and again extracted with EtOAc. The combined EtOAc extracts (1.3 g), which exhibited activity against the HCT-116 cell line, were chromatographed on Sephadex LH-20 using MeOH as eluant to obtain plakortamines A (**1**, 144 mg, 0.61% yield), B (**2**, 15 mg, 0.063% yield), and C (**3**, 4.9 mg, 0.021% yield). One

of the fractions from LH-20 was further purified by medium-pressure

chromatography on Diaion HP-20SS using gradient elution from 20% MeOH in

$H_2O$ to MeOH to obtain plakortamine D (**4**, 6.5 mg, 0.027% yield). Our first

attempts to separate the most cytotoxic LH-20 fractions were unsuccessful and

resulted in loss of the material, which consisted mainly of epiplakinic acids.

However, several cytotoxic LH-20 fractions were combined and chromatographed

on silica gel using a stepwise gradient from 20% EtOAc in hexanes to 100%

EtOAc to obtain several active fractions that contained phenyl signals in their [1]H

NMR spectra. The most active of these fractions were combined and

chromatographed by HPLC on silica using 20% EtOAc in hexanes to obtain

epiplakininc acid G (**5**, 4.7 mg) and epiplakinic acid H (**6**, 1 mg). The less polar

fractions were combined and chromatographed by HPLC on silica using 10%

EtOAc in hexanes to obtain (2*S**,4*R**)-2,4-dimethyl-4-hydroxy-16-

phenylhexadecanoic acid 1,4-lactone (**7**, 1.9 mg) and (2*R**,4*R**)-2,4-dimethyl-4-

hydroxy-16-phenylhexadecanoic acid 1,4-lactone (**8**, 0.7 mg).

**HCT-116 Assay.** The HCT-116 cells were plated by Catherine Sincich in 96-well

plates and incubated overnight at 37°C in 5% $CO_2$/air. Compounds were added to

the plate and serially diluted. The plate was then incubated for a further 72 h.

Cell viability was assessed at the end of this period through the use of a CellTiter

96 AQ$_{ueous}$ non-radioactive cell proliferation assay (Promega). Inhibition

concentration ($IC_{50}$) values are interpreted from the bioreduction of MTS/PMS by

living cells into a formazan product. The first step of the assay is the addition of MTS/PMS to the sample wells followed by a 3 h incubation. The quantity of the formazan product (proportional to the number of living cells) in each well was then determined using a Molecular Devices Emax microplate reader that measured the amount of 490 nm absorbance in each well, and the $IC_{50}$ value was calculated by a SOFTMax analysis program. Etoposide (Sigma) and DMSO (solvent) were used as positive and negative controls, respectively.

**Plakortamine A (1):** pale yellow oil; UV (MeOH) 243 nm ($\varepsilon$ 20 000), 295 nm ($\varepsilon$ 11 700); IR (film) 3200 (br), 1620, 1570 cm$^{-1}$; $^1$H NMR (CDCl$_3$, 300 MHz) $\delta_H$ 12.52 (br s, 1 H, -$N$H), 8.28 (d, 1 H, $J$ = 5.5 Hz, H-3), 7.95 (d, 1 H, $J$ = 8 Hz, H-5), 7.78 (d, 1 H, $J$ = 5.5 Hz, H-4), 7.67 (d, 1 H, $J$ = 1.5 Hz, H-8), 7.34 (dd, 1 H, $J$ = 8, 1.5 Hz, H-6), 3.36 (t, 2 H, $J$ = 5.5 Hz, H-10), 2.82 (t, 2 H, $J$ = 5.5 Hz, H-11), 2.47 (s, 6 H, NMe$_2$); $^{13}$C NMR (MeOH-$d_4$, 400 MHz) $\delta_C$ 144.0 (C-1), 143.1 (C-8a), 138.7 (C-3), 135.9 (C-9a), 129.8 (C-4a), 124.0 (C-5), 124.0 (C-6), 123.0 (C-7), 121.5 (C-4b), 115.7 (C-8), 114.5 (C-4), 58.5 (C-11), 44.7 (NMe$_2$), 30.9 (C-10); HREIMS [M + H]$^+$ $m/z$ 318.0596 (calcd for C$_{15}$H$_{17}$$^{79}$BrN$_3$, 318.0606).

**Plakortamine B (2):** yellow oil; UV (MeOH) 214 nm ($\varepsilon$ 32 000); IR (film) 3200 (br), 1620, 1560, 1235 cm$^{-1}$; $^1$H NMR (CDCl$_3$, 300 MHz) $\delta$8.61 (br s, 1 H, -$N$H), 8.48 (d, 1 H, $J$ = 5.5 Hz, H-3), 7.97 (d, 1 H, $J$ = 8 Hz, H-5), 7.84 (d, 1 H, $J$ = 5.5 Hz, H-4), 7.69 (d, 1 H, $J$ = 1.5 Hz, H-8), 7.41 (dd, 1 H, $J$ = 8, 1.5 Hz, H-6), 7.18 (dd, 1 H, $J$ = 17, 11 Hz, H-10), 6.40 (d, 1 H, $J$ = 17 Hz, H-11), 5.72 (d, 1 H, $J$ =

11 Hz, H-11); $^{13}$C NMR (MeOH-$d_4$, 400 MHz) δ141.9 (C-8a), 139.8 (C-1), 137.8

(C-3), 133.9 (C-9a), 131.6 (C-10), 129.4 (C-4a), 122.8 (C-5), 122.6 (C-6), 121.7

(C-7), 119.9 (C-4b), 118.5 (C-11), 114.3 (C-8), 113.8 (C-4); HREIMS [M + H]$^+$

*m/z* 275.0008 (calcd for C$_{13}$H$_{10}$$^{81}$BrN$_2$, 275.0007).

**Plakortamine C (3):** pale yellow oil; UV (MeOH) 243 nm (ε 57 400), 296 nm (ε

29 000); IR (film) 3200 (br), 1620, 1570 cm$^{-1}$; $^1$H NMR (MeOH-$d_4$, 300 MHz)

δ$_H$ 8.14 (d, 2 H, *J* = 5.5 Hz, H-3), 7.96 (d, 2 H, *J* = 8 Hz, H-5), 7.77 (d, 2 H, *J* =

5.5 Hz, H-4), 7.53 (d, 2 H, *J* = 1.5 Hz, H-8), 7.32 (dd, 2 H, *J* = 8, 1.5 Hz, H-6),

3.31 (t, 4 H, *J* = 5.5 Hz, H-10), 3.09 (t, 4 H, *J* = 5.5 Hz, H-11), 2.58 (s, 3 H,

NMe$_2$); $^{13}$C NMR (MeOH-$d_4$, 400 MHz) δ$_C$ 143.9 (C-1,1'), 142.9 (C-8a,8a'),

138.5 (C-3,3'), 135.8 (C-9a,9a'), 129.6 (C-4a,4a'), 124.0 (C-5,5'), 123.9 (C-6,6'),

122.9 (C-7,7'), 121.4 (C-4b,4b'), 115.7 (C-8,8'), 114.3 (C-4,4'), 56.3 (C-11,11'),

41.7 (NMe), 30.4 (C-10,10'); HREIMS [M + H]$^+$ *m/z* 578.0372 (calcd for

C$_{27}$H$_{24}$$^{79}$Br$^{81}$BrN$_5$, 578.0379).

**Plakortamine D (4):** pale yellow oil; [α]$_D$ -2.1° (*c* 0.6, MeOH); UV (MeOH) 243

nm (ε 26 600), 296 nm (ε14 700); IR (film) 3400 (br), 1625, 1570, 1420 cm$^{-1}$; $^1$H

NMR (CDCl$_3$, 300 MHz) δ$_H$ 11.37 (br s, 1 H, -*N*H), 8.29 (d, 1 H, *J* = 5.5 Hz, H-

3), 7.99 (d, 1 H, *J* = 8 Hz, H-5), 7.95 (d, 1 H, *J* = 5.5 Hz, H-4), 7.78 (d, 1 H, *J* =

1.5 Hz, H-8), 7.41 (dd, 1 H, *J* = 8, 1.5 Hz, H-6), 5.90 (dd, 1 H, *J* = 8.5, 7 Hz, H-

10) 3.61 (t, 1 H, *J* = 8 Hz, H-12), 3.08 (m, 1 H, H-11), 2.99 (s, 3 H, NMe), 2.80

(m, 1 H, H-12), 2.53 (m, 1 H, C-11); $^{13}$C NMR (CDCl$_3$, 400 MHz) δ$_C$ 145.3 (C-

1), 141.8 (C-8a), 134.5 (C-3), 132.0 (C-9a), 130.4 (C-4a), 123.6 (C-5), 123.1 (C-7), 122.9 (C-6), 119.9 (C-4b), 115.2 (C-8), 114.5 (C-4), 79.1 (C-10), 58.2 (C-12), 45.0 (NMe), 37.0 (C-11); HREIMS $[M + H]^+$ $m/z$ 332.0385 (calcd for $C_{15}H_{15}{}^{79}BrN_3O$, 332.0399).

**Epiplakinic acid G (5):** colorless oil; $[\alpha]_D$ -17.2° ($c$ 0.3, MeOH); UV (MeOH) 255 nm ($\varepsilon$ 253), 260 nm ($\varepsilon$ 276), 269 nm ($\varepsilon$ 218); IR (film) 3300 (br), 1705, 1450 cm$^{-1}$; $^1$H NMR (CDCl$_3$, 300 MHz) $\delta_H$ 7.24 (t, 2 H, $J$ = 7.5 Hz), 7.18 (m, 3 H), 2.77 (d, 1 H, $J$ = 16 Hz, H-2), 2.73 (d, 1 H, $J$ = 16 Hz, H-2), 2.59 (t, 2 H, $J$ = 8 Hz, H$_2$-17), 2.49 (d, 1 H, $J$ = 13 Hz, H-4), 2.22 (d, 1 H, $J$ = 13 Hz, H-4), 1.46 (s, 3 H, Me-24), 1.33 (s, 3 H, Me-25), 0.95 (d, 3 H, $J$ = 6.5 Hz, Me-26), 0.83 (d, 3 H, $J$ = 7 Hz, Me-27); $^{13}$C NMR (MeOH-$d_4$, 400 MHz) $\delta_C$ 174.3 (C-1), 143.8 (C-18), 129.2 (C-20,22), 129.0 (C-19,23), 126.4 (C-21), 87.8 (C-5), 84.9 (C-3), 58.3 (C-4), 47.9 (C-8), 47.5 (C-6), 45.3 (C-2), 37.9 (C-10), 36.9 (C-17), 32.7 (C-15), 31.1, 31.0, 30.7 (C-9), 30.6, 30.3, 28.1 (C-7), 27.9 (C-16), 24.8 (C-24), 24.1 (C-25), 22.2 (C-26), 20.7 (C-27); ESIMS (+ve) $m/z$ 455 [M + Na]$^+$, (-ve) 431 [M - H]$^-$; HRMALDIMS [M + Na]$^+$ $m/z$ 455.3127 (calcd for C$_{27}$H$_{44}$O$_4$Na, 455.3132).

**Epiplakinic acid H (6):** colorless oil; $[\alpha]_D$ +33° ($c$ 0.07, MeOH); UV (MeOH) 254 nm ($\varepsilon$ 269), 259 nm ($\varepsilon$ 270), 268 nm ($\varepsilon$ 212); IR (film) 3300 (br), 1705, 1455 cm$^{-1}$; $^1$H NMR (MeOH-$d_4$, 300 MHz) $\delta_H$ 7.22 (t, 2 H, $J$ = 7.5 Hz), 7.16 (m, 3 H), 2.76 (d, 1 H, $J$ = 16 Hz, H-2), 2.73 (d, 1 H, $J$ = 16 Hz, H-2), 2.59 (t, 2 H, $J$ = 8 Hz, H$_2$-17), 2.47 (d, 1 H, $J$ = 13 Hz, H-4), 2.22 (d, 1 H, $J$ = 13 Hz, H-4), 1.48 (s, 3 H,

Me-24), 1.37 (s, 3 H, Me-25), 0.91 (d, 3 H, $J$ = 6.5 Hz, Me-26), 0.83 (d, 3 H, $J$ = 7

Hz, Me-27); $^{13}$C NMR (MeOH-$d_4$, 400 MHz) $\delta_C$ 175.2 (C-1), 143.8 (C-18), 129.2

(C-20,22), 129.0 (C-19,23), 126.4 (C-21), 87.9 (C-5), 84.9 (C-3), 58.3 (C-4), 47.7

(C-8), 47.2 (C-6), 46.4 (C-2), 37.8 (C-10), 36.9 (C-17), 32.8 (C-15), 31.2, 31.0,

30.7 (C-9), 30.6, 30.3, 28.2 (C-7), 27.9 (C-16), 24.8 (C-24), 24.4 (C-25), 22.1 (C-

26), 20.7 (C-27); HRMALDIMS [M + Na]$^+$ $m/z$ 455.3128 (calcd for $C_{27}H_{44}O_4Na$,

455.3132).

**(2S\*,4R\*)-2,4-Dimethyl-4-hydroxy-16-phenylhexadecanoic acid 1,4-lactone**

**(7):** colorless oil; [α]$_D$ -7.1° ($c$ 0.13, MeOH); UV (MeOH) 254 nm (ε 196), 261

nm (ε 215) 268 nm (ε 170); IR (film) 1765, 1450 cm$^{-1}$; $^1$H NMR (MeOH-$d_4$, 300

MHz) $\delta_H$ 7.22 (t, 2 H, $J$ = 7.5 Hz), 7,16 (m, 3 H), 2.91 (m, 1 H), 2.58 (t, 2 H, $J$ = 8

Hz), 2.27 (dd, 1 H, $J$ = 12.5, 9 Hz), 1.72 (dd, 1 H, $J$ = 12.5, 11.5 Hz), 1.67 (m, 2

H), 1.59 (m, 2 H), 1.34 (s, 3 H), 1.31-1.28 (m, 18 H), 1.21 (d, 3 H, $J$ = 7 Hz); $^{13}$C

NMR (MeOH-$d_4$, 400 MHz) $\delta_C$ 181.6 (C-1), 143.8 (C-17), 129.2 (C-19,21), 129.0

(C-18,22), 126.4 (C-20), 86.1 (C-4), 42.8 (C-5), 42.5 (C-3), 36.9 (C-16), 36.3 (C-

2), 32.8 (C-14), 31.0, 30.6-30.7 (6C), 30.3 (C-15), 24.9 (C-24), 24.9 (C-6), 15.7

(C-23); HRMALDIMS [M + Na]$^+$ $m/z$ 381.2763 (calcd for $C_{24}H_{38}O_2Na$,

381.2764).

**(2R\*,4R\*)-2,4-Dimethyl-4-hydroxy-16-phenylhexadecanoic acid 1,4-lactone**

**(8):** colorless oil: [α]$_D$ +19.3° ($c$ 0.05, MeOH); UV (MeOH) 252 nm (ε 326), 258

nm (ε 296) 268 nm (ε 235); IR (film) 1765, 1455 cm$^{-1}$; $^1$H NMR (MeOH-$d_4$, 300

MHz) $\delta_H$ 7.22 (t, 2 H, $J$ = 7.5 Hz), 7,16 (m, 3 H), 2.86 (m, 1 H), 2.58 (t, 2 H, $J$ = 8 Hz), 2.43 (dd, 1 H, $J$ = 12.5, 9 Hz), 1.66 (dd, 1 H, $J$ = 12.5, 11.5 Hz), 1.59 (m, 4 H), 1.39 (s, 3 H), 1.31-1.28 (m, 18 H), 1.22 (d, 3 H, $J$ = 7 Hz); $^{13}$C NMR (MeOH-$d_4$, 400 MHz) $\delta_C$ 181.6 (C-1), 143.8 (C-17), 129.2 (C-19,21), 129.0 (C-18,22), 126.4 (C-20), 86.3 (C-4), 42.6 (C-3), 41.1 (C-5), 36.9 (C-16), 36.8 (C-2), 32.8 (C-14), 31.0, 30.6-30.7 (6C), 30.3 (C-15), 27.2 (C-24), 25.3 (C-6), 16.3 (C-23); HRMALDIMS [M + Na]$^+$ $m/z$ 381.2770 (calcd for $C_{24}H_{38}O_2Na$, 381.2764).

## References

1.  Tillequin, F., Michel, S., Seguin, E., *Methods in plant biochemistry. Tryptamine-derived indole alkaloids*, ed. Waterman PG. Vol. 8. 1993, London: Academic Press. 309-371.

2.  El-Rifaie, M. E.-S. (1980). *Peganum harmala*: its use in certain dermatoses. *Int. J. Dermatol.* **19**, 221-222.

3.  Sobhani, A. M., Ebrahimi, S.-A., Mahmoudian, M. (2002). An *in vitro* evaluation of human DNA topoisomerase I inhibition by *Peganum harmala* seeds extract and its β-carboline alkaloids. *J. Pharm. Pharmaceut. Sci.* **5**, 19-23.

4.  Chen, Q., Chao, R., Chen, H., Hou, X., Yan, H., Zhou, S., Peng, W., Xu, A. (2004). Antitumor and neurotoxic effects of novel harmine derivatives and structure-activity relationship analysis. *Int. J. Cancer* **114**, 675–682.

5.  Kanchanapoom, T., Kasai, R., Chumsri, P., Hiraga, Y., Yamasaki, K. (2001). Canthin-6-one and β-carboline alkaloids from *Eurycoma harmandiana*. *Phytochemistry* **56**, 383-386.

6.  Venkatachalam, S. R., Kunjappu, J. T., Nair, C. K. K. (1994). DNA binding studies on deoxytubulosine, an alkaloid from *Alangium lamarckii*. *Indian J. Chem.* **33B**, 809–811.

7.  Rao, K. N., Bhattacharya, R. K., Venkatachalam, S. R. (1998). Thymidylate synthase activity and the cell growth are inhibited by the β-carboline-benzoquinolizidine alkaloid deoxytubulosine. *J. Biochem. Mol. Toxicol.* **12**.

8.  Rao, K. N., Venkatachalam, S. R. (1999). Dihydrofolate reductase and cell growth activity inhibition by the β-carboline-benzoquinolizidine plant alkaloid deoxytubulosine from *Alangium lamarckii*: its potential as an antimicrobial and anticancer agent. *Bioorg. Med. Chem.* **7**, 1105-1110.

9.  Davidson, B. S. (1993). Ascidians: producers of amino acid-derived metabolites. *Chem. Rev.* **93**, 1771-91.

10. Rinehart, K. L., Kobayashi, J., Harbour, G. C., Gilmore, J., Mascal, M., Holt, T. G., Shield, L. S., Lafargue, F. (1987). Eudistomins A-Q, β-carbolines from the antiviral Caribbean tunicate *Eudistoma olivaceum*. *J. Am. Chem. Soc.* **109**, 3378-87.

11.    Tsuda, M., Kobayashi, J. (1997). Structures and biogenesis of manzamines and related alkaloids. *Heterocycles* **46**, 765-794.

12.    Yousaf, M., Rao, K. V., Gul, W., Kelly, M., Franzblau, S. G., Hill, R. T., Hamann, M. T. in *Abs. Pap. 6th Int. Mar. Biotech. Conf.* 2003, S14-13B-13.

13.    Jimenez, C., Quinoa, E., Adamczeski, M., Hunter, L. M., Crews, P. (1991). Novel sponge-derived amino acids. 12. Tryptophan-derived pigments and accompanying sesterterpenes from *Fascaplysinopsis reticulata. J. Org. Chem.* **56**, 3403-10.

14.    Bourguet-Kondracki, M. L., Martin, M. T., Guyot, M. (1996). A new β-carboline alkaloid isolated from the marine sponge *Hyrtios erecta. Tetrahedron Lett.* **37**, 3457-3460.

15.    Jung, M., Kim, H., Lee, K., Park, M. (2003). Naturally occurring peroxides with biological activities. *Mini Rev. Med. Chem.* **3**, 159-165.

16.    Casteel, D. A. (1999). Peroxy natural products. *Nat. Prod. Rep.* **16**, 55-73.

17.    Phillipson, D. W., Rinehart, K. L. (1983). Antifungal peroxide-containing acids from two Caribbean sponges. *J. Am. Chem. Soc.* **105**, 7735-6.

18.    Davidson, B. S. (1991). Cytotoxic five-membered cyclic peroxides from a *Plakortis* sponge. *J. Org. Chem.* **56**, 6722-4.

19.    Horton, P. A., Longley, R. E., Kelly-Borges, M.; McConnell, O. J., Ballas, L. M. (1994). New cytotoxic peroxylactones from the marine sponge, *Plakinastrella onkodes. J. Nat. Prod.* **57**, 1374-81.

20.    Qureshi, A., Salva, J., Harper, M. K., Faulkner, D. J. (1998). New cyclic peroxides from the Philippine sponge *Plakinastrella* sp. *J. Nat. Prod.* **61**, 1539-1542.

21.    Patil, A. D., Freyer, A. J., Bean, M. F., Carte, B. K., Westley, J. W., Johnson, R. K. (1996). The plakortones, novel bicyclic lactones from the sponge *Plakortis halichondrioides*: activators of cardiac SR-Ca2+-pumping ATPase. *Tetrahedron* **52**, 377-94.

22.    Chen, Y., Killday, K. B., McCarthy, P. J., Schimoler, R., Chilson, K., Selitrennikoff, C., Pomponi, S. A., Wright, A. E. (2001). Three new peroxides from the sponge *Plakinastrella* species. *J. Nat. Prod.* **64**, 262-264.

23. Rudi, A., Afanii, R., Gravalos, L. G., Aknin, M., Gaydou, E., Vacelet, J., Kashman, Y. (2003). Three new cyclic peroxides from the marine sponge *Plakortis* aff *simplex*. *J. Nat. Prod.* **66**, 682-685.

24. Cox, E. D., Cook, J. M. (1995). The Pictet-Spengler condensation: a new direction for an old reaction. *Chem. Rev.* **95**, 1797-842.

# CHAPTER 3

## ERYLOSIDES A, K, AND L: BIOACTIVE STEROIDAL GLYCOSIDES FROM THE MARINE SPONGE *ERYLUS LENDENFELDI*[*]

An assay was used to identify three compounds, erylosides A, K, and L (**1**-**3**), that were selectively toxic to a *Δrad50* yeast strain deficient in DNA double-strand break repair. The structures were established based mainly on 1D and 2D NMR data, and the absolute stereochemistry of erylosides A and K were determined by chemical means. The biological activity of these compounds was further investigated.

This work originally appeared in *Tetrahedron* **2005**, 61, 1199-1206 with co-authors Susan L. Forsburg and D. John Faulkner. It has been rewritten here for continuity and so that my contribution be clarified.

## Introduction

The modern approach to finding new anticancer drugs relies on the discovery of compounds that target the subtle molecular differences between malignant and healthy human cells.[1] In recent years, the integration of genetics and drug discovery has resulted in the engineering of a wide array of molecular

---

alterations in model organisms that can be used to screen for selectively bioactive small molecules. In particular, budding yeast (*Saccharomyces cerevisiae*) have proven to be an excellent model for discovering novel anticancer drugs.[2] Budding yeast is a simple, single-celled eukaryotic organism with a completely sequenced and comprehensively characterized genome. The advantages of using yeast as a model system include the high degree of conservation of DNA-repair pathways with higher eukaryotes, the ease of handling relative to human cell lines, and the availability of advanced molecular genetic techniques for subsequent analysis. The use of matched pairs of yeast strains (i.e. one strain with a defined genetic alteration and the other with the corresponding wild-type gene) has facilitated the identification of selectively toxic compounds whose mechanisms of action can take advantage of any differences between the strains.[3] A cell line containing a mutation in a gene whose human homolog is implicated in cancer (e.g. DNA-damage repair, cell-division checkpoint) can therefore be used as a model of a human cancer cell. However, unlike cancer cell lines that contain numerous genetic instabilities and complexities, yeast strains can be designed with single mutations, providing a simpler model for the identification of compounds that target specific biochemical pathways.

In 2000, Simon *et al.* developed a panel of isogenic yeast strains, each defective in a different DNA repair or cell cycle checkpoint function, and tested the panel for sensitivity to FDA-approved anticancer agents.[4] A wide range of
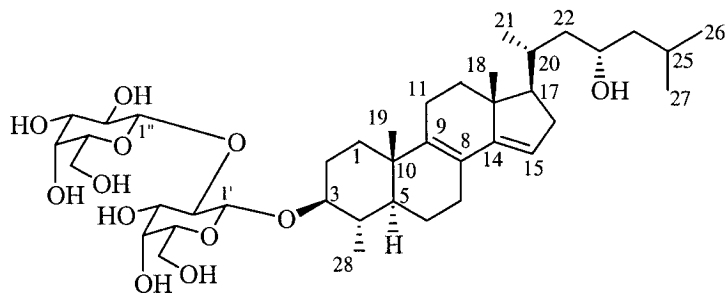
**1**
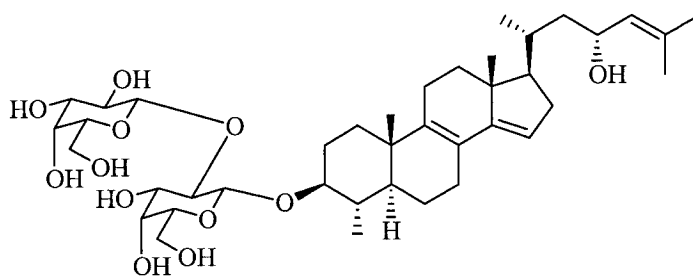


**2**
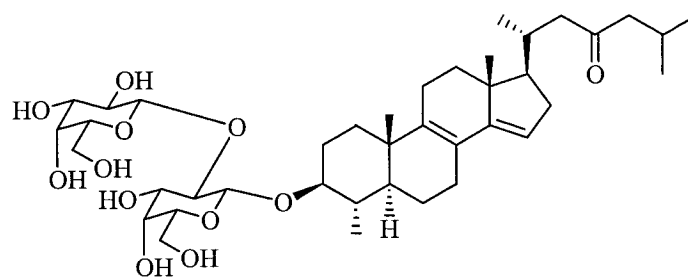


**3**

toxicity profiles were observed for the drugs, reflecting differences in their mechanisms of action. For example, alkylating agents such as cisplatin (**4**) and nitrogen mustard (**5**) were specifically toxic to strains defective for the Rad6/Rad18-controlled pathway of DNA damage tolerance during S-phase, exhibiting 10-fold higher toxicity in *Δrad6* and *Δrad18* strains than other sensitive strains. Cell lines deficient in nucleotide excision repair (*Δrad1* and *Δrad14*), recombinational repair (*Δrad50*, *Δrad51*, and *Δrad52*), and error-prone damage tolerance (*Δrev1*, *Δrev3*, and *Δrad6*) were also somewhat sensitive, reflecting the roles of such pathways in the repair of DNA cross-links caused by these alkylating agents. Cytarabine monophosphate (**6**), which is known to inhibit DNA synthesis,[5] exhibited selective toxicity against a *Δsgs1* strain. The *Δsgs1* yeast mutant and the homologous Bloom's and Werner's syndrome defects in humans cause hyperrecombination,[6] and sensitivity of the *Δsgs1* strain to **6** suggested an effect on recombination that required the Sgs1 protein for tolerance.

Several topoisomerase poisons exhibited selectivity for the double-strand break (DSB) repair-deficient mutants *Δrad50*, *Δrad51*, and *Δrad52*. Topoisomerase poisons stabilize the covalent complex of topoisomerase and DNA ends during DNA relaxation and lead to single-strand breaks and DSBs for topo I and topo II poisons, respectively.[7] The single-strand breaks caused by topo I poisons are converted to DSBs during DNA replication.[8] Rad50, Rad51, and Rad52 are needed for repair of double-strand DNA breaks,[9] and defects in both

human Rad50 and human topoisomerase enzymes have been associated with many types of cancer.[10-13] The topo I poison camptothecin (**7**), along with the topo II poisons mitoxantrone (**8**) and idarubicin (**9**), were selectively toxic to DSB repair mutants, providing a direct link between DSB repair defects and vulnerability to topoisomerase inhibition in yeast.

In addition to providing robust information regarding the mechanism of action for known anticancer agents, a panel of budding yeast mutants can be used to discover novel bioactive compounds. Dunstan *et al.* modified the aforementioned assay to identify new compounds that were selectively toxic to DSB repair mutants.[3] After screening 85,000 pure compounds, 126 were identified to be selectively toxic to DSB repair mutants, 39 of which were structurally unrelated to known topoisomerase poisons. Compounds identified in the screen were further analyzed by use of yeast and vertebrate cell-based and *in vitro* assays to distinguish between topo I and II poisons. Among these compounds, two novel topo II poisons were identified that were equipotent with the drug etoposide (**10**), and one compound was shown to directly bind DNA and induce strand breaks. The use of yeast strains with defined genetic alterations was thereby validated as a powerful tool for the discovery of novel, bioactive compounds that selectively target a biomedically relevant pathway.

In an attempt to identify compounds from marine organisms that targeted cancer-related pathways in yeast, I initiated a collaboration with Susan Forsburg's
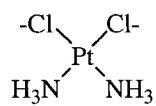
**4**
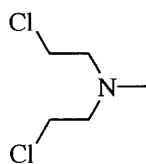
**5**
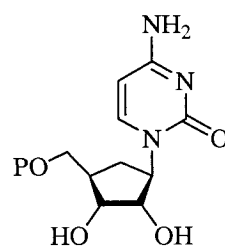
**6**
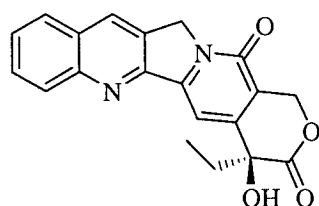
**7**
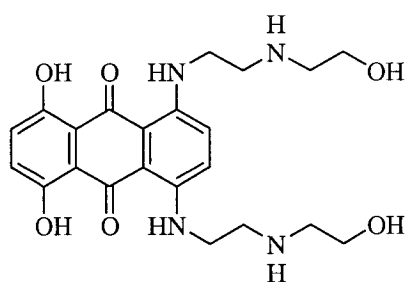
**8**
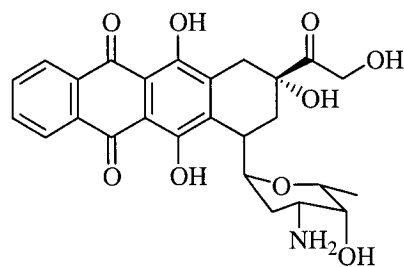
**9**
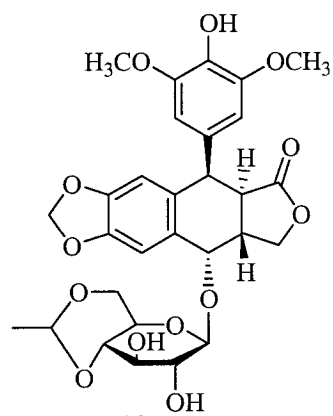
**10**

laboratory at the Salk Institute for Biological Studies. Dr. Forsburg's research is focused primarily on yeast cell biology and cell-cycle genetics, and her group provided an ideal environment in which to adapt and implement the yeast assay developed by Simon et al.[4] Our goal was to find new marine natural products that selectively targeted yeast strains deficient in DNA damage detection or damage repair pathways. Crude extracts from the Faulkner library of marine invertebrates were screened, and several extracts exhibited selective activity profiles against a panel a yeast mutants. The methanol extract from the Red Sea sponge *Erylus lendenfeldi* Sollas,[14] 1888 (Demospongiae, Astrophorida, Geodiidae) targeted a *Δrad50* strain deficient in DSB repair. The known compound, eryloside A (**1**), along with two new compounds, erylosides K (**2**) and L (**3**), were subsequently purified from the extract and their structures were determined by spectroscopic and chemical means.

The erylosides belong to a class of compounds collectively known as steroidal glycosides. Steroidal and triterpenoid oligoglycosides are the predominant metabolites of starfishes and sea-cucumbers, respectively.[15] More recently, glycosides have been isolated from some sponges. The erylosides are a series of unusual and bioactive steroidal glycosides isolated from sponges of the genus *Erylus*. Eryloside A (**1**), a 4-methyl steroidal diglycoside, was originally reported to possess anticancer and antifungal activity.[16] Surprisingly, this original

report also mentions the presence of an additional analog, eryloside B, but provides no structural information pertaining to this molecule. Erylosides C (**11**) and D (**12**),which are composed of three and four D-galactopyranose units respectively, were reported with no biological acitivty.[17] Eryloside E (**13**), however, displayed immunosuppressive activity without the presence of toxic side-affects.[18] Compounds **11-13** each possessed a rare penasterol nucleus with a $t$-butyl substituent on its side-chain. Eryloside F (**14**) was shown to possess potent thrombin receptor antagonist activity,[19] and erylosides G-J (**15-18**) all exhibited moderate cytotoxicity against a human leukemia cell line.[20] An analysis of the structural elucidation and bioactivity of erylosides A, K, and L is presented below.

## Isolation and structural elucidation

The marine sponge *Erylus lendenfeldi* was collected in February, 2000 in the Red Sea just north of Hurghada. Bioassay-guided fractionation led to the isolation of the known steroidal glycoside, eryloside A (**1**, 720 mg, 0.4% dry weight), along with two new steroidal glycosides, eryloside K (**2**, 145 mg, 0.08% dry weight), and eryloside L (**3**, 90 mg, 0.05% dry weight). The molecular formula of eryloside A (**1**) was determined to be $C_{40}H_{66}O_{12}$ by high resolution MALDI-MS ($m/z$ 761.4472 ([M+Na]$^+$). The spectral properties of **1** (Table 3.1) were identical with the reported values for eryloside A,[16] a 3β-$O$-{β-D-
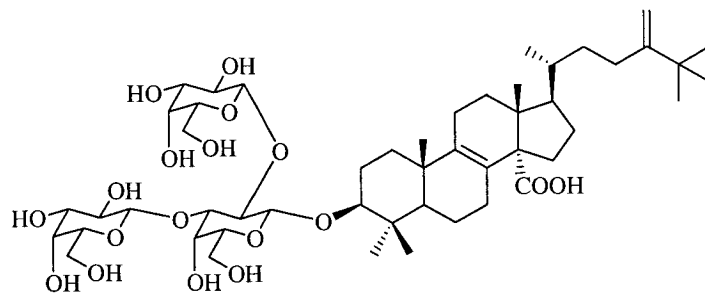
**11**
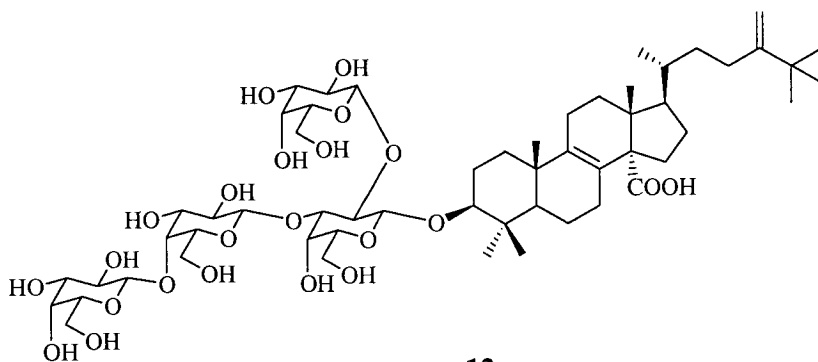
**12**
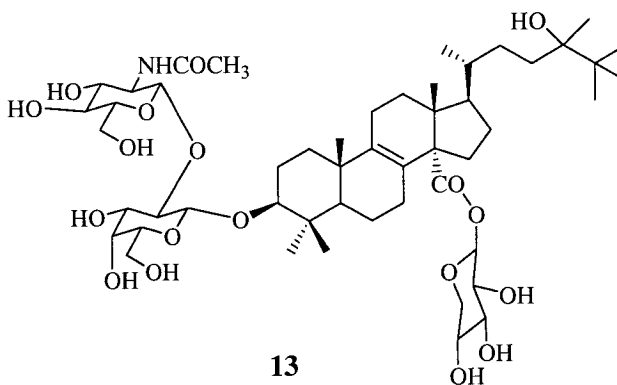
**13**
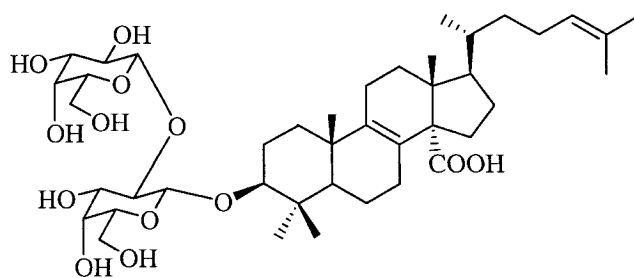
**14**
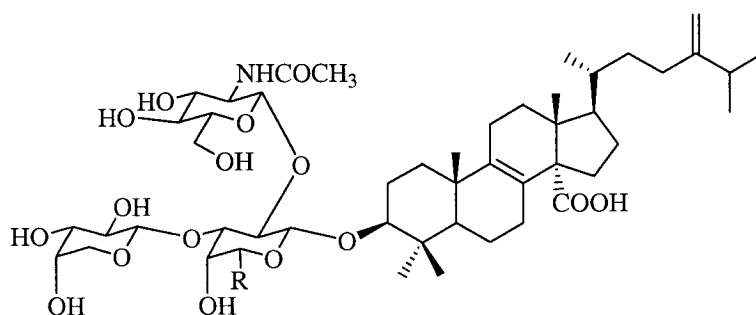


**15** R = CH₂OH
**16** R = H
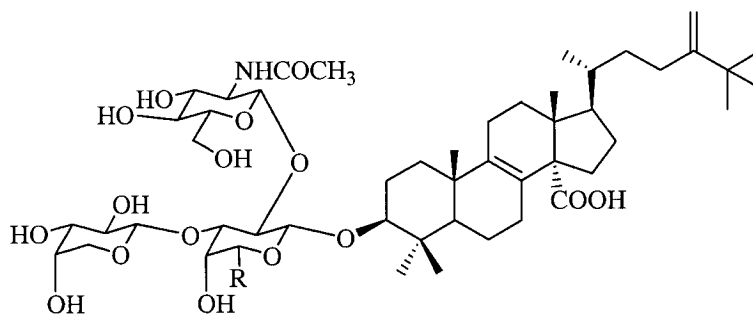


**17** R = CH₂OH
**18** R = H

**Table 3.1** $^{13}$C (100 MHz, MeOH-$d_4$) and $^1$H (300 MHz, MeOH-$d_4$) NMR data for compounds **1** and **3**.

| C# | $^{13}$C NMR in ppm | | $^1$H NMR in ppm, mult. ($J$ in Hz) | |
|---|---|---|---|---|
| | **1** | **3** | **1** | **3** |
| 1 | 36.6 | 36.2 | 1.24 m | 1.25 m |
| | | | 1.87 m | 1.89 m |
| 2 | 31.0 | 30.5 | 1.61 m | 1.62 m |
| | | | 2.13 m | 2.13 m |
| 3 | 87.9 | 87.4 | 3.16 dt (10.6, 5.2) | 3.17 dt (10.6, 5.1) |
| 4 | 39.1 | 38.7 | 1.51 dd (11.4, 10.6) | 1.51 dd (11.0, 10.8) |
| 5 | 49.1 | 48.7 | 1.07 ddd (12.2, 11.4, 2.4) | 1.08 ddd (12.0, 10.8, 2.4) |
| 6 | 21.9 | 21.5 | 1.30 m | 1.31 m |
| | | | 1.85 m | 1.88 m |
| 7 | 28.1 | 27.6 | 2.13 m | 2.13 m |
| | | | 2.25 m | 2.25 m |
| 8 | 124.1 | 123.6 | | |
| 9 | 141.6 | 141.5 | | |
| 10 | 38.0 | 37.6 | | |
| 11 | 22.9 | 22.5 | 2.21 m | 2.23 m |
| 12 | 38.5 | 38.0 | 1.37 m | 1.38 m |
| | | | 2.05 m | 2.02 m |
| 13 | 46.3 | 46.2 | | |
| 14 | 152.1 | 152.2 | | |
| 15 | 118.2 | 117.4 | 5.34 s | 5.34 s |
| 16 | 37.1 | 36.7 | 2.07 m | 2.07 m |
| | | | 2.34 m | 2.30 m |
| 17 | 59.4 | 58.1 | 1.48 m | 1.55 m |
| 18 | 16.3 | 15.8 | 0.84 s | 0.86 s |
| 19 | 19.9 | 19.4 | 1.02 s | 1.04 s |
| 20 | 31.9 | 31.7 | 1.94 m | 2.22 m |
| 21 | 19.5 | 20.2 | 0.97 d (6.6) | 0.94 d (5.6) |
| 22 | 45.6 | 50.9 | 1.01 m | 2.21 m |
| | | | 1.47 m | 2.49 m |
| 23 | 67.5 | 213.3 | 3.75 m | |
| 24 | 49.3 | 53.0 | 1.15 m | 2.32 m |
| | | | 1.37 m | 2.29 m |
| 25 | 25.9 | 25.3 | 1.75 m | 2.08 m |
| 26 | 23.9 | 22.5 | 0.90 d (6.4) | 0.90 d (6.4) |
| 27 | 22.7 | 22.6 | 0.92 d (6.2) | 0.91 d (6.4) |
| 28 | 16.0 | 15.6 | 1.08 d (6.4) | 1.10 d (6.4) |
| 1' | 104.8 | 104.4 | 4.43 d (8.0) | 4.45 d (7.6) |
| 2' | 80.7 | 80.2 | 3.79 m | 3.83 m |
| 3' | 75.3 | 74.8 | 3.67 m | 3.67 m |
| 4' | 70.1 | 69.8 | 3.85 m | 3.86 m |
| 5' | 76.2 | 75.9 | 3.49 m | 3.50 m |
| 6' | 62.3 | 62.2 | 3.71 | 3.71 m |
| 1" | 105.9 | 105.4 | 4.57 d (7.4) | 4.57 d (7.6) |
| 2" | 73.2 | 72.1 | 3.62 m | 3.64 m |
| 3" | 74.8 | 74.4 | 3.50 m | 3.51 m |
| 4" | 70.1 | 69.8 | 3.85 m | 3.82 m |
| 5" | 77.0 | 76.6 | 3.52 m | 3.54 m |
| 6" | 62.2 | 62.3 | 3.70 m | 3.72 m |

galactopyranosyl-(1→2)-β-D-galactopyranosyl}-23β-hydroxy-4α-methyl-5α-

cholesta-8,14-diene.

The absolute configuration of eryloside A, which had never been fully

characterized, was determined using the modified Mosher's method.[21]

Compound 1 was hydrolyzed with HCl to afford the aglycon (19), which was

converted to the (R)- and (S)-MTPA diesters (20a,b). Interpretation of Δδ values

(Figure 3.1) allowed the absolute configuration of C-3 and C-23 to be assigned as

3S and 23S, respectively. This is in agreement with other sponge-derived

steroidal glycosides for which the absolute configurations have been

determined,[22, 23] as well as cholesterol and ergosterol.[21]
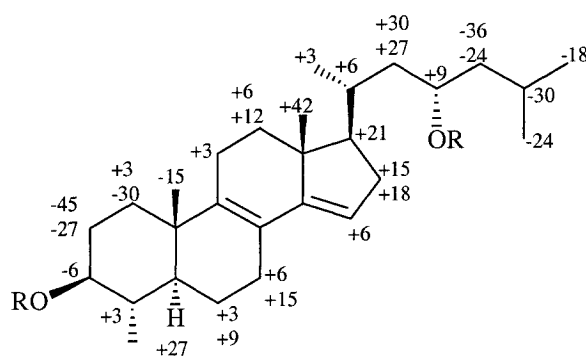


19:  R=H
20a: R=(R)-MTPA
20b: R=(S)-MTPA

**Figure 3.1** Distribution of Δδ_{S-R} values (Hz) for the MTPA esters of **19**.

Eryloside K (2) had the molecular formula of $C_{40}H_{64}O_{12}$, which was determined by high resolution MALDI-MS ($m/z$ 759.4320; [M+Na]$^+$) and analysis of $^{13}C$ NMR data. Careful analysis of the $^{13}C$ NMR and multiplicity-edited HSQC spectra showed that 2 contained six methyl, ten methylene, eighteen methine, and six quaternary carbons (Table 3.2). Chemical shifts indicated that two of the methylene and ten of the methine carbons were associated with two sugar units, and that the remaining twenty-eight carbons belonged to the steroidal portion. Four quaternary and two methine carbons were associated with three double bonds ($\delta_C$ 124.1, 141.6, 152.1, 117.8, 130.2, 133.3), while two of the remaining steroid methines were oxygenated ($\delta_C$ 87.4, 66.3). A major portion of the tetracyclic backbone was assembled through interpretations of HMBC correlations from two methyl singlets ($\delta_H$ 0.86, 1.04), a methyl doublet ($\delta_H$ 1.10) and an olefinic methine ($\delta_H$ 5.34) to ring junction carbons (Me-18 to C-14; Me-19 to C-5, C-9; Me-28 to C-5; H-15 to C-8, C-13). Additional HMBC correlations from the methyl signals established all carbons two and three bonds removed from the methyls. Analysis of the COSY and TOCSY data allowed for assignment of the C-1/C-2/C-3/C-4/C-28/C-5/C-6/C-7, C-11/C-12, and C-15/C-16/C-17 spin systems.

The UV spectrum for 2 suggested the presence of a chromophore derived from a conjugated diene system ($\lambda_{max}$ 249 nm). Whereas one double bond ($\delta_C$ 130.2, 133.3) was shown by COSY and HMBC experiments to be on the side-

**Table 3.2** $^{13}$C (100 MHz, MeOH-$d_4$), $^1$H (300 MHz, MeOH-$d_4$), and HMBC (300 MHz, MeOH-$d_4$) NMR data for compound **2**.

| C# | $^{13}$C NMR in ppm | | $^1$H NMR in ppm, mult. ($J$ in Hz) | HMBC |
|---|---|---|---|---|
| 1 | 36.3 | CH$_2$ | 1.28 m | C-10, C-19 |
|  |  | CH$_2$ | 1.87 m | C-10, C-19 |
| 2 | 30.6 | CH$_2$ | 1.62 m |  |
|  |  | CH$_2$ | 2.14 m |  |
| 3 | 87.4 | CH | 3.16 dt (10.7, 5.1) | C-4, C-28, C-1' |
| 4 | 38.8 | CH | 1.51 dd (10.8, 11.2) | C-3, C-5, C-28 |
| 5 | 48.7 | CH | 1.07 ddd (12.2, 11.4, 2.4) |  |
| 6 | 21.6 | CH$_2$ | 1.30 m | C-5, C-7 |
|  |  | CH$_2$ | 1.86 m | C-7, C-8 |
| 7 | 27.7 | CH$_2$ | 2.12 m | C-5, C-8, C-9 |
|  |  | CH$_2$ | 2.25 m | C-8, C-9 |
| 8 | 124.1 | C |  |  |
| 9 | 141.6 | C |  |  |
| 10 | 37.8 | C |  |  |
| 11 | 22.6 | CH$_2$ | 2.21 m | C-13 |
| 12 | 38.2 | CH$_2$ | 1.36 m | C-11, C-13, C-17, C-18 |
|  |  | CH$_2$ | 2.06 m | C-11, C-13, C-18 |
| 13 | 46.3 | C |  |  |
| 14 | 152.1 | C |  |  |
| 15 | 117.8 | CH | 5.34 s | C-8, C-13, C-16, C-17 |
| 16 | 36.7 | CH$_2$ | 2.11 m | C-14, C-15, C-17, C-20 |
|  |  | CH$_2$ | 2.36 m | C-13, C-14, C-15, C-17 |
| 17 | 59.0 | CH | 1.46 m | C-12, C-13, C-16, C-18, C-20 |
| 18 | 15.9 | CH$_3$ | 0.86 s | C-12, C-13, C-14, C-17 |
| 19 | 19.2 | CH$_3$ | 1.04 s | C-1, C-5, C-9, C-10 |
| 20 | 31.6 | CH | 1.87 m |  |
| 21 | 19.2 | CH$_3$ | 1.02 d (6.8) | C-17, C-20, C-22 |
| 22 | 45.0 | CH$_2$ | 1.00 m |  |
|  |  | CH$_2$ | 1.66 m | C-23 |
| 23 | 66.3 | CH | 4.42 m |  |
| 24 | 130.2 | CH | 5.17 dt (8.4, 1.2) | C-22, C-26, C-27 |
| 25 | 133.3 | C |  |  |
| 26 | 25.6 | CH$_3$ | 1.70 d (1.2) | C-24, C-25, C-27 |
| 27 | 17.8 | CH$_3$ | 1.67 d (1.2) | C-26 |
| 28 | 15.7 | CH$_3$ | 1.10 d (6.4) | C-3, C-4, C-5 |
| 1' | 104.5 | CH | 4.45 d (8.0) | C-3, C-2', C-3', C-5', C-1" |
| 2' | 80.2 | CH | 3.81 m | C-1', C-1" |
| 3' | 74.9 | CH | 3.65 m | C-2' |
| 4' | 69.8 | CH | 3.85 m | C-2' |
| 5' | 76.1 | CH | 3.50 m | C-1', C-3', C-4', C-6' |
| 6' | 62.2 | CH$_2$ | 3.71 m | C-4' |
| 1" | 105.9 | CH | 4.58 d (7.6) | C-2', C-2", C-3" |
| 2" | 72.8 | CH | 3.62 m | C-1", C-3" |
| 3" | 74.5 | CH | 3.49 m | C-1" |
| 4" | 69.8 | CH | 3.85 m | C-2", C-3", C-6" |
| 5" | 76.8 | CH | 3.53 m | C-2", C-4", C-6" |
| 6" | 62.3 | CH$_2$ | 3.72 m | C-4", C-5" |

chain of the steroid, the remaining diene appeared to be within the tetracyclic ring system. Since three of the four olefinic carbons were quaternary, only two locations for a conjugated system were possible: $\Delta^{8,14}$ and $\Delta^{9(11),8(14)}$. Comparison with $^{13}$C NMR values for 5$\alpha$-cholesta-8,14-dien-3$\beta$-ol[24] and 3$\beta$-hydroxy-5$\alpha$-cholesta-8(14),9(11)-dien-15-one[25] allowed the elimination of the $\Delta^{9(11),8(14)}$ system and established the 8,14 diene as the correct location.

A comparison of the HSQC spectra for **2** and **1** suggested differences in their side-chain substituents (Figure 3.2). HMBC correlations from H-17 ($\delta_H$ 1.46) to C-20 ($\delta_C$ 31.6) established attachment of the side-chain at C-17. An HMBC correlation from Me-21 ($\delta_H$ 1.02) to C-22 ($\delta_C$ 45.0), along with COSY correlations between H$_2$-22 ($\delta_C$ 1.00, 1.66), H-23 ($\delta_H$ 4.42) and H-24 ($\delta_H$ 5.17), firmly established the configuration of the side-chain, including the C-23 allylic alcohol and the C-24/C25 alkene. The side-chain methyl doublets at $\delta$ 1.70 and 1.67 were assigned to the vinyl methyl groups at C-26 and C-27 respectively, on the basis of HMBC correlations to the fully substituted olefinic carbon at C-25 ($\delta_C$ 133.3) and the olefinic methine at C-24 ($\delta_C$ 130.2). Analysis of the $^{13}$C NMR data further supported the presence of a double bond in **2** that was not present in **1** (Figure 3.3).

The identity and arrangement of the glycon moiety was established by a combination of 1D and 2D NMR experiments. The $^{13}$C NMR shifts of the anomeric methine carbons ($\delta_C$ 104.5, 105.9) suggested that both sugars were

(a)



(b)



(c)
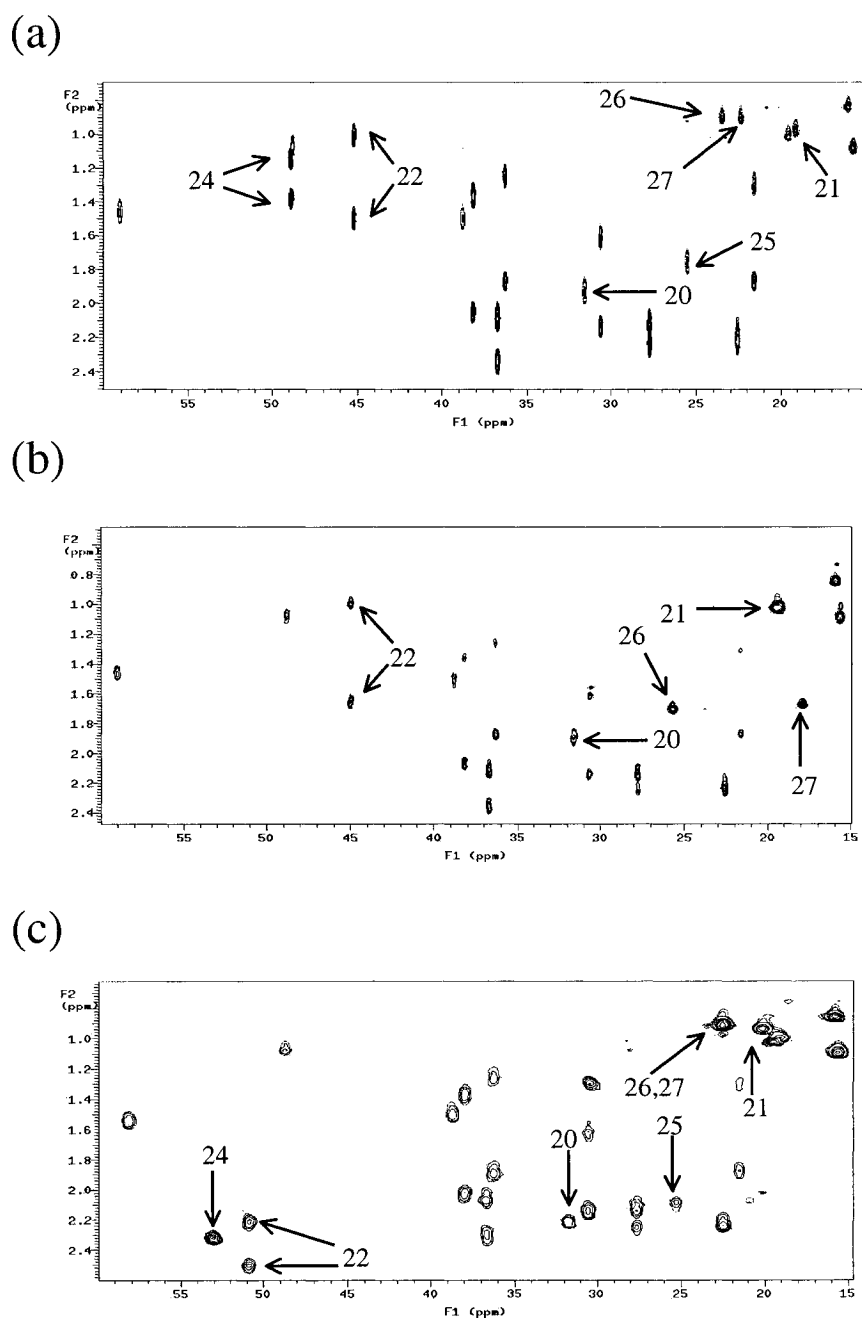


**Figure 3.2** Enlargement of the upfield region of the HSQC spectra for compounds (a) **1**, (b) **2**, and (c) **3**. Direct proton-carbon coupling can be used to differentiate between these related analogs. Numbers and arrows indicate chemical shifts of side-chain protons. Note that other (non-side chain) shifts do not change between compounds.
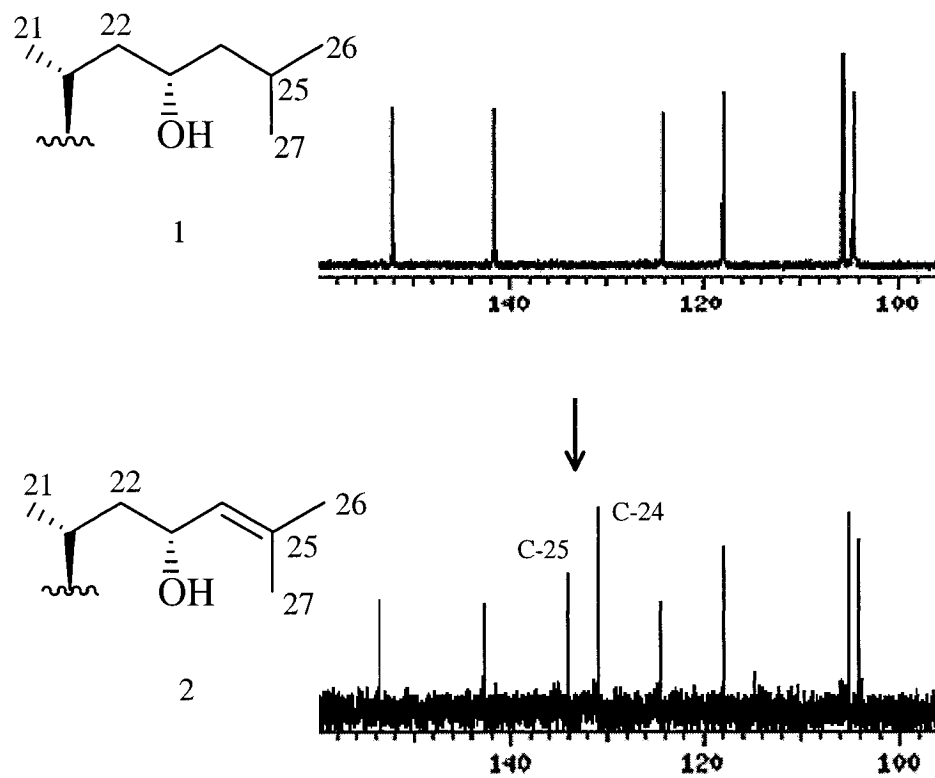
**Figure 3.3** Comparison of the downfield region of $^{13}$C NMR spectra for **1** (top) and **2** (bottom). Arrow indicates the appearance two signals due to the presence of the side-chain olefin in **2**. Truncated portion of the molecules shown for clarity.

connected through β-glycosidic linkages.[26] An HMBC correlation between H-3α

($\delta_H$ 3.16) and C-1'($\delta_C$ 104.5) established the location of the glycosidic linkage at

C-3, and a correlation from H-2'to C-1"defined the linkage between the two

sugar units. This latter finding was supported by an observed NOE between H-2'

($\delta_H$ 3.81) and H-1"($\delta_H$ 4.58).    Comparison of the COSY data and proton $J$-

values with the literature[16] established both sugars as β-galactopyranoside units.

The relative stereochemistry of the steroidal portion of **2** was assigned on

the basis of NOE enhancements (Figure 3.4) and $^1$H-$^1$H coupling constants.

Observed 1,3-diaxial NOE correlations between Me-19, H-2β ($\delta_H$ 1.62), H-4β ($\delta_H$

1.51), and H-6β ($\delta_H$ 1.86) established the chair conformation and the *trans*-ring

fusion of the A and B rings, as well as the axial orientation of Me-19 and the $10S^*$

stereochemistry for C-10. The 4α-methyl configuration was determined by a large

diaxial coupling ($J$ = 10.7) between H-3α ($\delta_H$ 3.16) and H-4β ($\delta_H$ 1.51). Since the

H-5 $^1$H NMR signal was obscured by the Me-28 doublet ($\delta_H$ 1.10), a 1D TOCSY

experiment was used to determine the 11.2-Hz diaxial coupling constant between

H-4β and H-5 ($\delta_H$ 1.07). This established the α position for H-5, as well as the $4S^*$

and $5R^*$ stereochemistries at C-4 and C-5. It was not possible to distinguish the $H_2$-

11 methylene signals ($\delta_H$ 2.21) by $^1$H NMR, making it difficult to determine the

orientation of Me-18. However, the axial orientation of Me-18 was assignable

based on NOE enhancements from Me-18 to both Me-21 ($\delta_H$ 1.02) and H-20
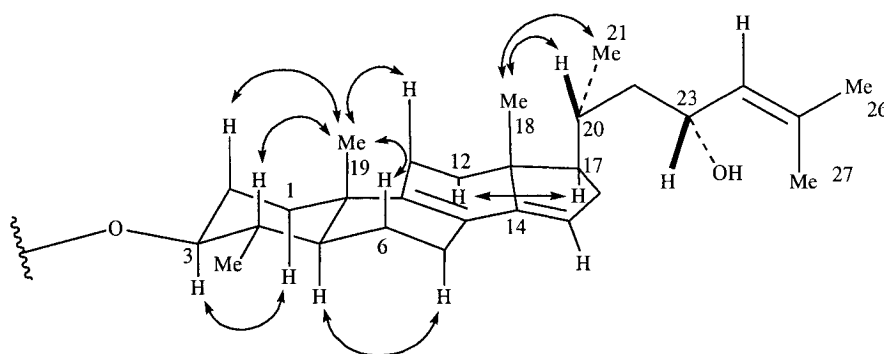
**Figure 3.4** NOE correlations for the steroidal portion of **2**.

($\delta_H$ 1.87). In addition, a long-range COSY correlation between Me-18 and H-12$\alpha$

suggested that both groups were axial. Finally, the $\beta$-orientation for the side-

chain could be assigned based on an NOE between H-12$\alpha$ ($\delta_H$ 1.36) and H-17 ($\delta_H$

1.46). The relative stereochemistries at C-13 and C-17 were thus established as

13$R^*$ and 17$R^*$. Eryloside K is a 3$\beta$-$O$-{$\beta$-D-galactopyranosyl-(1→2)-$\beta$-D-

galactopyranosyl}-23$\beta$-hydroxy-4$\alpha$-methyl-5$\alpha$-cholesta-8,14,24-triene.

Eryloside L (**3**) had a molecular formula of $C_{40}H_{64}O_{12}$, which was

determined by high-resolution MALDI-MS ($m/z$ 759.4283; $C_{40}H_{64}O_{12}$ Na) and by

interpretation of the ^{13}C NMR data. The spectral data of **3** were very similar to

those of **1** and **2**. Careful examination of the $^1$H and $^{13}$C NMR data (Table 3.1)

revealed that both the disaccharide chain and the tetracyclic backbone were

conserved in **3**, but an analysis of the HSQC spectrum suggested an alteration in

the alkyl side-chain (Figure 3.2). Unlike **1** and **2**, **3** lacked a side-chain hydroxyl

group. The presence of a strongly deshielded $^{13}$C signal ($\delta_C$ 213.3), combined

with an IR band at 1705 cm$^{-1}$ and a downfield alpha methylene signal ($\delta_H$ 2.32),

suggested the presence of a side-chain ketone. HMBC correlations from the

carbonyl carbon to H$_2$-22 and H$_2$-24 established the location of the ketone at C-

23. Thus, **3** has been assigned as 3β-*O*-{β-ᴅ-galactopyranosyl-(1→2)-β-ᴅ-

galactopyranosyl}-4α-methyl-5α-cholesta-8,14-dien-23-one.

To establish the absolute configuration for eryloside K, I attempted to

obtain the aglycon of **2** via acid hydrolysis. Not surprisingly, the allylic alcohol

readily dehydrated upon exposure to HCl or milder acids. To circumvent this

problem, I decided to reduce the side-chain alkene in **2** and compare the

properties of the resulting product to the product of **1** when exposed to the same

conditions. Rhodium was chosen as the catalyst since it is known to minimize

hydrogenolysis of allylic alchohols.[27] Hydrogenation of both **1** and **2** in the

presence of 5% rhodium catalyst yielded compound **21** (Figure 3.5), in which the

C-24/25 alkene (**2**) and the C-14/15 alkene (**1** and **2**) were reduced, while the

more highly substituted C-8/9 alkene remained intact. The resulting products

exhibited identical $^1$H NMR spectra, optical rotations, and HPLC retention times

(Figure 3.6). Eryloside K must therefore have the same absolute configuration as 1.[28] Eryloside L also has the same absolute stereochemistry as 1 and 2 based on similarities in optical rotation and biogenetic reasoning.

## Biological Activity

Glycosylated marine natural products tend to exhibit potent and/or selective bioactivity.[29] The erylosides have been reported with anticancer, antifungal, and anticoagulative activity,[16-20] and erylosides A, K, and L all exhibited selective cytotoxicity against a Δrad50 yeast strain deficient in DSB repair. Modifications in the side-chain between 1, 2, and 3 corresponded to noticeable differences in both the potency and selectivity of the erylosides against the yeast strains (Table 3.3). The aglycon (19) did not exhibit significant activity against any of the yeast strains, suggesting that glycosylation of these molecules is integral to their bioactivity.

In order to determine if the erylosides caused cell-cycle arrest in yeast, wildtype cells were exposed to eryloside A (1) and monitored by microscopy. *S. cerevisiae* divides by budding, and the cell-cycle stage of an actively dividing cell can be determined by examining the size of the bud and the number of DNA copies. Cells treated with a sublethal dose of 1 (8.5 μM) were fixed and DAPI stained every hour. When DAPI binds to DNA, its fluorescence is strongly enhanced, allowing me to assess the number of DNA copies in each cell by
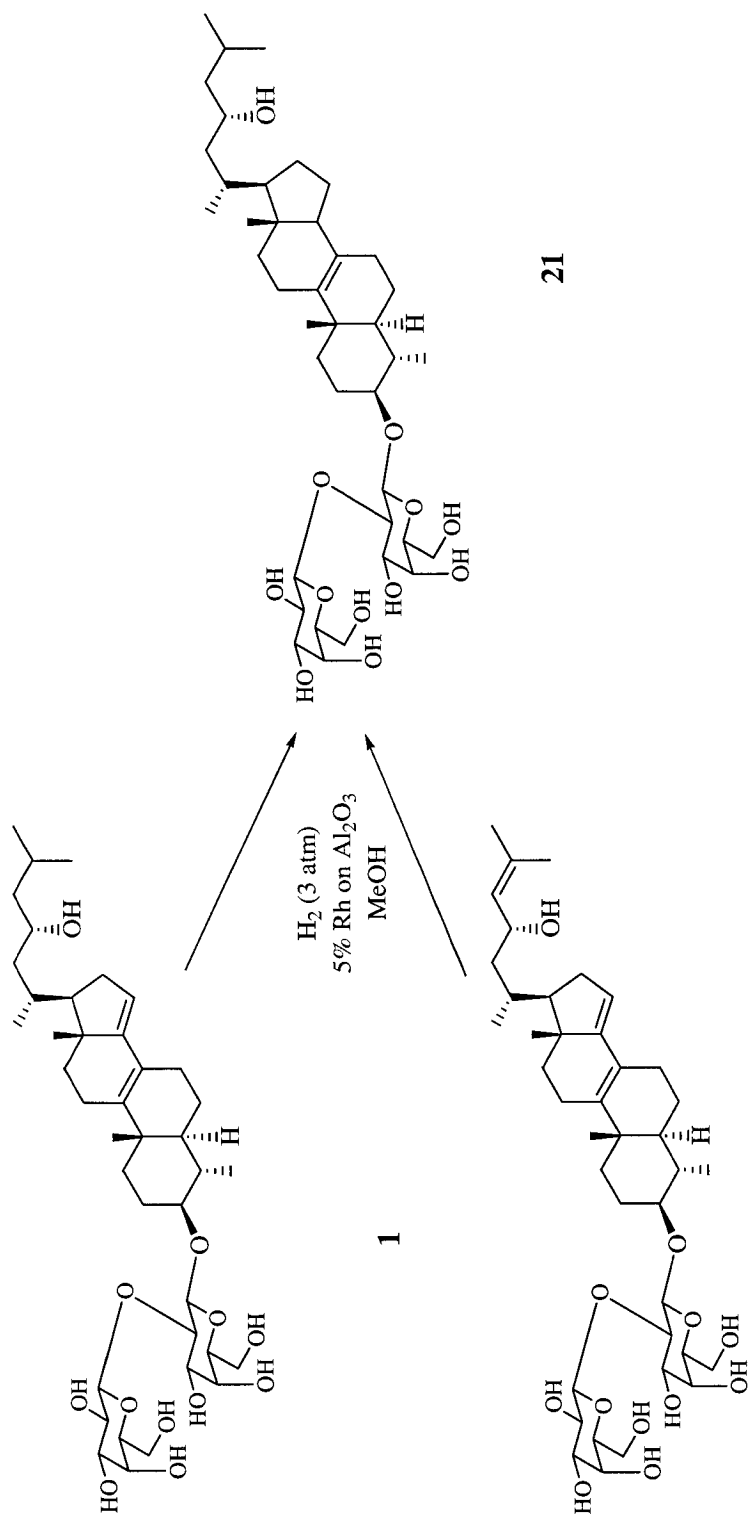
**Figure 3.5** Catalytic hydrogenation of **1** and **2**.
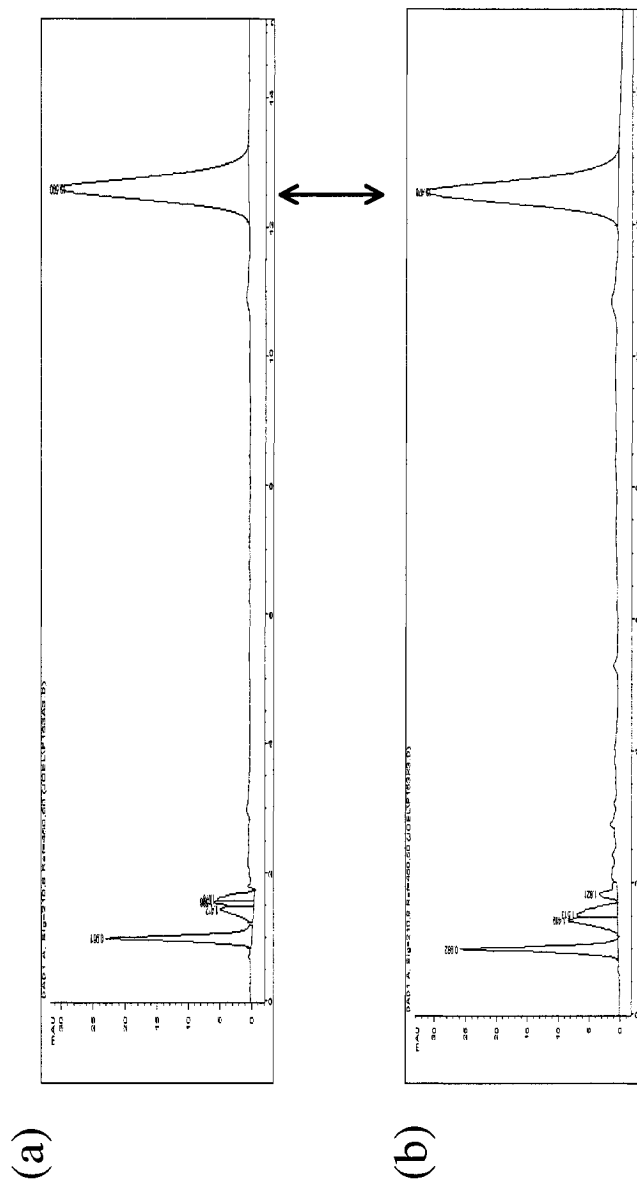
**Figure 3.6** HPLC chromatograms of hydrogenation products from (a) **1** and (b) **2**. Double-sided arrow indicates peaks associated with compound **21**. Phenomenex Luna C18 column; 46% $CH_3CN$; detected at 254 nm; $t_R = 12.6$ minutes.

**Table 3.3** Activity[a] of erylosides and some reference topoisomerase poisons against different yeast strains[b].

| Compound | Yeast strains | | | |
| --- | --- | --- | --- | --- |
| | Parent | *Δrad50*[c] | TOP1oe[d] | TOP2oe[e] |
| Eryloside A (**1**) | 3.5 | 0.8 | 5.7 | 10.8 |
| Eryloside K (**2**) | 6.1 | 2.0 | 7.5 | 12.2 |
| Eryloside L (**3**) | 11.4 | 3.4 | 10.9 | 9.5 |
| Aglygon (**4**) | >50 | >50 | NT[f] | NT |
| Camptothecin (**7**)[g] | 3.8 | 0.1 | 0.4 | 1.5 |
| Idarubicin (**9**)[g] | 3.5 | 0.2 | 3.5 | 0.2 |

[a] $IC_{50}$ ($\mu$M).
[b] Log-phase culture of *S. cerevisiae* strains (135 $\mu$L, $OD_{600}$ of 0.5) treated with serial dilution of drug or DMSO (15 $\mu$L) for 18 hours and optical density monitored (n=3).
[c] *S. cerevisiae* strain with a deletion in the rad50 gene.
[d] *S. cerevisiae* strain overexpressing topoisomerase I enzyme.
[e] *S. cerevisiae* strain overexpressing topoisomerase II enzyme.
[f] Indicates not tested.
[g] See reference.[3]

microscopy. In comparison with untreated controls, the number of treated cells in $G_1$ phase slightly increased with time (Figure 3.7), suggesting that **1** may have been causing cell-cycle arrest at this stage. $G_1$ is a critical point at which the cell assesses whether it should enter another full round of cell division. Proteins involved in $G_1$ progression are frequently mutated in human cancers and are among the most attractive targets for the development of new anticancer drugs.[30] Rapamycin (**22**) and wortmannin (**23**) are two well-known examples of bioactive natural product that cause $G_1$-specific arrest.

Several studies have suggested that selective cytotoxicity against yeast mutants deficient in DSB repair may be an indicator of topoisomerase poisons.[3, 31] Topoisomerase inhibitors such as camptothecin (**7**) and idarubicin (**9**), exhibit marked selectivity against DSB repair mutants (Table 3.3). Topo I and topo II poisons can be distinguished by selective cytotoxicity against yeast strains overexpressing TOP1 and TOP2 respectively, as compared to a wild-type yeast strain.[3] Based on this, compounds **1-3** do not appear to be topoisomerase poisons (Table 3.3). In addition, **1-3** failed to stabilize the covalent complex between DNA and human topoisomerase I or II when screened for DNA strand-break activity[32] at a dose of 500 µM (Figure 3.8).

In contrast, results obtained from the National Cancer Institute 60-cell line antitumor assay suggested that **1-3** may be topoisomerase II inhibitors. Analysis of the assay data was performed using the COMPARE algorithm,[33] which ranks

the bioactivity profile of the test compound according to similarity with 175

standard anticancer drugs. The results obtained by analyzing 60-cell line data

with COMPARE often reflect the mechanism of action by which chemical

substances act upon cells. Since COMPARE does not use chemical data in its

analysis, it can detect structurally novel compounds that act by known

mechanisms. As a result, novel classes of compounds can be recognized as

topoisomerase I or II agents, tubulin-binding agents, or inhibitors of protein

synthesis. A COMPARE analysis of eryloside K (2) revealed that it correlated

principally with etoposide (10) and the anthracycline analog morpholino-ADR

(24), both selective topo II inhibitors (Table 3.4). Similarly, eryloside L (3)

correlated highly with three anthracycline analogs (25-27).

The primary mode of action for anthracylcines such as 24-27 is believed to

be their reversible binding to nucleolar DNA, which causes inhibition of the

replication process and thence death. Numerous biochemical studies including

evidence from NMR spectroscopic and X-ray crystallographic studies have shown

that these compounds intercalate into double-stranded DNA with guanine-

cytosine site-specific interactions.[34] The base pairs above and below the drug

'buckle' in conformation to afford a distorted DNA helix, thereby preventing

association with the DNA helicase, DNA topoisomerase[35] and polymerase

enzymes. Despite the fact that the erylosides lack TOP2 cleavage activity in a

DNA strand-break assay, COMPARE analysis suggests that these compounds

exhibit a similar (albeit weaker) mechanism of action with known topo II poisons.

(a)



(b)
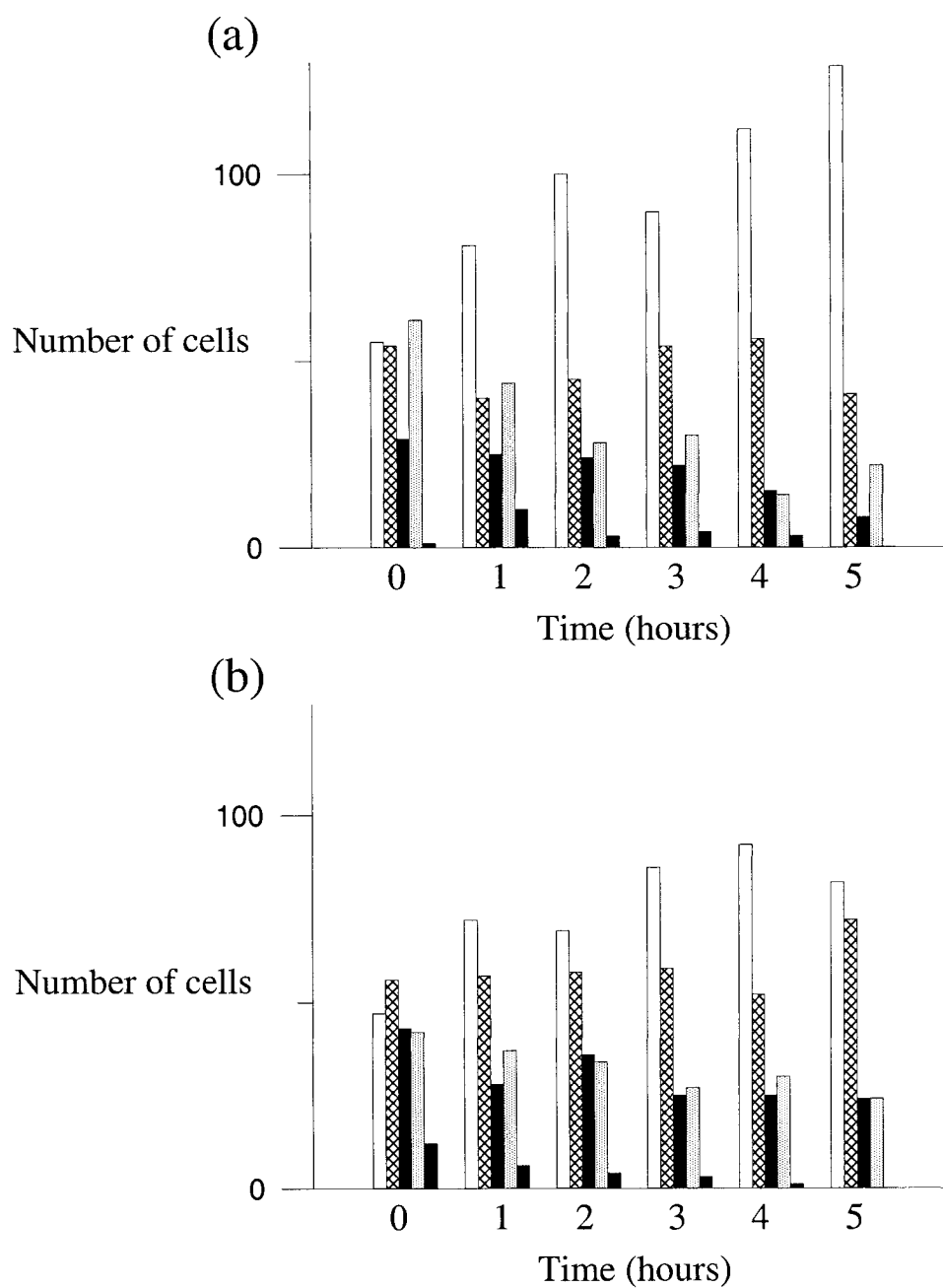


**Figure 3.7** Effect of compound **1** on cell cycle of wild type yeast: (a) Cells treated with 6.25 μg/ml (8.5 μM) of **1** and (b) untreated control cells (n=200). ∏ = no bud ($G_1$-phase); ⊠ = small bud (S-phase); ■= large bud, 1 nucleus or mitotic ($G_2$/M-phase); ▣ = large bud, 2 nuclei (M-phase); ▨ = missegregated/ messy DNA.

(a)
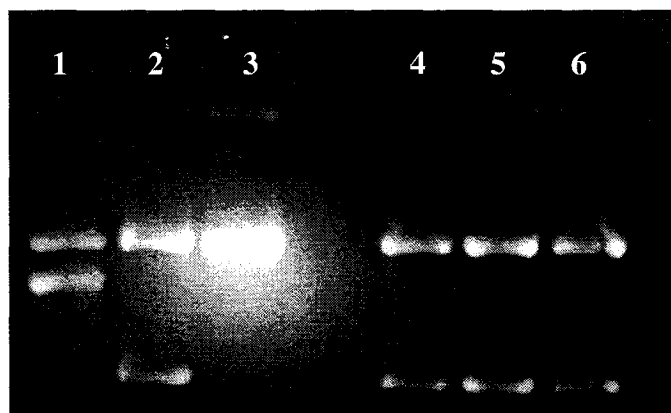


(b)
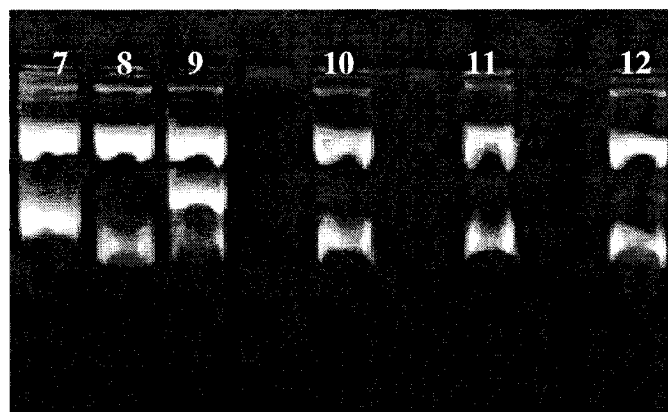


**Figure 3.8** Effects of compounds **1-3** on (a) topoisomerase I and (b) topoisomerase II. Lanes 1 = untreated supercoiled (sc) DNA; Lane 2 = TOP1 + scDNA; Lane 3 = topo I poison (topotecan) + TOP1 + scDNA; Lane 4 = **1** + TOP1 + scDNA; Lane 5 = **2** + TOP1 + scDNA; Lane 6 = **3** + TOP1 + scDNA; Lane 7 = scDNA; Lane 8 = TOP2 + scDNA; Lane 9 = topo II poison (etoposide; 200 μM) + TOP2 + scDNA; Lane 10 = **1** + TOP2 + scDNA; Lane 11 = **2** + TOP2 + scDNA; Lane 12 = **3** + TOP2 + scDNA. Unless otherwise noted, 500 μM of each compound was used.
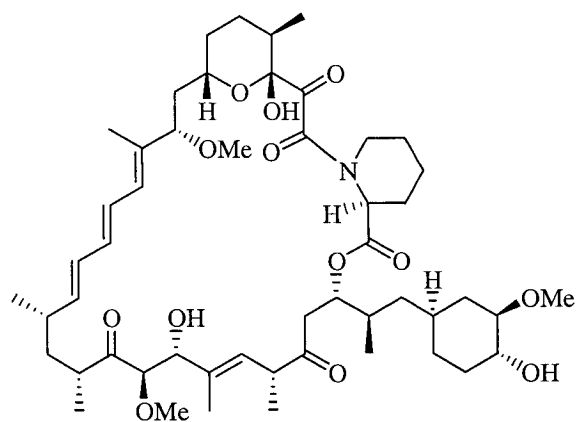
**22**
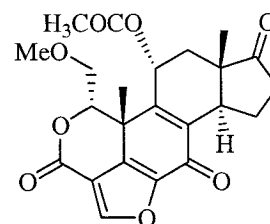
**23**
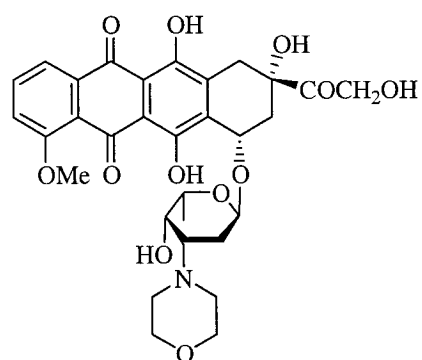
**24**
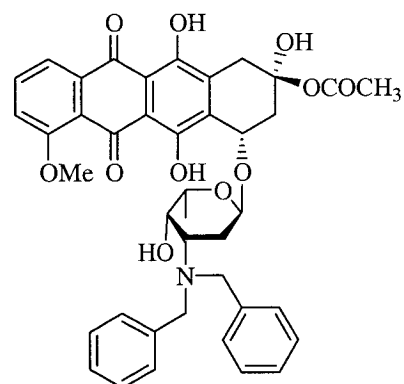
**25**
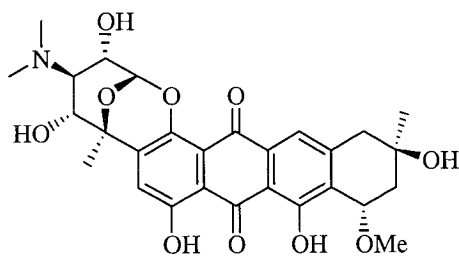
**26**
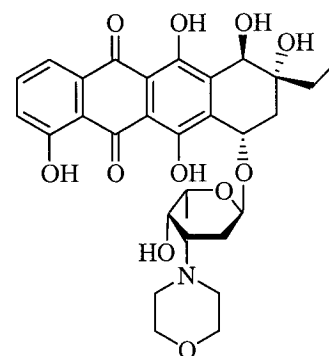
**27**

**Table 3.4** Results from COMPARE analysis of compounds **1**-**3**.

| Compound | Rank | Correlation* | Compound | Target |
|---|---|---|---|---|
| Eryloside A (1) | | | | |
| | 1 | 0.422 | Didemnin B | Protein synthesis |
| | 2 | 0.411 | Thaliblastine | Cell membrane |
| | 3 | 0.359 | Acivicin | Glutamine amidotransferase |
| Eryloside K (2) | | | | |
| | 1 | 0.522 | Morpholino-ADR (24) | Topo II |
| | 2 | 0.348 | Etoposide (10) | Topo II |
| | 3 | 0.298 | Floxuridine | DNA synthesis |
| Eryloside L (3) | | | | |
| | 1 | 0.425 | Dibenzyldaunorubicin (25) | Topo II |
| | 2 | 0.419 | Menogaril (26) | Topo II |
| | 3 | 0.359 | MX2-HCl (27) | Topo II |

*The correlation coefficient can range from -1 to +1, with -1 indicating a perfect negative correlation, +1 indicating a perfect positive correlation.

There is further evidence to suggest that the erylosides inhibit topoisomerase II. In 2000, Abdel-Kader *et al.* isolated a series of chemically related metabolites from a tropical plant species.[36] Interestingly, this class of steroidal glycosides was reported to have selective cytotoxicity against a panel of yeast mutants deficient in topoisomerase function. The panel consisted of three strains (1138, 1140, and 1353), and topo II inhibitors were distinguished as those compounds that inhibited strain 1138 only. Three of the compounds (**28-30**) exhibited two-fold or greater inhibition of strain 1138 than the other strains, suggesting that these compounds are topo II inhibitors.

The erylosides are not the first examples of selective topoisomerase inhibitors being isolated from a marine invertebrate. Kalihinol F (**31**), a naturally occurring diterpene from a marine sponge *Acanthella* sp., inhibited topoisomerase I activity in vitro, but had no effects on activities of DNA polymerases alpha, beta, and gamma, and of topoisomerase II.[37] Ascididemin (**32**), a pyridoacridine alkaloid from the Okinawan tunicate *Didemnumn* sp., was shown to exhibit potent DNA cleavage activity.[38, 39] Relaxation assays using supercoiled DNA showed that **32** stimulated double-stranded cleavage of DNA by topoisomerase II, but exerted only a very weak effect on topoisomerase I.[40] Other pyridoacridine alkaloids have also been shown to target topoisomerase II.[41]

This work has validated the use of a simple, cell-based assay to rapidly identify and isolate selectively bioactive compounds from a crude marine extract. The structural determination of two compounds (**2** and **3**), along with the absolute

configuration of the known compound **1** provides an important addition to the

knowledge of this unique class of secondary metabolites. Although the precise

molecular mechanism of action has not been determined, it is reasonable to

assume that these compounds are weakly selective inhibitors of human

topoisomerase II, an important target in the fight against cancer. One must not

overlook the possibility that the saponic nature of these compounds contributes to

their ability as selectively cytostatic or cytotoxic agents (i.e. as surfactants).

However, this does not explain the selective bioactivity profiles observed from the

multiple, independently monitored investigations mentioned above. Well-known

surfactants, such as the triton-X 100 detergent, do not exhibit any selectivity

against yeast mutants deficient in DSB repair (J. Simon, *pers. comm.*).

**28** $R_1 = H$; $R_2 = H$
**29** $R_1 = $ xylose; $R_2 = $ glucose
**30** $R_1 = $ glucose; $R_2 = $ glucose
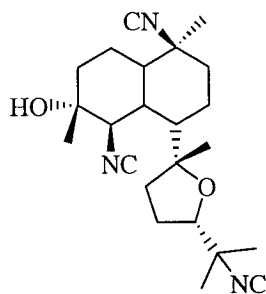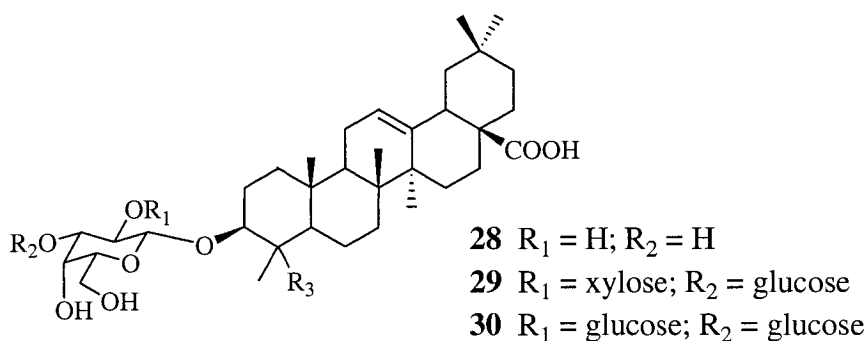
**31**
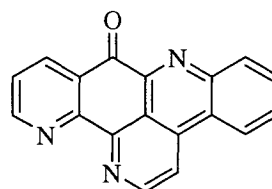
**32**

The text of this chapter is, in part, a reprint of the material as it appears in

Tetrahedron 2005, 61, 1199-1206 with co-authors Susan L. Forsburg and D. John

Faulkner. I was the primary researcher and author, and the co-authors listed in

this publication helped direct and supervise the research, which forms the basis of

this chapter.

**Experimental**

**General Methods.** Optical rotations were measured on a Rudolf Autopol III

polarimeter at 598 nm. IR spectra were recorded on a Perkin-Elmer 1600 FT-IR

spectrophotometer. UV spectra were obtained using a Perkin-Elmer Lambda Bio-

20 spectrophotometer. $^{1}$H, COSY, HMBC, HSQC, 1D-NOESY, 1D-TOCSY, and

ROESY NMR spectra were measured on a Varian Inova 300 MHz spectrometer.

$^{13}$C and DEPT spectra were measured on a Varian Gemini 400 MHz

spectrometer. ESIMS spectra were recorded using a Finnigan LCQ mass

spectrometer. High-resolution MALDI-MS data were obtained on a PE

Biosystems DE-STR MALDI TOF system at the U.C. Riverside Regional

Facility. All solvents were distilled prior to use.

**Extraction and Purification.** The sponge *Erylus lendenfeldi* was collected by

SCUBA in February, 2000 in the Red Sea just north of Hurghada. The crude

methanol extract exhibited selective cytotoxicity against a *Δrad50* yeast strain,

and was thus selected for further study. A portion of the freeze-dried sponge (180

g) was extracted three times in methanol to give 1 L of crude extract. Roughly

half of the methanol was removed *in vacuo*, and the remaining extract was

partitioned on HP20 (Supelco Diaion®) using an increasing concentration of

acetone in water.[42] The 50% aqueous acetone fraction (200 mg) exhibited the

most potent and selective activity against Δ*rad50* mutants and was thus purified

using reversed-phase HPLC (Dynamax C8 semi-prep, 75% MeOH, 3 mL/min) to

give eryloside A (1, 720 mg, 0.4% dry weight), eryloside K (2, 145 mg, 0.08%

dry weight), and eryloside L (3, 90 mg, 0.05% dry weight).

**Eryloside A (1):** white powder; $[\alpha]_D$ +6° (*c* 1.11, MeOH); mp: 168-172°C; UV

(MeOH) $\lambda_{max}$ (log ε) 250 (4.24); IR $\nu_{max}$ (MeOH) 3360, 2930, 1060 cm$^{-1}$; $^1$H

NMR (400 MHz, CD$_3$OD) see Table 3.1; $^{13}$C NMR (100 MHz, CD$_3$OD) see

Table 3.1; HRMALDI-MS *m/z* 761.4472 ([M+Na]$^+$ calcd for C$_{40}$H$_{66}$O$_{12}$Na,

761.45543).

**Eryloside K (2):** white powder; $[\alpha]_D$ +10° (*c* 0.12, MeOH); mp: 208-212°C; UV

(MeOH) $\lambda_{max}$ (log ε) 249 (4.31); IR $\nu_{max}$ (MeOH) 3400, 2925, 1380, 1060 cm$^{-1}$;

$^1$H NMR (400 MHz, CD$_3$OD) see Table 3.2; $^{13}$C NMR (100 MHz, CD$_3$OD) see

Table 3.2; HRMALDI-MS *m/z* 759.4320 ([M+Na]$^+$ calcd for C$_{40}$H$_{64}$O$_{12}$Na,

759.4290).

**Eryloside L (3):** white powder; $[\alpha]_D$ +10° (*c* 0.34, MeOH); mp: 200-204°C; UV

(MeOH) $\lambda_{max}$ (log ε) 250 (4.33); IR $\nu_{max}$ (MeOH) 3375, 2930, 1705, 1370, 1060

cm$^{-1}$; $^1$H NMR (400 MHz, CD$_3$OD) see Table 3.1; $^{13}$C NMR (100 MHz, CD$_3$OD)

see Table 3.1; HRMALDI-MS *m/z* 759.4283 ([M+Na]$^+$ calcd for $C_{40}H_{64}O_{12}Na$, 759.4290).

**Acid Hydrolysis of Eryloside A (1):** A portion of **1** (90 mg) was dissolved in 9 mL of a 1:1:48 mixture of HCl:benzene:EtOH and stirred at 65°C. After 3 hours, the mixture was neutralized with $NaCO_3$. The filtered slurry was dried down *in vacuo*, and the purified aglycon (**19**) was obtained in roughly quantitative yield by silica gel chromatography eluting with ethyl acetate.

**19:** $^1$H NMR ($CD_3OD$) $\delta_H$ 0.84 (3H, s, H-18), 0.91 (3H, d, H-26), 0.91 (3H, d, H-27), 0.97 (3H, d, H-21), 0.98 (3H, d, H-28), 1.01 (3H, s, H-19), 1.01 (1H, m, H-22a), 1.06 (1H, m, H-5), 1.15 (1H, m, H-24a), 1.27 (1H, m, H-1a), 1.32 (1H, m, H-6a), 1.34 (1H, m, H-4), 1.38 (1H, m, H-24b), 1.38 (1H, m, H-12a), 1.47 (1H, m, H-17), 1.51 (1H, m, H-22b), 1.54 (1H, m, H-2a), 1.76 (1H, m, H-25), 1.84 (1H, m, H-2b), 1.86 (1H, m, H-6b), 1.90 (1H, m, H-1b), 1.94 (1H, m, H-20), 2.06 (1H, m, H-12b), 2.10 (1H, m, H-16a), 2.14 (1H, m, H-7a), 2.22 (2H, m, H-11), 2.25 (1H, m, H-7b), 2.32 (1H, m, H-16b), 3.02 (1H, m, H-3), 3.75 (1H, m, H-23), 5.33 (1H, s, H-15); ESIMS *m/z* 415 (M+H)$^+$.

**MTPA esterification of 19:** To a solution of 14.5 mg of 4 in 250 µL dry DCM and 28 µL pyridine was added 200 µL of (*S*)-MTPACl. The mixture was stirred over an ice bath for 4 hours. After the consumption of the starting material was confirmed by TLC, the solution was twice washed with 5% aq. $NaHCO_3$. The organic phase was dried under $N_2$ and chromatographed on silica gel (95:5

CHCl$_3$/MeOH) to give 5.2 mg of **20a**. Using the same procedure, 200 µL of (*R*)-

MTPACl and 14.5 mg of **19** were reacted to obtain 3.8 mg of **20b**.

**20a:** $^1$H NMR (CD$_3$OD) $\delta_H$ 0.64 (3H, s, H-18), 0.92 (3H, d, H-26), 0.96 (3H, d,

H-27), 0.90 (3H, d, H-21), 0.98 (3H, s, H-19), 1.22 (1H, m, H-1a), 1.14 (1H, m,

H-5), 1.23 (1H, m, H-6a), 1.34 (3H, d, H-28), 1.38 (1H, m, H-12a), 1.43 (1H, m,

H-24a), 1.43 (1H, m, H-20), 1.57 (1H, m, H-25), 1.60 (1H, m, H-17), 1.62 (1H,

m, H-22a), 1.65 (1H, m, H-24b), 1.69 (1H, m, H-2a), 1.72 (1H, m, H-6b), 1.72

(1H, m, H-22b), 1.97 (1H, m, H-1b), 2.02 (1H, m, H-12b), 2.04 (1H, m, H-4),

2.05 (1H, m, H-16a), 2.09 (1H, m, H-2b), 2.20 (2H, m, H-11), 2.20 (1H, m, H-

7a), 2.38 (1H, m, H-16b), 2.55 (1H, m, H-7b), 4.6 (1H, m, H-3), 5.34 (1H, m, H-

23), 5.53 (1H, s, H-15).

**20b:** $^1$H NMR (CD$_3$OD) $\delta_H$ 0.78 (3H, s, H-18), 0.86 (3H, d, H-26), 0.88 (3H, d,

H-27), 0.91 (3H, d, H-21), 0.93 (3H, s, H-19), 1.23 (1H, m, H-1a), 1.23 (1H, m,

H-5), 1.24 (1H, m, H-6a), 1.31 (1H, m, H-24a), 1.37 (3H, d, H-28), 1.40 (1H, m,

H-12a), 1.45 (1H, m, H-20), 1.47 (1H, m, H-25), 1.54 (1H, m, H-2a), 1.57 (1H,

m, H-24b), 1.67 (1H, m, H-17), 1.72 (1H, m, H-22a), 1.75 (1H, m, H-6b), 1.81

(1H, m, H-22b), 1.87 (1H, m, H-1b), 2.00 (1H, m, H-2b), 2.05 (1H, m, H-4), 2.06

(1H, m, H-12b), 2.10 (1H, m, H-16a), 2.21 (2H, m, H-11), 2.22 (1H, m, H-7a),

2.44 (1H, m, H-16b), 2.60 (1H, m, H-7b), 4.58 (1H, m, H-3), 5.37 (1H, m, H-23),

5.55 (1H, s, H-15).

**Catalytic Hydrogenation Product 21:** Compounds **1** and **2** (10 mg) were each

dissolved in 10 ml of MeOH. Hydrogenation was effected under $H_2$ gas (~3 atm)

in the presence of 5% rhodium on $Al_2O_3$. The reaction was complete after 50

minutes as indicated by TLC. The filtered slurry was dried to give the identical

product (**21**) in both cases. Products from hydrogenation reactions using **1** and **2**

had identical masses (ESIMS, $m/z$ 764 [M+Na]) corresponding to the reduction of

one double bond in **1**, and two double bonds in **2**. The products from **1** and **2** had

similar optical rotation values of $[\alpha]_D = +12.4°$ ($c$ 0.20, MeOH) and $[\alpha]_D =$

+12.3° ($c$ 0.21, MeOH) respectively, the same $^1H$ NMR spectra (data not shown),

and identical HPLC retention times on C8 (Zorbax XDB; 67% MeOH; detected at

254 nm; $t_R$ = 20.7 min.) and C18 (Phenomenex Luna; 46% $CH_3CN$; detected at

254 nm; $t_R$ = 12.6 min.).

**Yeast Strains.** All budding yeast strains were obtained from the Molecular

Pharmacology Program at the Fred Hutchinson Cancer Research Center in

Seattle, WA. Six strains were used, each with drug-sensitizing mutations that

increased membrane porosity ($\Delta erg6$)[43] and hindered drug efflux ($\Delta pdr1$ and

$\Delta pdr3$).[44] In addition to these mutations, two of the strains contained a mutation

in a double-strand break repair gene (yMP11406; $\Delta rad50$)[45] and a DNA damage

checkpoint gene (yMP10605; $mec2-1/rad53$)[46] respectively. Three other strains

contained double mutations in a postreplication repair gene (yMP10425;

$\Delta rad18$)[47] and a mismatch repair gene (SP50248; $\Delta mlh1$)[48], a nucleotide excision

repair gene (yMP10691; *Δrad14*) (review in ref.[49]) and overexpression of the $G_1$

cyclin CLN2 (*CLN2oe*)[50], and a 5' to 3' helicase gene (SP50265; *Δsgs1*)[51] and an

alkylguanine transferase gene (yMP10612; *Δmgt1*).[52] The parent strain

(yMP10381) was used as a control.

**Yeast Assay.** Exponentially growing yeast in enriched liquid media were diluted

to $OD_{600} = 0.07$, and 135 μL of cells along with 15 μL of extract in DMSO was

dispensed into each well of flat-bottomed 96-well microtiter plates. The assay

was conducted in two stages. In stage 1, extracts (50 μg/mL) that produced a

70% or greater inhibition of growth in any or all strains advanced to stage 2. In

stage 2, extracts were tested at 50, 25, 12.5, 6.3, 3.1, and 1.6 μg/mL. Extracts that

produced a two-fold or greater difference in sensitivity between the most sensitive

strain and less sensitive strains were studied further. Plates were incubated on a

shaker plate for 18h at 25°C, and the optical density (600 nm) of the cultures was

determined using a Bio-Tek Instruments $EL_x808$ microplate reader to assess

relative growth. DMSO and cycloheximide were used as negative and positive

controls respectively.

**Staining cells for DAPI analysis.** Clean glass slides were coated in 10 μl of

0.01% polylysine for 3 minutes. Excess polylysine was removed and slides were

air dried. 150 μl of cell broth from 96-well plate was centrifuged and excess

media was removed by aspiration. Cold 70% ethanol (1 ml) was added and

solution was vortexed. Ethanol-fixed cells were washed with water (200 μl,

milliQ), and 5 µl of cells were placed on slide. After three minutes, excess cells were aspirated and slide air dried for 5 minutes. Mount media (2 µl) and DAPI® (0.6 µl; 1 mg/ml) were added to slide prior to viewing.

**Staining cells for FACS analysis.** Cell broth (150 µl) from 96-well plate was centrifuged and excess media was aspirated. Cold 70% ethanol (1 ml) was added, solution was vortexed, and centrifuged. Excess ethanol was aspirated, and 1 ml 50mM sodium citrate was added. Cells were vortexed, centrifuged, and sodium citrate was aspirated. Sodium citrate (500 ml; 50 mM) was added, cells were vortexed and transferred to FACS tubes. RNase A (500 ml; 0.5 mg/ml in 50 mM sodium citrate) was added. Cells were incubated at 50°C for 1 hour, centrifuged, and excess supernatant was aspirated. SytoxGreen® (0.5 ml; 2 µM) was added prior to FACS analysis.

**DNA strand-break activity.** *In vitro* assays assessing TOP1- and TOP2-specific activity were conducted as reported previously.[32]

# References

1. Hartwell, H. L., Szankasi, P., Roberts, C. J., Murray, A.W., Friend, S. H (1997). Integrating genetic approaches into the discovery of anticancer drugs. *Science* **278**, 1064-1068.

2. Perego, P., Jiminez, G. S., Gatti, L., Howell, S. B., Zunino, F. (2000). Yeast mutants as a model system for identification of determinants of chemosensitivity. *Pharm. Rev.* **52**, 477-491.

3. Dunstan, H. M., Ludlow, C., Goehle, S., Cronk, M., Szankasi, P., Evans, D. R. H., Simon, J. A., Lamb, J. R (2002). Cell-based assays for identification of novel double-strand break-inducing agents. *J. Nat. Cancer. Inst.* **94**, 88-92.

4. Simon, J. A., Szankazi, P. ,Nguyen, D. K., Ludlow, C., Dunstan, H. M., Roberts, C. J., Jensen, E. L., Hartwell, L. H., Friend, S. H. (2000). Differential toxicities of anticancer agents among DNA repair and checkpoint mutants of *Saccharomyces cerevisiae. Cancer Res.* **60**, 328-333.

5. Kaplan, A. S., Brown M., Ben-Porat, T. (1968). Effect of 1-beta-D-arabinofuranosylcytosine on DNA synthesis. *Mol Pharmacol.* **4**, 131-8.

6. Yamagata, K., Kato, J., Shimamoto, A., Goto, M., Furuichi, Y., Ikeda, H. (1998). Bloom's and Werner's syndrome genes suppress hyperrecombination in yeast sgs1 mutant: Implication for genomic instability in human diseases. *Proc. Nat. Acad. Sci.* **95**, 8733-8738.

7. Holm, C., Covey, J. M., Kerrigan, D., Pommier, Y. (1989). Differential requirement of DNA replication for the cytotoxicity of DNA topoisomerase I and II inhibitors in Chinese hamster DC3F cells. *Cancer Res* **49**, 6365-6368.

8. Levin, N. A., Bjornsti, M. A., Fink, G. R. (1993). A novel mutation in DNA topoisomerase I of yeast causes DNA damage and RAD9-dependent cell cycle arrest. *Genetics* **133**, 799-814.

9. Vishnevetskaia, O. I., Luchnik A. N., Arutiunova L. S., Shestakov S. V. (1983). Disorder of the repair of DNA double-stranded breaks in radiosensitive mutants of *Saccharomyces cerevisiae* yeasts. *Genetika* **19**, 26-32.

10. Angele, S., Treilleux, I., Bremond, A., Taniere, P., Hall, J. (2003). Altered expression of DNA double-strand break detection and repair proteins in breast carcinomas. *Histopathology* **43**, 347-53.

11. Djuzenova, C., Muhl, B., Schakowski, R., Oppitz, U., Flentje, M. (2004). Normal expression of DNA repair proteins, hMre11, Rad50 and Rad51 but protracted formation of Rad50 containing foci in X-irradiated skin fibroblasts from radiosensitive cancer patients. *Br. J. Cancer* **90**, 2356-63.

12. Donahue, S. L., Campbell, C. (2004). A Rad50-dependent pathway of DNA repair is deficient in Fanconi anemia fibroblasts. *Nucl. Acids Res.* **32**, 3248-3257.

13. Wang, H.-K., Morris-Natschke, S.L., Lee, K.-H. (1997). Recent advances in the discovery and development of topoisomerase inhibitors as antitumor agents. *Med. Res. Rev.* **17**, 367-425.

14. Sollas, W. J., *Report on the Tetractinellida collected by HMS 'Challenger' during the years 1873-76*. 1888, London: Her Majesty's Stationary Office.

15. Stonik, V. A., Elyakon, G. B., *Bioorganic Marine Chemistry*, ed. P.J. Sheuer. Vol. 2. 1988, New York: Springer Verlag. 43.

16. Carmely, S., Roll, M., Loya, Y., Kashman, Y. (1989). The structure of eryloside A, a new antitumor and antifungal 4-methylated steroidal glycoside from the sponge *Erylus lendenfeldi*. *J. Nat. Prod.* **52**, 167-170.

17. D'Auria, M. V., Gomez, P., Minale, L., Riccio, R., Debitus, C. (1992). Structure chacterization by two-dimensional NMR spectroscopy, of two marine triterpene oligoglycosides from a pacific sponge of the genus *Erylus*. *Tetrahedron* **48**, 491-498.

18. Gulavita, N. K., Wright, A. E., Kelly-Borges, M., Longley, R. E., Yarwood, D., Sills, M. A. (1994). Eryloside E from an atlantic sponge *Erylus goffrilleri*. *Tetrahedron Lett.* **35**, 4299-4302.

19. Stead, P., Hiscox, S., Robinson, P. S., Pike, N. B., Sidebottom, P. J., Roberst, A. D., Taylor, N. L., Wright, A. E., Pomponi, S. A., Langley, D. (2000). Eryloside F, a novel penasterol disaccharide possessing potent thrombin receptor antagonist activity. *Bioorg. Med. Chem. Lett.* **10**, 661-664.

20. Shin, J., Lee, H.-S., Woo, L., Rho, J.-R., Seo, Y., Cho, K. W., Sim, C. J. (2001). New triterpenoid saponins from the sponge *Erylus nobilis*. *J. Nat. Prod.* **64**, 767-771.

21. Ohtani, I., Kusumi, T., Kashman, Y., Kakisawa, H. (1991). High-field FT NMR application of mosher's method: the absolute configuration of marine terpenoids. *J. Am. Chem. Soc.* **113**, 4092-4096.

22. Takada, K., Nakao, Y., Matsunaga, S., van Soest, R. W. M., Fusetani, N. (2002). Nobiloside, a new neuraminidase inhibitory triterpenoidal saponin from the marine sponge *Erylus nobilis*. *J. Nat. Prod.* **65**, 411-413.

23. Ryu, G., Choi, B. W., Lee, B. H., Hwang, K.-H. (1999). Wondosterols A-C, three steroidal glycosides from a korean marine two-sponge association. *Tetrahedron* **55**, 13171-13178.

24. Wilson, W. K., Sumpter, R. M., Warren, J. J., Rogers, P. S., Ruan, B., Schroepfer, G. J. (1996). Analysis of unsaturated C27 sterols by nuclear magnetic resonance spectroscopy. *J. Lipid Res.* **37**, 1529-1547.

25. Sidduqui, A. U., Swaminathan, S., Pinkerton, F. D., Gerst, N., Wilson, W. K., Choi, H., Schroepfer, G. J. (1994). Inhibitors of sterol synthesis: synthesis and spectral properties of derivatives of 3β-hydroxy-25,26,26,26,27,27,27-heptafluoro-5α-cholest-8(14)-en-15-one fluorinated at carbon 7 or carbon 9 and their effects on 3-hydroxy-3-methylglutaryl coenzyme A reductase activity in cultured mammalian cells. *Chem. Phys. Lipids* **72**, 59-75.

26. Beier, R. C., Mundy, B. P., Stobel, G. A. (1980). Assignment of anomeric configuration and identification of carbohydrate residues by 13C NMR. 1. Galacto- and glucopyranosides and furanosides. *Can. J. Chem.* **58**, 2800-2804.

27. Freifelder, M., *Practical catalytic hydrogenation; techniques and applications*. 1971, New York: M.Wiley-Interscience. 13-15.

28. Due to a change in prioritization of groups surrounding the C-23 chiral center, 2 has the 23R configuration while 1 has the 23S configuration.

29. Faulkner, D. J. (2002). Marine Natural Products. *Nat. Prod. Rep.* **19**, 1-48, and previous reports in this series.

30. Hung, D. T., Jamison, T. F., Schreiber, S. L. (1996). Understanding and controlling the cell cycle with natural products. *Chem. Biol.* **3**, 623-639.

31. Nitiss, J., Wang, J. C. (1988). DNA topoisomerase-targeting antitumor drugs can be studied in yeast. *Proc. Natl. Acad. Sci.* **85**, 7501-7505.

32. Matsumoto, S. S., Haughey, H. M., Schmehl, D. M., Venables, D. A., Ireland, C. M., Holden, J. A., Barrows, L. R. (1999). Makaluvamines vary in ability to induce dose-dependent DNA cleavage via topoisomerase II interaction. *Anticancer Drugs* **10**, 39-45.

33. Boyd, M. R., DeVita, V. T., Jr., Hellman, S., Rosenberg, S. A., *Cancer: Principles and Practice of Oncology*, ed. Lippincott. Vol. 3. 1989, Philadelphia, PA. 1-12.

34. Frederick, C. A., Williams, L. D., Ughetto, G., Van der Marel, G. A., van Boom, J. H., Rich, A.,Wang, A. H. J. (1990). Structural comparison of anticancer drug-DNA complexes: adriamycin and daunomycin. *Biochemistry* **29**, 2538 - 2549.

35. Capanico, G., Zunino, F., *Molecular basis of specificty in nucleic acid-drug interactions*, ed. B Pullman, Jortner, J. 1990, Netherlands: Kluwer Academic Publishers.

36. Abdel-Kader, M. S., Bahler, B. D., Malone, S.,Werkhoven, M. C. M., Wisse, J. H., Neddermann, K. M., Bursuker, I., Kingston, D. G. I. (2000). Bioactive saponins from *Swartzia schomburgkii* from the Suriname rainforest. *J. Nat. Prod.* **63**, 1461-1464.

37. Ohta, E., Ohta, S., Hongo, T., Hamagu, Y., Andoh, T., Shioda, M., Ikegami, S. (2003). Inhibition of chromosome separation in fertilized starfish eggs by kalihinol F, a topoisomerase I inhibitor obtained from a marine sponge. *Biosci. Biotech. Biochem.* **67**, 2365-72.

38. Kobayashi, J., Cheng, J.-F., Nakamura, H., Ohizumi, Y., Hirata, Y., Sasaki, T., Ohta, T., Nozoe, S. (1988). Ascididemin, a novel pentacyclic aromatic alkaloid with potent antileukemic activity from the okinawan tunicate *Didemnumn* sp. *Tetrahedron Lett.* **29**, 1177-1180.

39. Matsumoto, S. S., Sidford, M. H., Holden, J. A. (2000). Mechanism of action studies of cytotoxic marine alkaloids: ascididemin exhibits thiol-dependent oxidative DNA cleavage. *Tetrahedron Lett.* **41**, 1667-70.

40. Dassonneville, L., Wattez, N., Baldeyrou, B., Mahieu, C., Lansiaux, A., Banaigs, B., Bonnard, I., Bailly, C. (2000). Inhibition of topoisomerase II by the marine alkaloid ascididemin and induction of apoptosis in leukemia cells. *Biochemical Pharmacology* **60**, 527-537.

41. McDonald, L. A., Eldredge, G. S., Barrows, L. R., Ireland, C. M. (1994). Inhibition of topoisomerase II catalytic activity by pyridoacridine alkaloids from a *Cystodytes* sp. ascidian: a mechanism for the apparent intercalator-induced inhibition of topoisomerase II. *J. Med. Chem.* **37**, 3819 - 3827.

42. West, L. M., Northcote, P. T., Battershill, C. N. (2000). Peloruside A: a potent cytotoxic macrolide isolated from the New Zealand marine sponge *Mycale* sp. *J. Org. Chem.* **65**, 445-449.

43. Gaber, R. F., Copple, D. M., Kennedy, B. K., Vidal, M., Bard, M. (1989). The yeast gene ERG6 is required for normal membrane function but is not essential for biosynthesis of the cell-cycle-sparking sterol. *Mol. Cell. Biol.* **9**, 3447-3456.

44. Balzi, E., Goffeau, A. J. (1995). Yeast multidrug resistance: the PDR network. *Bioenerg. Biomem.* **27**, 71-76.

45. van den Bosch, M., Bree, R. T., Lowndes, N. F. (2003). The MRN complex: coordinating and mediating the response to broken chromosomes. *EMBO Rep.* **4**, 844-849.

46. Kim, S., Weinert, T. A. (1997). Characterization of the checkpoint gene RAD53/MEC2 in *Saccharomyces cerevisiae*. *Yeast* **13**, 735-745.

47. Bailly, V., Lamb, J., Sung, P., Prakash, S., Prakash, L. (1994). Specific complex formation between yeast RAD6 and RAD18 proteins: a potential mechanism for targeting RAD6 ubiquitin-conjugating activity to DNA damage sites. *Genes Dev.* **8**, 811-820.

48. Prolla, T. A., Christie, D. M., Liskay, R. M. (1994). Dual requirement in yeast DNA mismatch repair for MLH1 and PMS1, two homologs of the bacterial mutL gene. *Mol. Cell. Biol.* **14**, 407-415.

49. Prakash, S., Prakash, L. (2000). Nucleotide excision repair in yeast. *Mutat. Res.* **451**, 13-24.

50. Richardson, H. E., Wittenberg, C., Cross, F., Reed, S. I. (1989). An essential $G_1$ function for cyclin-like proteins in yeast. *Cell* **59**, 1127-1133.

51. Watt, P. M., Louis, E. J., Borts, R. H., Hickson, I. D. (1995). Sgs1: a eukaryotic homolog of E. coli RecQ that interacts with topoisomerase II in vivo and is required for faithful chromosome segregation. *Cell* **81**, 253-260.

52.    Xiao, W., Derfler, B., Chen, J., Samson, L. (1991). Primary sequence and biological functions of a *Saccharomyces cerevisiae* O6-methylguanine/O4-methylthymine DNA-repair methyltransferase gene. *EMBO J.* **10**, 2179-2186.

# CHAPTER 4

## NOVEL MACROLIDES FROM A NEW DEEP-WATER

## PALAUAN SPONGE *LEIODERMATIUM* SP.

An investigation of a new deep-water marine sponge *Leiodermatium* sp. resulted in the isolation of two novel macrolides, leiodelides A (**1**) and B (**2**). The leiodelides represent the first members of a new class of marine-derived macrolides, incorporating several unique functional groups including a conjugated oxazole ring and an $\alpha,\alpha$-hydroxy-methyl carboxylic acid terminus. The structures were established primarily by interpretation of NMR data. A model for the relative stereochemistry of five chiral centers was proposed based on detailed interpretation of spectroscopic data. The leiodelides inhibited the growth of HCT-116 human colon tumor cells at low micromolar concentrations.

**Introduction**

Lithistid demosponges are a highly prolific source of novel bioactive secondary metabolites and are renowned for their ability to produce a diverse array of polyketides, cyclic peptides, alkaloids, pigments, and novel sterols.[1] The order Lithistida is, in fact, a phylogenetically artificial assemblage of diverse species that all contain fused spicules called desmas.[2] In addition to the physical protection

118

afforded by these siliceous spicules, lithistids are typically characterized by the presence of potently bioactive secondary metabolites that provide chemical defense against competition, predation, and microbial fouling. The extreme diversity of secondary metabolites found among lithistids defies simple chemotaxonomic reasoning, and symbiotic microorganisms have been shown to be responsible for the production of at least some of these compounds.[3] Regardless of which organism is the actual producer, lithistid sponges have been a remarkably fruitful source of novel compounds with potent and unique biological activities.
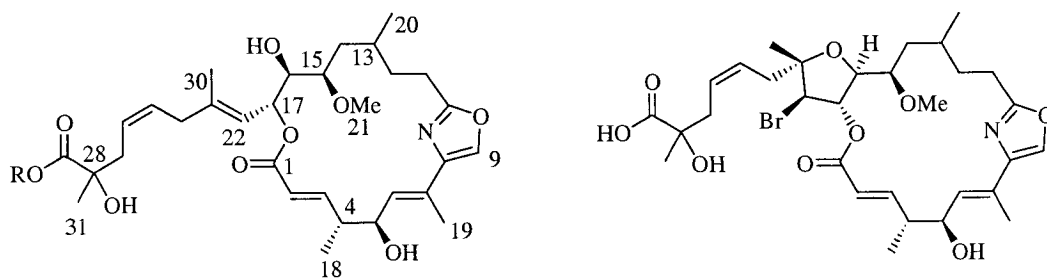
Despite the fact that lithistids are found predominantly in deep-water habitats, chemical investigations have tended to focus on shallow species that are readily accessible by SCUBA. Swinholide A (3) is a potent cytotoxic macrolide that was first isolated by Carmely and Kashman from a Red Sea specimen of *Theonella swinhoei*.[4] It was originally reported as a monomeric 22-membered macrolide (4), a structure that was supported by NMR data, elemental analysis, and mass spectroscopy. A subsequent study of an okinawan specimen of *T. swinhoei* resulted in the isolation of a macrolide that was spectroscopically identical to swinholide A.[5] The positive and negative FABMS spectra from this compound, however, showed ion peaks suggesting that swinholide A had a dimeric dilactone structure. The revised structure (3), along with its absolute stereochemistry, was unambiguously proven by X-ray crystallographic analysis.[6] Swinholide A was shown to disrupt the actin cytoskeleton, sequester actin dimers, and rapidly sever F-actin of cells grown in culture, suggesting that the compound

might be therapeutically useful in certain cancers where filamentous actin

contributes to pathology.[7] Callipeltoside A (5) is a cytotoxic glycoside macrolide

isolated from a New Caledonian sponge, *Callipelta* sp.[8] Although only moderately

cytotoxic, a flow cytometry assay of lung cancer cells treated with 5 revealed the

compound induced a cell-cycle dependent cytotoxicity involving arrest during G1

phase. Theoneberine (6) is an unusual alkaloid that was isolated from an

unidentified Okinawan *Theonella* sponge.[9] Compound 6 showed moderate

cytotoxicity against lymphoma and carcinoma cells, but lacked specificity and was

therefore not pursued further. Cyclotheonamides A (7) and B (8) belong to an

interesting family of cyclic peptides that contain a rare $\alpha$-keto amide functionality.

These compounds were shown to potently inhibit thrombin,[10] resulting in

anticoagulant activity. The structural elucidation of theonellamide F (9),[11] an

antifungal bicyclic peptide from *Theonella* sp., was particularly challenging for its

time and paved the way for the characterization of other lithistid metabolites such

as theonegramide (10)[12] and theopalauamide (11).[13] Aciculitins A-C (12-14) were

obtained from the lithistid sponge *Aciculites orientalis* and inhibited the growth of

HCT-116 human colon tumor cells at low micromolar concentrations.[14]

A few interesting compounds have been isolated from deep-water lithistid

sponges that were collected by submersible or sea-floor dredging. A particularly

noteworthy example is the case of discodermolide (15), a polyhydroxylated

lactone from the Atlantic deep-water sponge *Discodermia dissoluta*.[15] While it
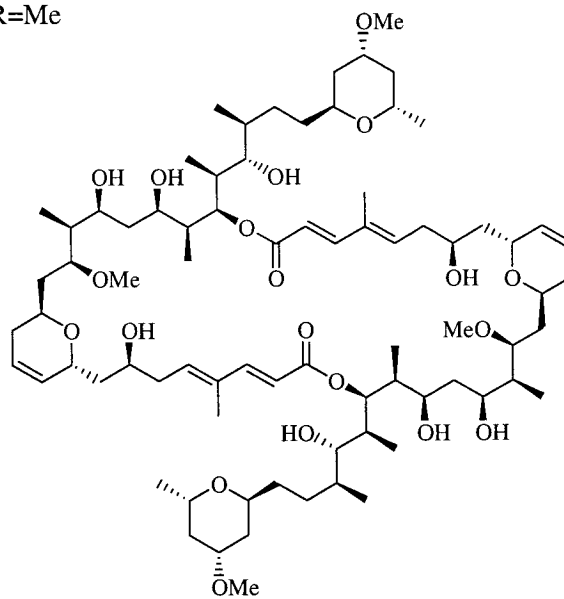
was originally reported as a cytotoxic anti-inflammatory compound, **15** was

subsequently shown to stabilize microtubules in the same manner as Taxol™ and

is now in clinical trials as an anticancer drug.[16] Other interesting compounds from

deep-water *Discodermia* sponges include the discobahamins **(16-17)**[17] and

polydiscamide A **(18)**,[18] an anticancer cyclic peptide. A deep-water

*Microscleroderma* species obtained by sea-floor dredging in New Caledonia

contained two antifungal cyclic peptides, microsclerodermins A **(19)** and B **(20)**.[19]

Since their discovery, several other microsclerodermin analogs have been

reported.[20, 21] Superstolide A **(21)** is a unique macrolide that was isolated from a

New Caledonian deep-water sponge *Neosiphonia superstes*.[22] Although

superstolide A exhibited potent cytotoxicity against several cancer cell lines, the

molecular mode of action of this compound remains undetermined.

Aside from the New Caledonian reefs, the deep-water habitats of the

tropical Pacific, including those in Micronesia and Polynesia, have been largely

inaccessible and few sponges from these regions have been examined due to the

difficulties involved in their procurement. Recently, use of the *Deep Worker*, a

manned submersible, has provided access to the remote depths along the barrier

reefs of Palau, providing an unprecedented opportunity to collect new species of

lithistid sponges. As part of my ongoing search for anticancer compounds from

marine sponges, I examined a specimen of a new deep-water species of lithistid
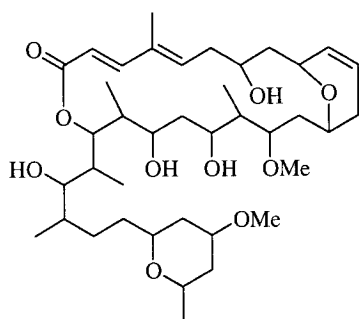
sponge, *Leiodermatium* sp.[23] No secondary metabolites have been reported from

**1** R=H
**22** R=Me
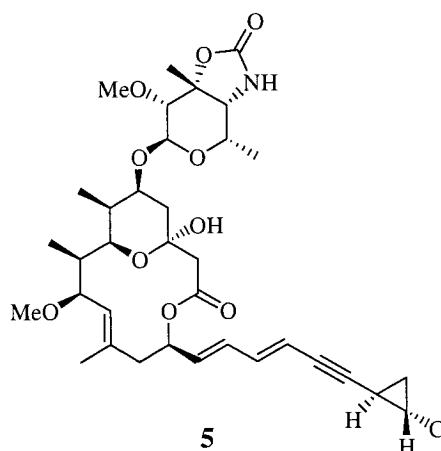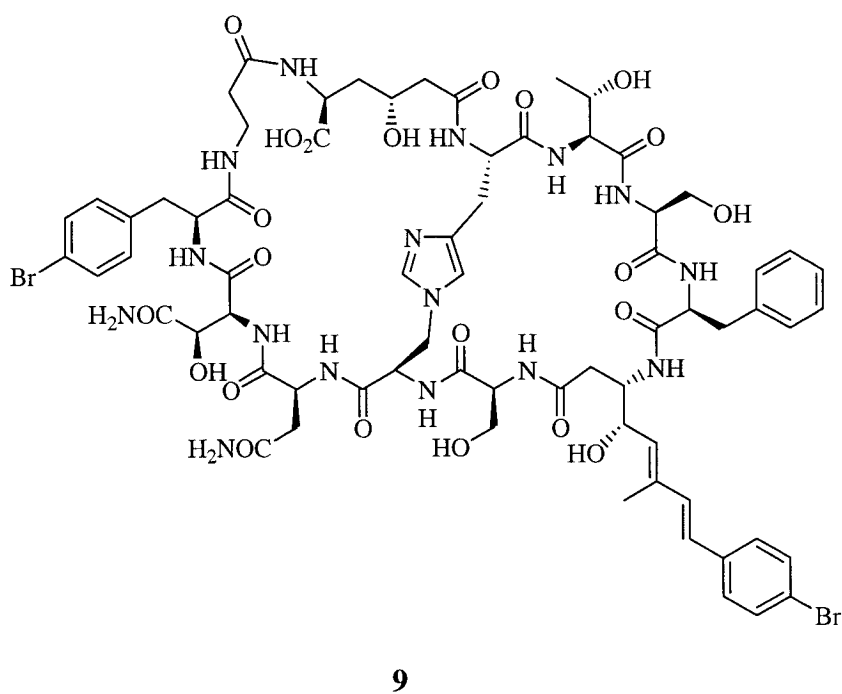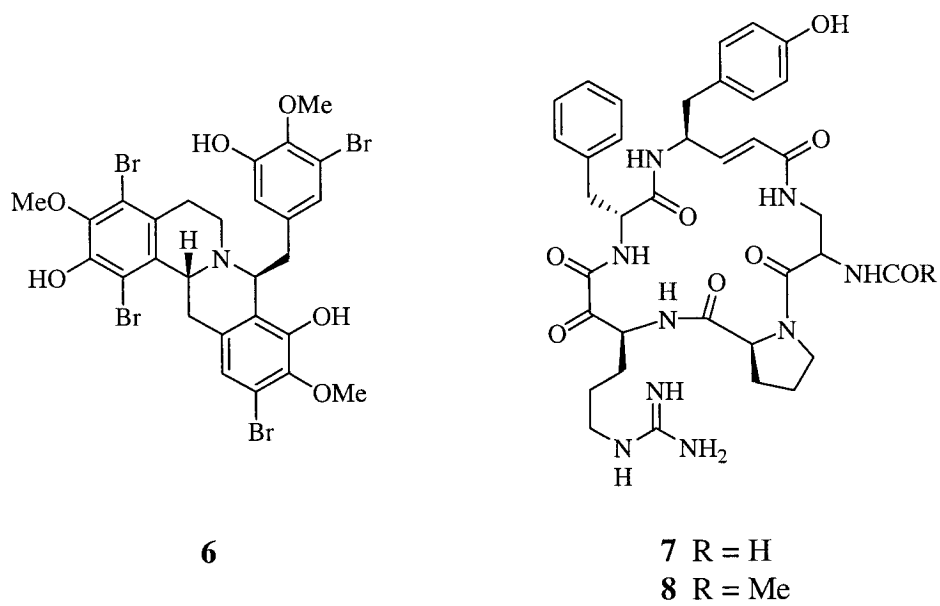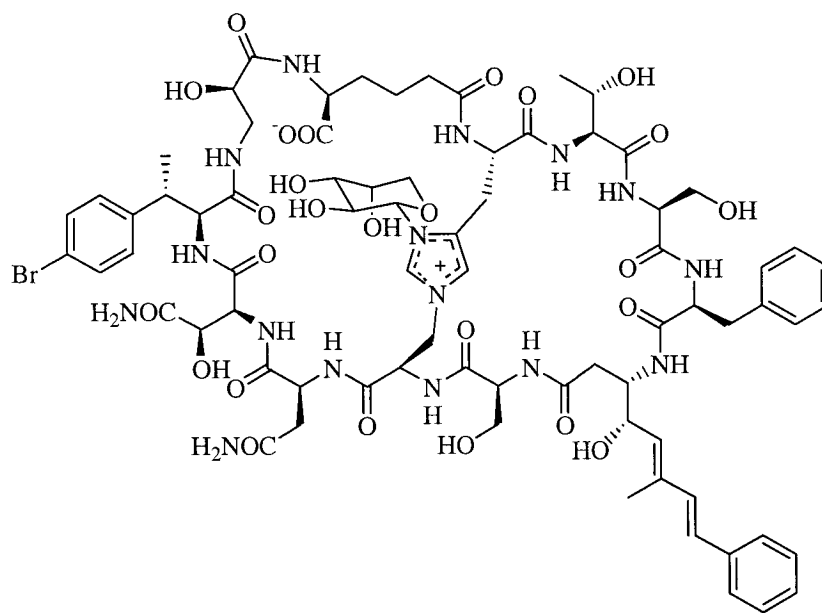
**2**

**3**

**4**

**5**

**6**

**7** R = H
**8** R = Me

**9**

**10**

**11**

**12** R = C$_5$H$_{11}$
**13** R = C$_6$H$_{13}$
**14** R = C$_7$H$_{15}$



**15**



**16** R = H
**17** R = CH$_3$

**18**

**19** R = OH
**20** R = H

**21**
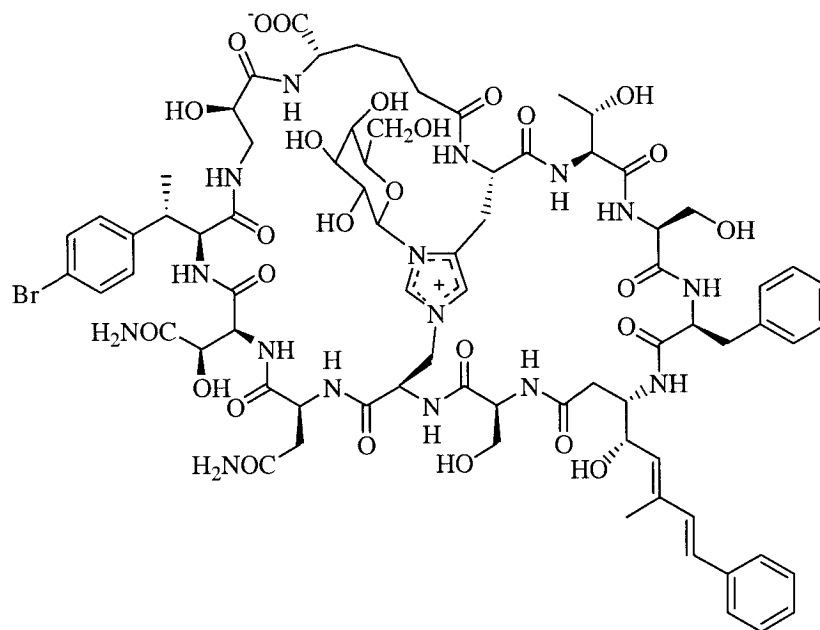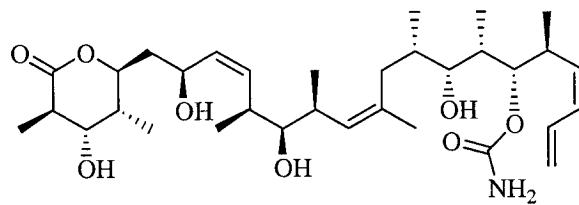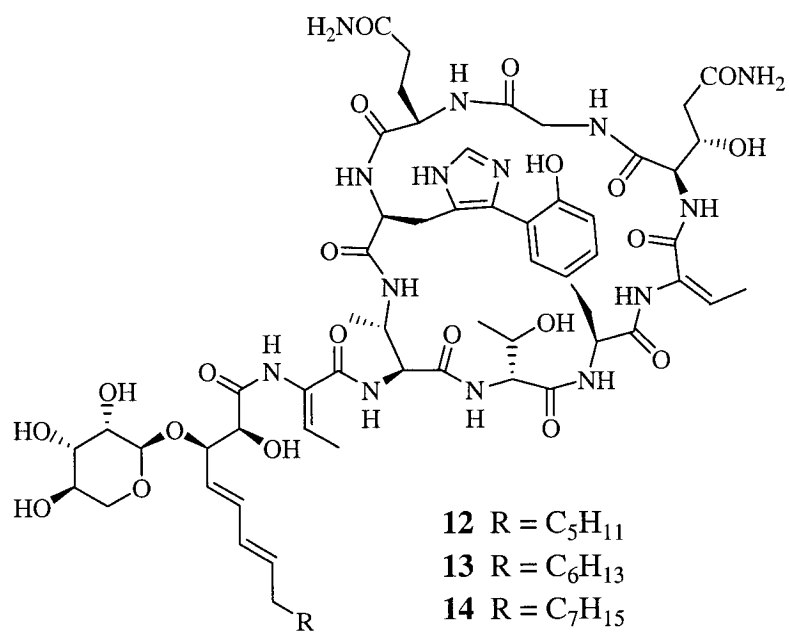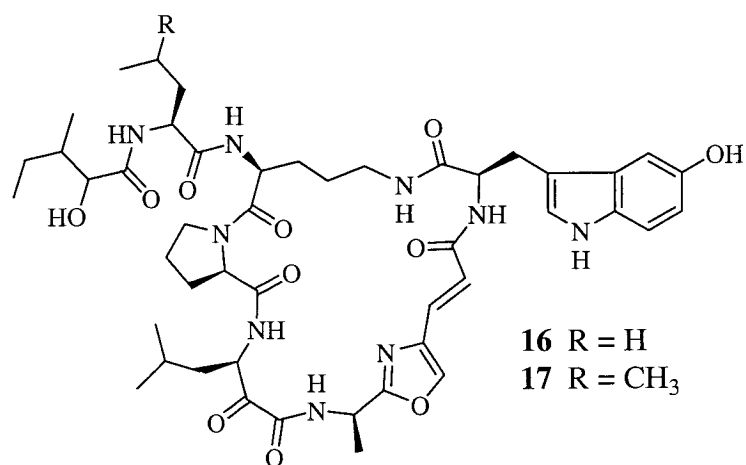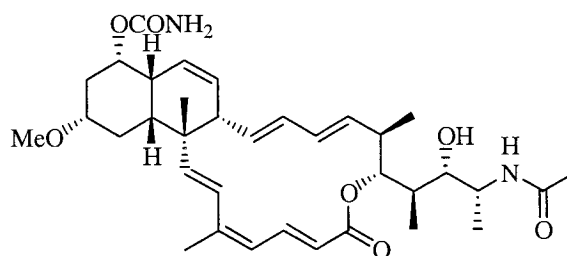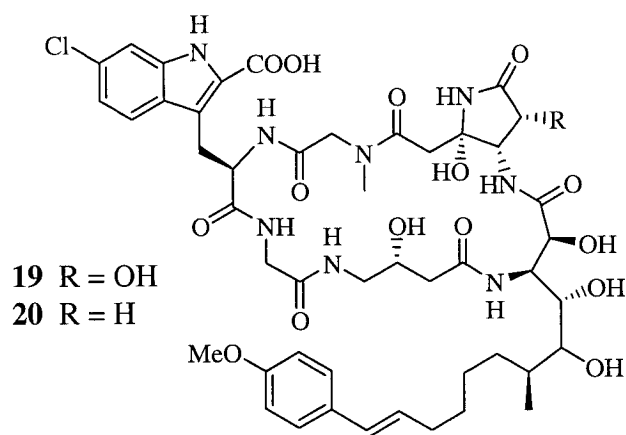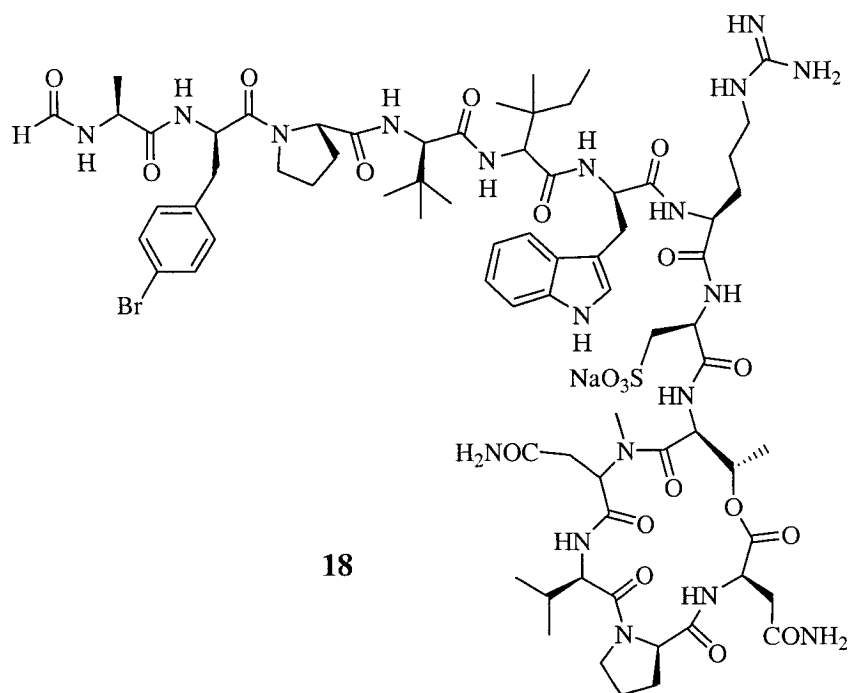
this genus until now. An analysis of the isolation, structural eludcidation, and bioactivity of two novel macrocyclic lactones, leiodelides A (1) and B (2), is presented below.

## Isolation and structural elucidation

Using the manned submersible, *Deep Worker 2000*, Patrick Colin collected the sponge on the West side of Uchelbeluu Reef in Palau from a depth of 240 m. The sponge is a new species of the genus *Leiodermatium* ('Lithistid' Demospongiae: Family Azoriciidae) presently being described.[23] The lyophilized sponge (730 g, dry weight) was exhaustively extracted with methanol to give 1 L of crude extract. Roughly half of the methanol was removed *in vacuo*, and the remaining extract was partitioned on HP20 (Supelco Diaion®) using an increasing concentration of acetone in water as previously described.[24] The 50% and 75% aqueous acetone fractions exhibited the most potent activity against HCT-116 cells and were thus purified using reversed-phase HPLC (PRP-1 semi-prep, 27.5% acetonitrile, 2 mL/min) to give leiodelide A (1, 14 mg, 0.002% dry weight) and leiodelide B (2, 0.8 mg, 0.0001% dry weight).

The molecular formula of leiodelide A (1) was deduced from the high resolution MALDI-MS spectrum (598.2992, $[M + Na]^+$, $\Delta$ 0.9 ppm) as $C_{31}H_{45}NO_9$, which was consistent with both the $^{13}C$ and $^1H$ NMR data (Table 4.1). Analysis of the proton (Figure 4.1) and carbon (Figure 4.2) NMR data revealed signals due to

**Table 4.1** $^{13}C$ (75 MHz, MeOH-$d_4$), $^1H$ (500 MHz, MeOH-$d_4$), and HMBC (500 MHz, MeOH-$d_4$) NMR data for **1**

| C# | $^{13}C$ NMR in ppm | | $^1H$ NMR in ppm, mult. ($J$ in Hz) | HMBC |
|---|---|---|---|---|
| 1 | 166.9 | C | | |
| 2 | 124.3 | CH | 5.69 d (15.5) | C-1, C-4 |
| 3 | 151.2 | CH | 6.88 dd (15.5, 9.5) | C-1, C-2, C-4, C-18 |
| 4 | 44.9 | CH | 2.38 m | C-2, C-3, C-5, C-18 |
| 5 | 72.3 | CH | 4.54 dd (9.5, 3.0) | C-3, C-4, C-6, C-7, C-18 |
| 6 | 131.4 | CH | 6.31 dd (9.0, 1.0) | C-4, C-7, C-8, C-19 |
| 7 | 125.6 | C | | |
| 8 | 143.5 | C | | |
| 9 | 135.0 | CH | 7.66 s | C-6, C-8, C-10 |
| 10 | 166.3 | C | | |
| 11 | 25.2 | CH$_2$ | 2.71 m | C-10, C-12, C-13 |
| | | CH$_2$ | 2.83 m | C-10, C-12, C-13 |
| 12 | 34.6 | CH$_2$ | 1.60 m | C-10, C-11, C-13, C-14, C-20 |
| | | CH$_2$ | 2.05 m | C-10, C-11, C-13, C-14, C-20 |
| 13 | 29.5 | CH | 1.28 m | C-11, C-12, C-14, C-15, C-20 |
| 14 | 35.9 | CH$_2$ | 1.62 m | C-12, C-13, C-15, C-16, C-20 |
| 15 | 80.3 | CH | 3.22 ddd (9.5, 4.5, 0.5) | C-13, C-14, C-21 |
| 16 | 73.1 | CH | 3.45 d (9.5) | C-17, C-22 |
| 17 | 70.8 | CH | 5.75 t (9.5) | C-1, C-15, C-16, C-22, C-23 |
| 18 | 16.8 | CH$_3$ | 1.25 d (7.0) | C-3, C-4, C-5 |
| 19 | 13.8 | CH$_3$ | 1.92 d (1.0) | C-4, C-5, C-6, C-7, C-8 |
| 20 | 21.5 | CH$_3$ | 0.97 d (6.5) | C-13, C-14 |
| 21 | 58.1 | CH$_3$ | 3.38 s | C-15 |
| 22 | 123.1 | CH | 5.14 dd (9.5, 1.0) | C-16, C-24, C-30 |
| 23 | 143.5 | C | | |
| 24 | 38.1 | CH$_2$ | 2.75 m | C-22, C-23, C-25, C-26, C-30 |
| | | CH$_2$ | 2.81 m | C-22, C-23, C-25, C-26, C-30 |
| 25 | 129.5 | CH | 5.45 m | C-27 |
| 26 | 128.2 | CH | 5.57 m | C-27, C-22 |
| 27 | 39.0 | CH$_2$ | 2.30 m | C-25, C-26, C-28, C-29, C-31 |
| | | CH$_2$ | 2.48 m | C-25, C-26, C-28, C-31 |
| 28 | 76.5 | C | | |
| 29 | 182.8 | C | | |
| 30 | 17.9 | CH$_3$ | 1.79 d (1.0) | C-22, C-23, C-24 |
| 31 | 26.7 | CH$_3$ | 1.29 s | C-27, C-28, C-29 |
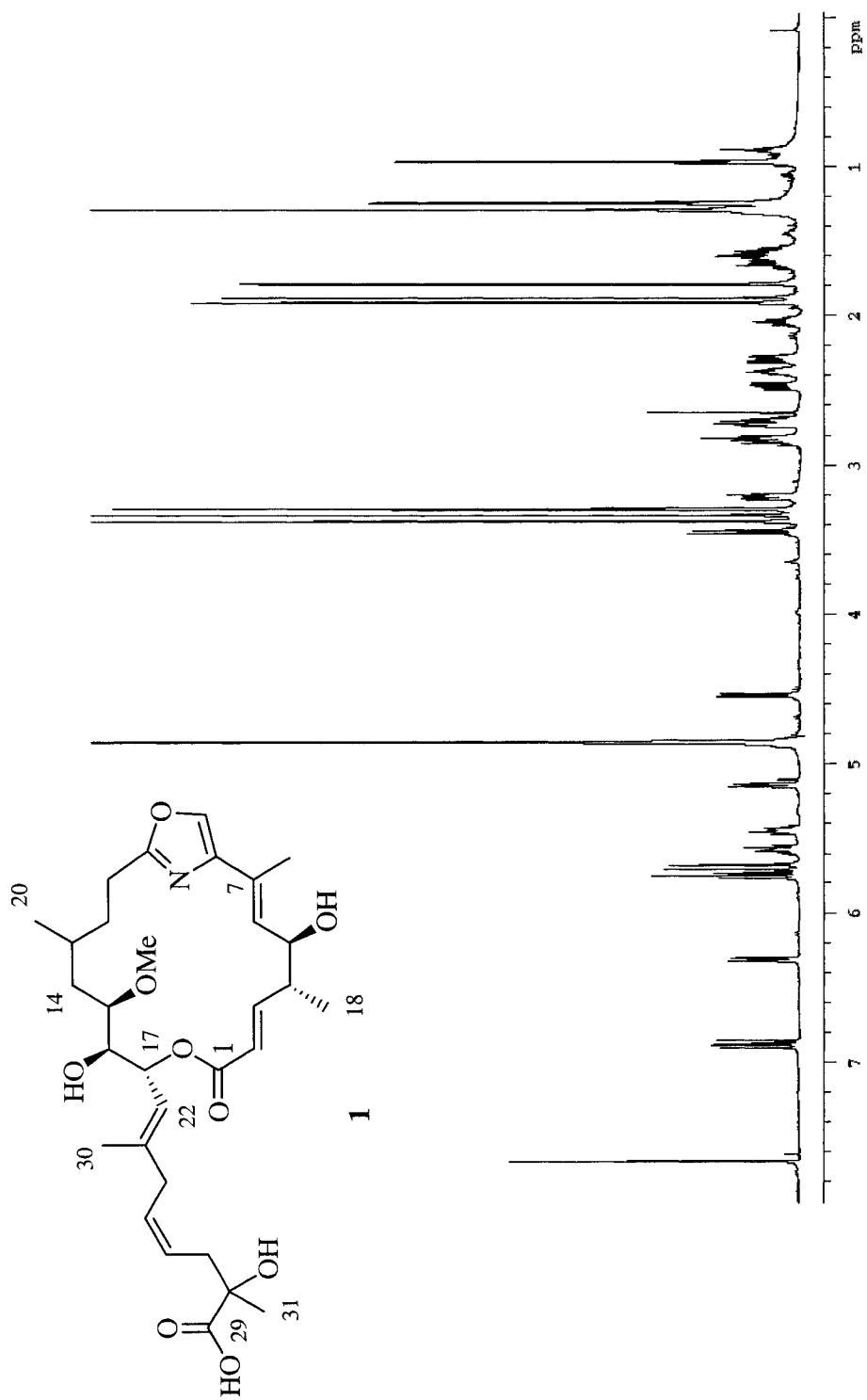
**Figure 4.1** $^1$H NMR spectrum for leiodelide A (**1**) in MeOH-$d_4$.
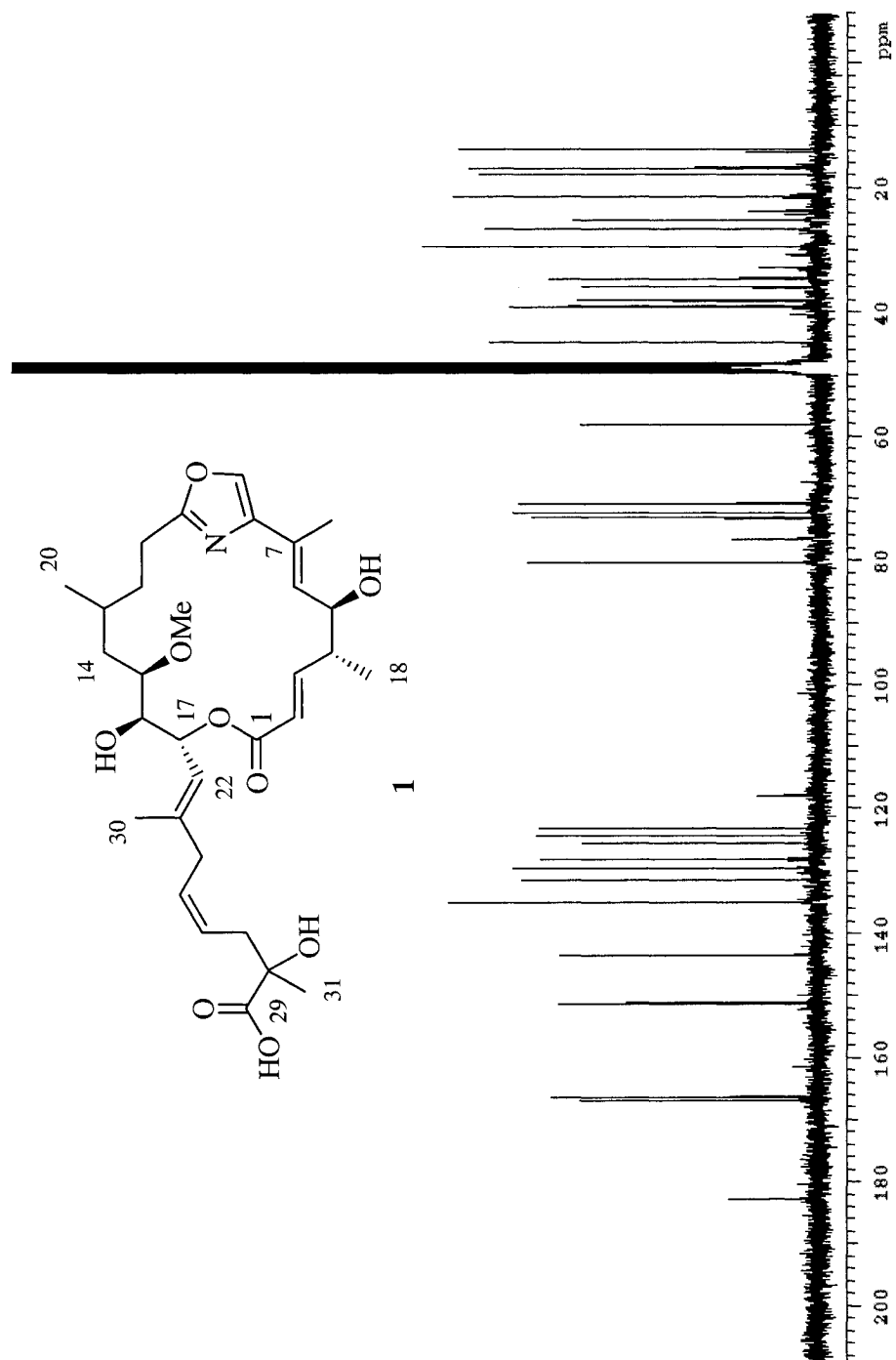
**Figure 4.2** ^{13}C NMR spectrum for leiodelide A (**1**) in MeOH-$d_4$.

two di- and two trisubstituted double bonds, four oxymethines, a methoxy group, a

saturated carboxyl acid, an α,β-unsaturated ester or carboxyl acid, and possibly a

small heteroaromatic ring ($\delta_H$ 7.66, $\delta_C$ 135.0, $\delta_C$ 143.5, $\delta_C$ 166.3). Combined,

these data suggested that **1** was an oxygenated polyketide.

Interpretation of cross peaks from the COSY spectrum (Figure 4.3)

established the connectivity between two olefinic methines, C-2 ($\delta_H$ 5.69, $\delta_C$

124.2) and C-3 ($\delta_H$ 6.88, $\delta_C$ 151.2). A large coupling constant (15.5 Hz) between

H-2 and H-3 established the *E* configuration for this disubstituted double bond.

COSY correlations revealed a linear system comprised of the $\Delta^{2,3}$ olefin, a

methylated methine, C-4 ($\delta_H$ 2.38, $\delta_C$ 44.8), a methyl doublet, C-18 ($\delta_H$ 1.25, $\delta_C$

16.8), and an oxymethine, C-5 ($\delta_H$ 4.54, $\delta_C$ 72.3). The H-5 methine resonance

also showed coupling to an olefinic proton resonance at C-6 ($\delta_H$ 6.31, $\delta_C$ 131.4) of

a trisubstituted double bond. Allylic coupling between H-6 and the C-19 methyl

protons ($\delta_H$ 1.92, $\delta_C$ 13.8) was evident from the COSY spectrum and established

the presence of these two substituents in a trisubstituted double bond. A NOESY
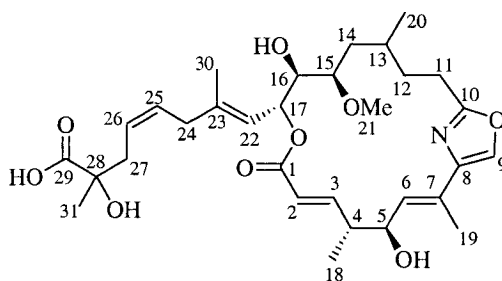


**1**

correlation between H-19 and H-5, combined with the lack of a NOESY correlation between H-19 and H-6, established the configuration of this double bond as *E*.

COSY correlations were also used to elucidate a linear subunit comprised of two methylenes, C-11 ($\delta_H$ 2.71, 2.83; $\delta_C$ 25.3) and C-12 ($\delta_H$ 1.60, 2.05; $\delta_C$ 34.6), a methylated methine, C-13 ($\delta_H$ 1.28, $\delta_C$ 29.5), a methyl doublet, C-20 ($\delta_H$ 0.97, $\delta_C$ 21.4), a methylene, C-14 ($\delta_H$ 1.62, $\delta_C$ 35.8), and three oxymethines, C-15 ($\delta_H$ 3.22, $\delta_C$ 80.2), C-16 ($\delta_H$ 3.45, $\delta_C$ 73.3), and C-17 ($\delta_H$ 5.75, $\delta_C$ 70.7). The downfield H-17 methine resonance was also coupled to an olefinic proton at C-22 ($\delta_H$ 5.14, $\delta_C$ 123.2), which in turn showed allylic coupling to a vinyl methyl resonance at C-30 ($\delta_H$ 1.79, $\delta_C$ 17.9). NOESY cross-peaks (H-22 and H-24, H-30 and H-25) established the *E* configuration for $\Delta^{22,23}$. The remaining proton couplings observed in the COSY spectrum were assigned to a linear four-carbon subunit consisting of a downfield methylene, C-24 ($\delta_H$ 2.75, 2.81; $\delta_C$ 38.1), two olefinic methines, C-25 ($\delta_H$ 5.45, $\delta_C$ 130.1) and C-26 ($\delta_H$ 5.57, $\delta_C$ 127.4), and an additional methylene, C-27 ($\delta_H$ 2.30, 2.48; $\delta_C$ 38.9). Selective decoupling of the C-24 methylene protons in a homonuclear decoupling experiment (HOMODEC) revealed an 11.0 Hz coupling constant between H-25 and H-26, suggesting a *Z* configuration for the $\Delta^{25,26}$ olefin (Figure 4.4). Additional support for this orientation was provided by NOESY correlations between the methylene protons at C-24 and C-27.
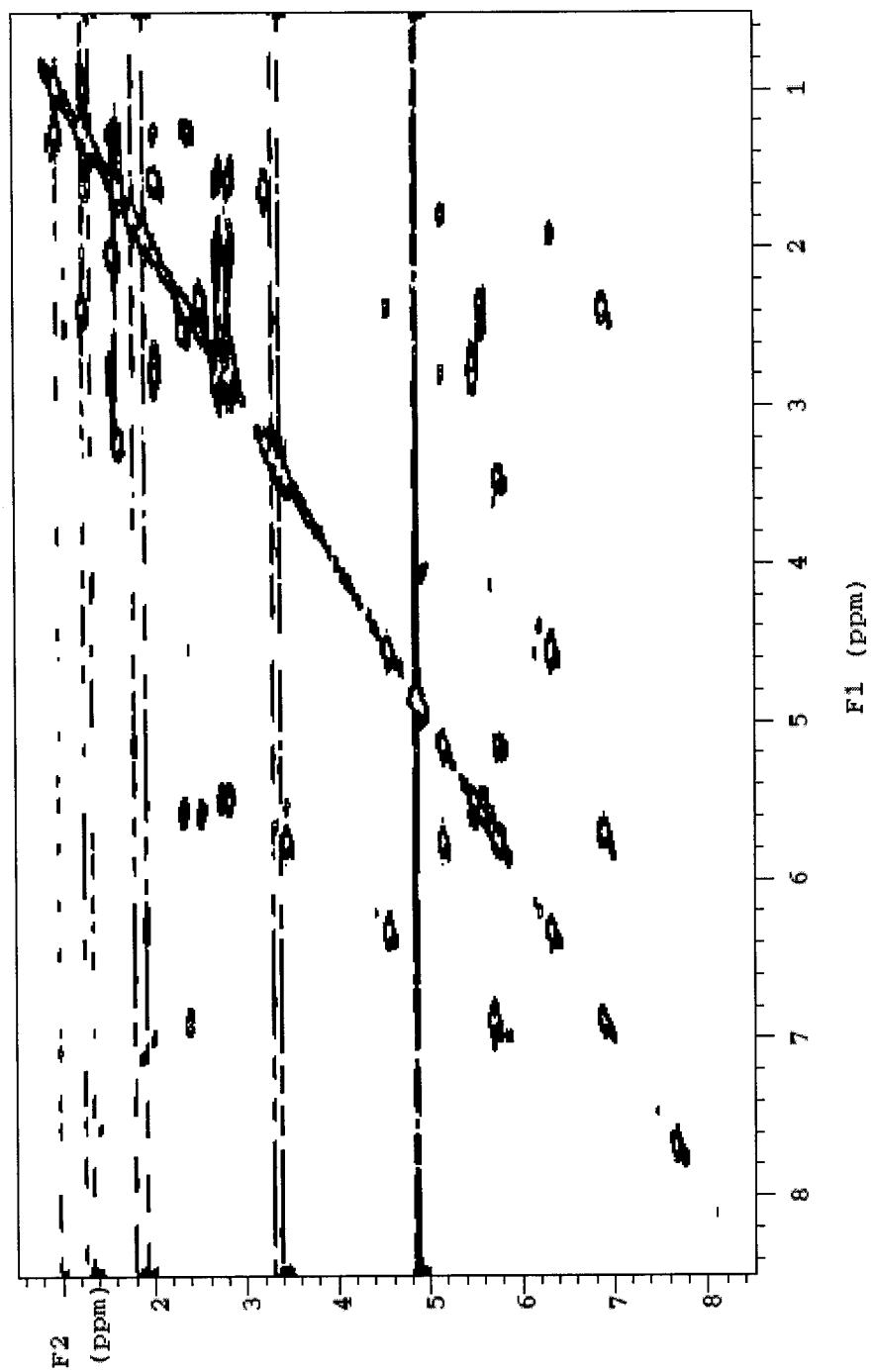
**Figure 4.3** gCOSY spectrum for leiodelide A (**1**) in MeOH-$d_4$.

F1 (ppm)

F2 (ppm)
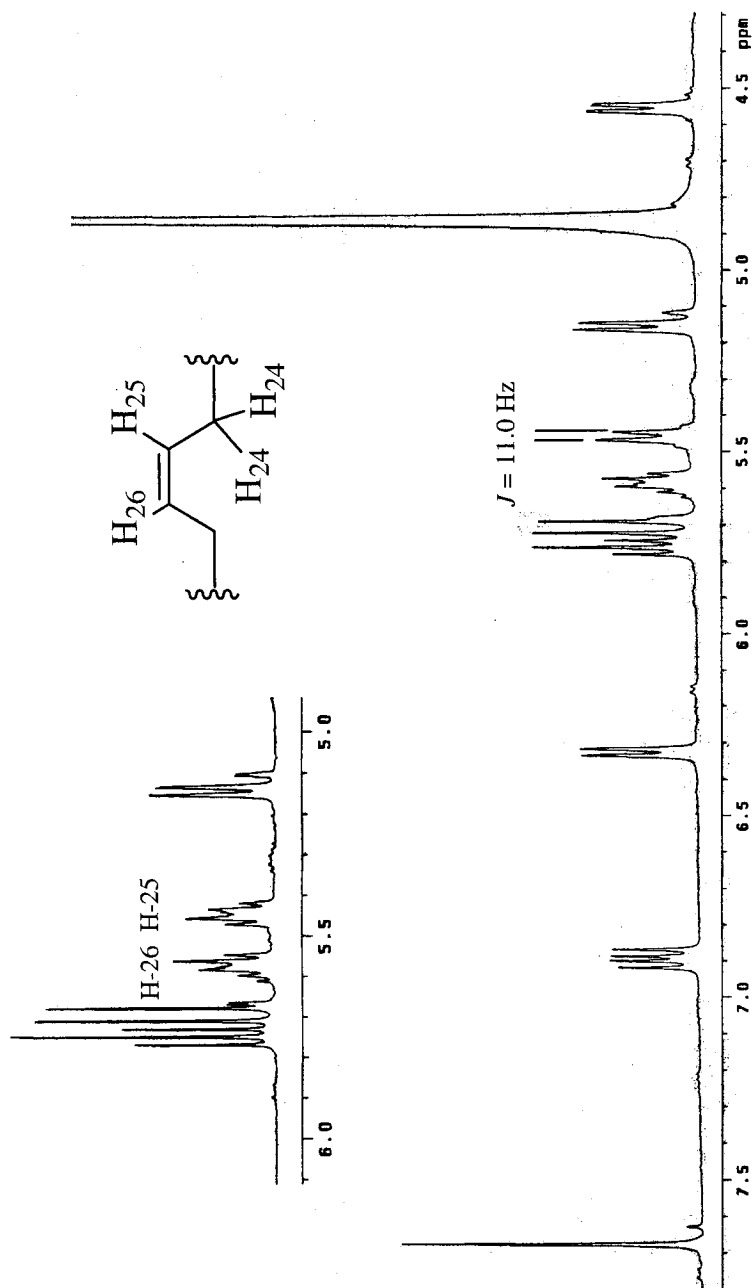
**Figure 4.4** Homonuclear decoupling $^1$H NMR experiment for leiodelide A (**1**). Selective decoupling of the C-24 methylene protons ($\delta_H$ 2.75 and 2.81) reveals an 11.0 Hz coupling constant between H-25 and H-26. Inset shows normal (fully coupled) $^1$H NMR spectrum for comparison. Truncated portion of the molecule shown for clarity.

Long-range proton-carbon correlations observed in the HMBC spectrum

(Table 4.1, Figure 4.5) provided corroborative evidence to support the three

subunits deduced by analysis of the COSY spectrum (C-2 to C-6, C-11 to C-22,

and C-24 to C-27). In addition, HMBC correlations were observed from the

olefin protons at C-2 and C-3 to the carbonyl C-1 ($\delta_C$ 166.9), establishing this as

an $\alpha,\beta$-unsaturated ester moiety. HMBC correlations suggested a link between

the olefinic methyl group at C-19 and a substituted olefin carbon ($\delta_C$ 125.6)

assigned as C-7. In addition, the methoxy group C-21 ($\delta_H$ 3.38, $\delta_C$ 58.1) was

shown to be attached to the C-15 oxymethine. An HMBC correlation from the

olefinic methyl protons of C-30 to the substituted olefin carbon C-23 and the

methylene C-24 established a link between C-24 and the $\Delta^{22,23}$ trisubstituted

double bond.

The presence of a disubstituted 1,3-oxazole was revealed by the NMR

signals at C-8 ($\delta_C$ 143.5), C-9 ($\delta_H$ 7.66, $\delta_C$ 135.0), and C-10 ($\delta_C$ 166.3), along with

a characteristic $^1J_{C,H}$ value for C-9 (205.8 Hz).[25] The heteroaromatic proton

resonance H-9 exhibited long-range coupling to the quaternary carbons C-8 and

C-10. HMBC correlations were observed from both H-6 and Me-19 to C-8, and

from the methylene protons at C-11 and C-12 to C-10, which established the

location of the oxazole moiety as shown.

An analysis of the NMR and IR spectra indicated that the remaining

portion of the molecule consisted of an oxygenated quaternary carbon, C-28 ($\delta_C$
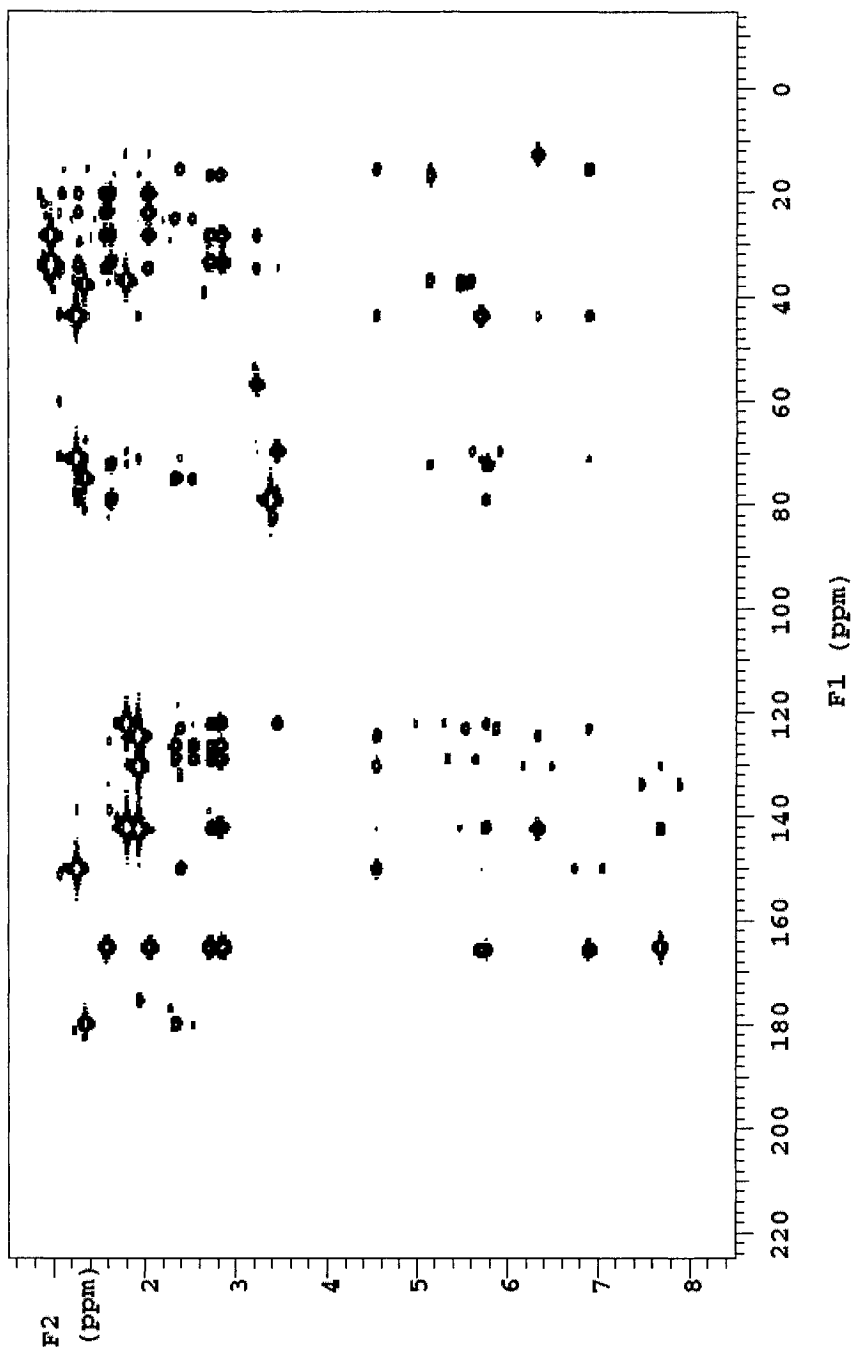
**Figure 4.5** gHMBC spectrum for leiodelide A (**1**) in MeOH-*d4*.

76.1), a methyl singlet, C-31 ($\delta_H$ 1.29, $\delta_C$ 26.4), and an aliphatic carboxyl acid carbon, C-29 ($\delta_C$ 180.1; IR 1715 cm$^{-1}$). HMBC correlations (H-27 to C-28, C-29, and C-31; H-31 to C-27, C-28, C-29) established a link between the C-27 methylene and this terminal group. With all other atoms in compound **1** already accounted for, the molecular formula only allowed for an additional three carbons, five protons, and three oxygen atoms in this functional group. Taken together, these data established the unusual α-hydroxy-α-methyl carboxylic acid terminal moiety, which matches reported values for this type of functional group.[26, 27] Methylation of **1** with diazomethane to give compound **22** verified the presence of a carboxyl acid, providing further support for the proposed structure. The presence of an α-oxy-α,α-disubstituted acetic acid moiety has been reported for natural products such as quinic acid derivatives[28] and okadaic acid derivatives.[29] However, this is the first reported case of an α-hydroxy-α-methyl carboxylic acid positioned at the chain terminus of a macrocyclic lactone.

The molecular formula of (**1**) suggested the presence of a total of ten unsaturation equivalents. With all carbon connectivities accounted for, the remaining degree of unsaturation required a cyclic structure. An HMBC correlation from H-17 to the carbonyl carbon C-1 suggested an ester linkage between C-1 and C-17, thereby establishing the structure of **1** as an 18-membered macrolide.

The observation that chemical shift differences of methylene protons and $^1$H-$^1$H coupling constants at centers throughout compound **1** were not dependent on temperature (0-40°C) or NMR solvent (MeOH-$d_4$, DMSO-$d_6$) confirmed the existence of a single predominant conformer.[30] This implied that an assignment of the relative stereochemistry for at least some of the chiral centers would be possible from a combination of NOE and vicinal coupling constants.[31] For the most part, vicinal proton-proton ($^3J_{H,H}$) and carbon-proton ($^3J_{C,H}$) coupling constants follow a Karplus-type equation and thus can be used for stereochemical analysis.[32] NOE correlations were detected with NOESY and selective 1D NOESY experiments at 500 MHz. Approximate $^3J_{H,H}$ values were determined by careful analysis of the $^1$H NMR spectrum along with homonuclear decoupling experiments at 500 MHz, and a gHSQMBC[33] experiment was used to determine the $^3J_{C,H}$ values. This latter experiment can be used to calculate long-range heteronuclear coupling constants by comparison with combined antiphase $^1$H NMR spectra that are offset by the coupling constant in question (Figure 4.6, Figure 4.7).

The relative configuration of C-2 to C-7 is shown in Figure 4.8. The methine proton attached to C-5 appeared as a doublet of doublets with a large vicinal coupling to H-6 (9.5 Hz) and a small vicinal coupling (3.0 Hz) to the oxymethine H-4, suggesting that H-4 and H-5 are *gauche* to one another. A large
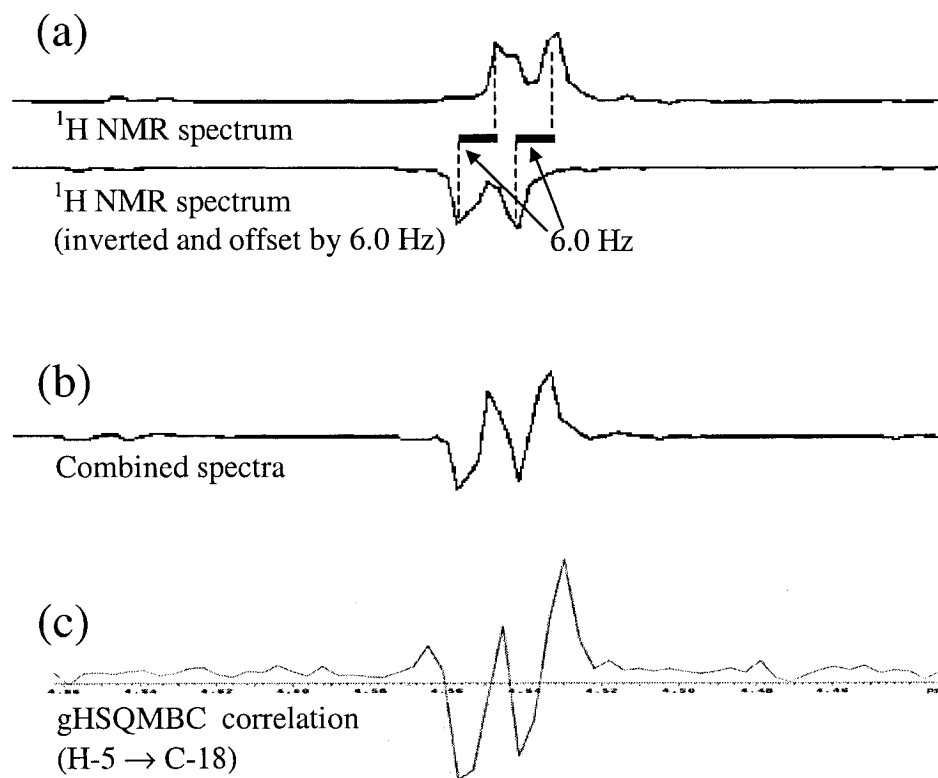
**Figure 4.6** Comparison of $^1$H NMR and gHSQMBC spectra ($J_{C18, H5}$) of **1**: (a) Two antiphase $^1$H NMR spectra showing the H-5 peak horizontally shifted by the heteronuclear coupling constant between H-5 and C-18 (6.0 Hz); (b) Addition of the two shifted antiphase peaks pictured in (a); (c) Slice from the 2D gHSQMBC spectrum showing the correlation between H-5 and C-18.
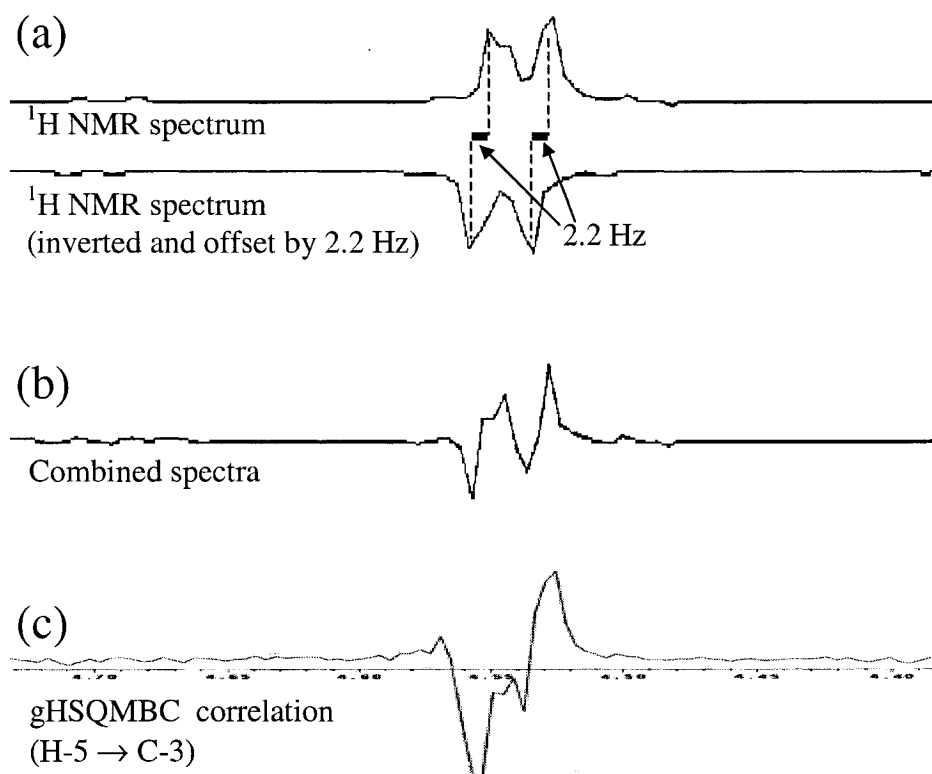
**Figure 4.7** Comparison of $^1$H NMR and gHSQMBC spectra ($J_{C3, H5}$) of **1**: (a) Two antiphase $^1$H NMR spectra showing the H-5 peak horizontally shifted by the heteronuclear coupling constant between H-5 and C-3 (2.2 Hz); (b) Addition of the two shifted antiphase peaks pictured in (a); (c) Slice from the 2D gHSQMBC spectrum showing the correlation between H-5 and C-3.
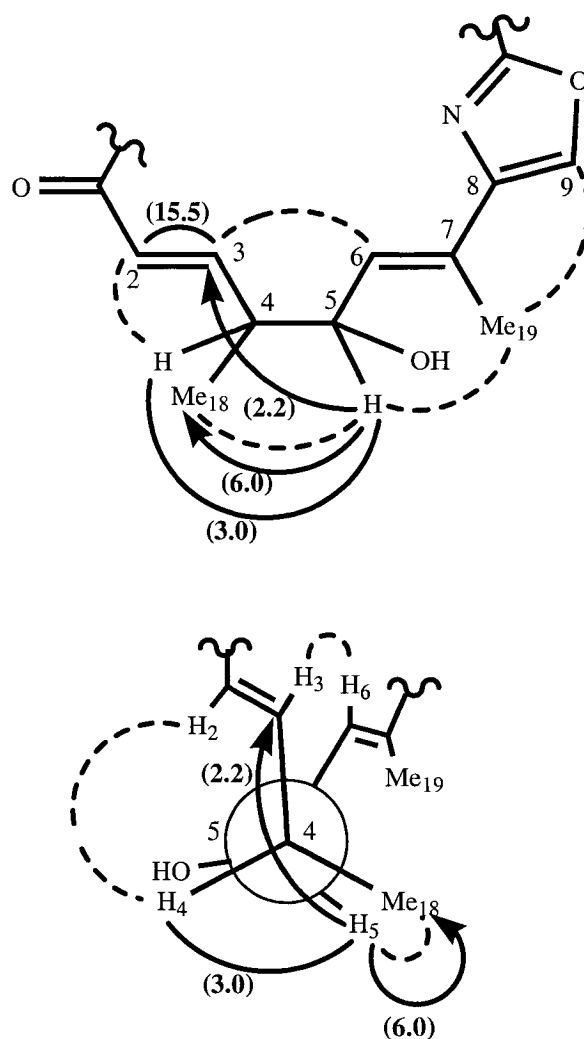
**Figure 4.8** Relative stereochemistry of C-2 to C-7 in leiodelide A (**1**). Important NOE's are illustrated with dashed lines. Vicinal proton-carbon couplings ($^3J_{C,H}$) are indicated with solid arrows (H→C), whereas vicinal proton-proton couplings ($^3J_{H,H}$) are indicated with solid lines (H—H). Coupling constants are shown in parenthesis and given in Hertz.

vicinal coupling (6.0 Hz) between H-5 and C-18 (Figure 4.6), along with the presence of a NOE enhancement between H-5 and H-18 established the near-parallel *syn* relationship between these two centers, which is consistent with the observation of a smaller coupling (2.2 Hz) between H-5 and C-3 (Figure 4.7). These data, combined with the presence of a positive NOE enhancement between H-3 and H-6, established an eclipsing orientation for C-4 and C-5, with Me-18 *gauche* to the hydroxyl group at C-5 as shown (Figure 4.8).

An analysis of the coupling constants and NOE enhancements revealed the relative configuration of C-15 to C-17 (Figure 4.9). A large vicinal coupling (9.5 Hz) and the absence of an NOE enhancement between H-16 and H-17 established the antiperiplanar relationship for these two protons. A NOESY experiment performed in DMSO-$d_6$ revealed a NOE enhancement between H-22 and the hydroxyl proton at C-16, establishing an *erythro* configuration with the two oxygen functionalities (hydroxyl at C-16 and O-acyl at C-17) *anti* to one another. This is supported by the fact that, in *threo* 1,2-dioxygenated methine systems, the *anti* rotamer would be disfavored due to steric (C↔C) and electrostatic (O↔O) repulsion.[32] An NOE enhancement between H-16 and H-22 and a small $^3J_{C,H}$ of 2.5 Hz between H-16 and C-22 indicated a dihedryl angle of approximately 60° for these atoms, further supporting the proposed *anti* orientation of H-16 and H-17 (Figure 4.9).
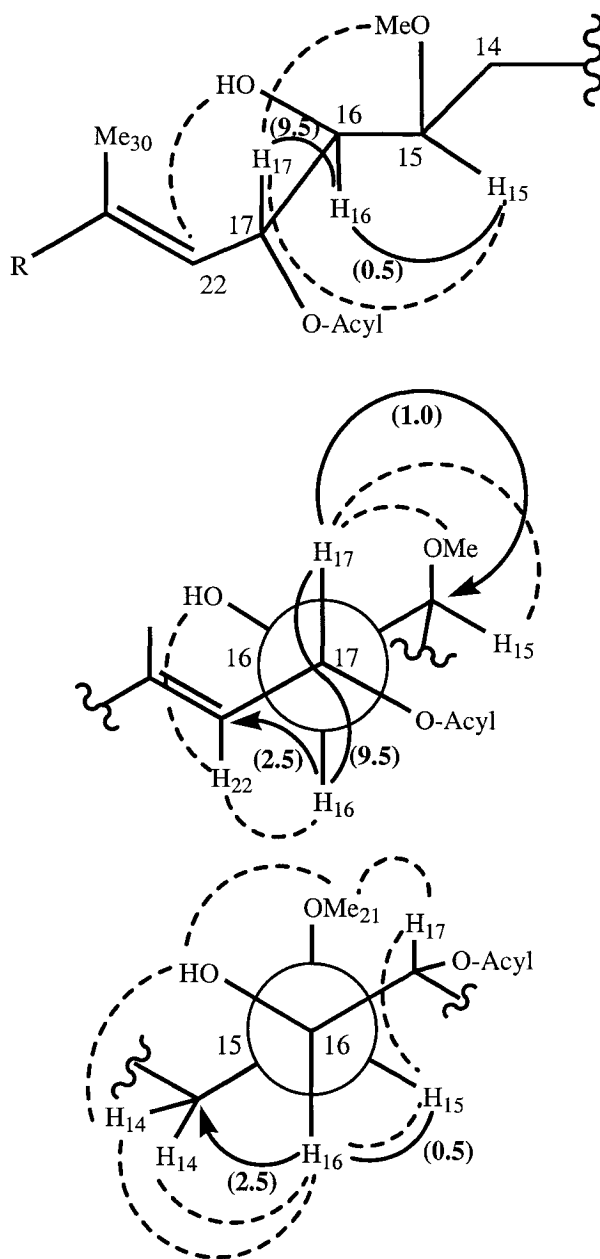
**Figure 4.9** Relative stereochemistry of C-15 to C-17 in leiodelide A (1). Important NOE's are illustrated with dashed lines. Vicinal proton-carbon couplings ($^3J_{C,H}$) are indicated with solid arrows (H→C), whereas vicinal proton-proton couplings ($^3J_{H,H}$) are indicated with solid lines (H—H). Coupling constants are shown in parenthesis and given in Hertz.

A negligible coupling (0.5 Hz) between H-15 and H-16 suggested a system in which both protons are opposite the oxygen atoms.[32] A small $^3J_{C,H}$ (2.5 Hz) observed for H-16 and C-14 indicated a *gauche* orientation for these atoms. NOE enhancements (H-17 to H-15 and Me-21; C-16OH to H-14 and Me-21; $H_2$-14 to H-16) established the configuration of C-15 relative to C-16, with the C-21 methoxy *anti* to H-16 (Figure 4.9). The relative configuration of a 1,3-methine system can be determined if the C-2 diastereotopic methylene protons can be assigned stereospecifically.[32] Although it was possible to determine both the $^1H$ chemical shifts and the coupling constants of the C-14 methylene protons in DMSO-$d_6$, the presence of multiple NOE enhancements (H-14a to H-13, H-14b to H-13, H-14a to Me-20, and H-14b to Me-20) and intermediate vicinal coupling constants made an assignment of the C-13 stereochemistry relative to C-15 via C-14 difficult. Nonetheless, strong transannular NOE enhancements from H-15 to the C-12 and C-11 methylene protons indicated a turn in the macrolide skeleton at C-13. On the basis of the above arguments, the relative stereochemistry of leiodelide A (1) is proposed to be 2*E*, 4*R**, 5*S**, 6*E*, 15*R**, 16*S**, 17*R*, 22E, 25Z. All vicinal coupling constants ($^3J_{H,H}$ and $^3J_{C,H}$) and NOE correlations are consistent with this configurational assignment in a single conformation.

The EIMS spectrum of leiodelide B (2) exhibited peaks of equal intensity at *m/z* 654/656, suggesting the presence of bromine (Figure 4.10). The molecular formula of $C_{31}H_{44}{}^{79}BrNO_9$ was deduced by high resolution MALDI-MS

(676.2074, [M + Na]$^+$, $\Delta$ -2.7 ppm). The spectral data of **2** suggested that it was a related analog of **1** (Table 4.2). Detailed examination of the $^1$H and $^{13}$C NMR data revealed that certain portions of the molecule (C-1 to C-14; C-23 to C-28) were fundamentally conserved, while other centers were altered (Table 4.2, Figure 4.11). In particular, the oxymethines C-16 ($\delta_C$ 80.5) and C-17 ($\delta_C$ 78.4) were shifted downfield and the multiplicities of H-16 and H-17 were noticeably modified in **2**. In addition, the C-22 methine ($\delta_H$ 4.28, $\delta_C$ 56.2) appeared to be brominated, while the quaternary carbon at C-23 ($\delta_C$ 84.0) was oxygenated. The disappearance of the $\Delta^{22,23}$ olefin, despite the fact that **2** has the same number of double bond equivalents as **1**, introduced the possibility of an additional ring system. These data, combined with chemical reasoning, suggested an ether linkage between C-16 and C-23 to form the stable five-membered tetrahydrofuran ring as shown. NOE enhancements from H-17 to Me-30 and from H-16 to H-22 established the relative configuration around the ring (Figure 4.12). Although an HMBC correlation from H-16 to C-23 through the ether linkage was not observed, the lack of long-range correlations across a furan ring has been reported,[34] and can be rationalized by an unfavorable dihedral angle between these centers.

The proposed mechanism for the formation of the 16,23-ether bridge in **2** from **1** is illustrated in Figure 4.13. In an enzyme catalyzed reaction, addition of an electrophilic bromine atom to the $\Delta^{22,23}$ alkene results in the formation of a
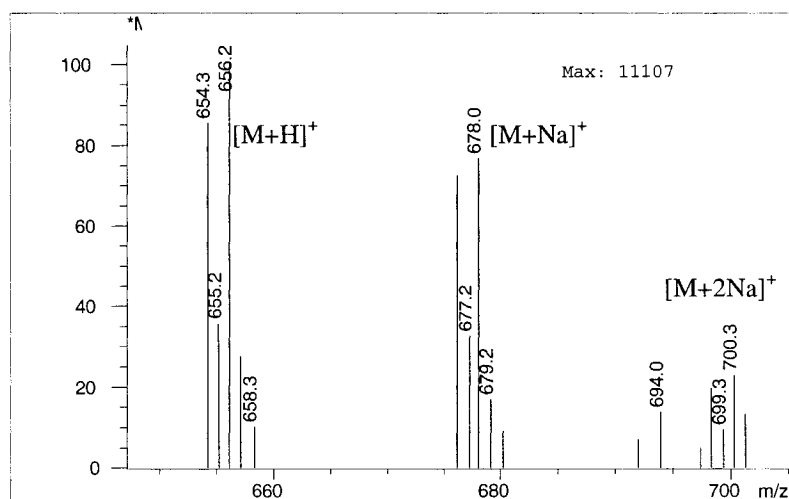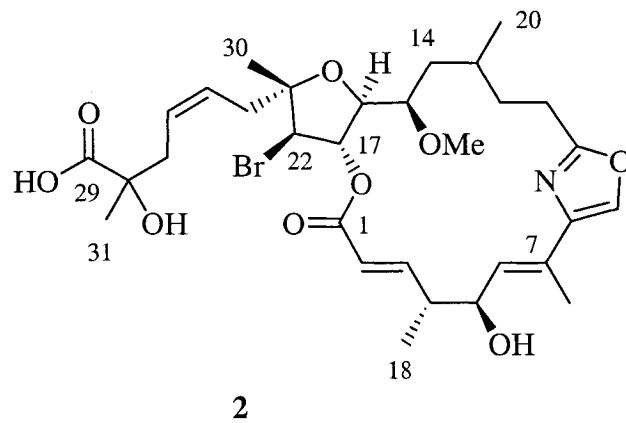
**Figure 4.10** Low-resolution mass spectrum for leiodelide B (**2**), illustrating the parent ion cluster indicative of bromine.

**Table 4.2** $^{13}$C (75 MHz, MeOH-$d_4$) and $^1$H (500 MHz, MeOH-$d_4$) NMR data for **1** and **2**.

| C# | $^{13}$C NMR (ppm) 1 | 2[a] | $^1$H NMR (ppm) 1 | 2 |
|---|---|---|---|---|
| 1 | 166.9 | 166.6 | | |
| 2 | 124.3 | 122.8 | 5.69 d (15.5) | 5.79 d (15.5) |
| 3 | 151.2 | 153.1 | 6.88 dd (15.5, 9.5) | 7.02 dd (15.5, 10.0) |
| 4 | 44.9 | 45.1 | 2.38 m | 2.44 m |
| 5 | 72.3 | 71.7 | 4.54 dd (9.5, 3.0) | 4.54 m |
| 6 | 131.4 | 131.2 | 6.31 dd (9.0, 1.0) | 6.22 dd (8.0, 0.5) |
| 7 | 125.6 | 125.5 | | |
| 8 | 143.5 | 143.3 | | |
| 9 | 135.0 | 134.5[b] | 7.66 s | 7.64 s |
| 10 | 166.3 | 166.4 | | |
| 11 | 25.2 | 25.7 | 2.71 m | 2.61 m |
| | | | 2.83 m | 2.79 m |
| 12 | 34.6 | 33.9 | 1.60 m | 1.41 m |
| | | | 2.05 m | 2.06 m |
| 13 | 29.5 | 30.5 | 1.28 m | 1.27 m |
| 14 | 35.9 | 36.7 | 1.62 m | 1.50 m |
| 15 | 80.3 | 78.0 | 3.22 ddd (9.5, 4.5, 0.5) | 3.09 m |
| 16 | 73.1 | 80.5 | 3.45 d (9.0) | 3.62 dd (8.0, 2.0) |
| 17 | 70.8 | 78.4 | 5.75 t (9.5) | 5.75 t (8.0) |
| 18 | 16.8 | 16.3 | 1.25 d (7.0) | 1.24 d (7.0) |
| 19 | 13.8 | 13.7 | 1.92 d (1.0) | 1.89 d (1.0) |
| 20 | 21.5 | 20.7 | 0.97 d (6.5) | 0.97 d (6.5) |
| 21 | 58.1 | 58.0 | 3.38 s | 3.41 s |
| 22 | 123.1 | 56.2 | 5.14 dd (9.5, 1.0) | 4.28 d (8.5) |
| 23 | 143.5 | 84.0 | | |
| 24 | 38.1 | 37.6 | 2.75 m | 2.33 m |
| | | | 2.81 m | 2.47 m |
| 25 | 129.5 | 126.5 | 5.45 m | 5.50 m |
| 26 | 128.2 | 130.4 | 5.57 m | 5.66 m |
| 27 | 39.0 | 39.2 | 2.30 m | 2.34 m |
| | | | 2.48 m | 2.43 m |
| 28 | 76.5 | 76.4 | | |
| 29 | 182.8 | 182.7 | | |
| 30 | 17.9 | 26.0 | 1.79 d (1.0) | 1.33 s |
| 31 | 26.7 | 26.4 | 1.29 | 1.28 |

[a] $^{13}$C shifts assigned indirectly by gHSQC
[b] determined by gHMBC
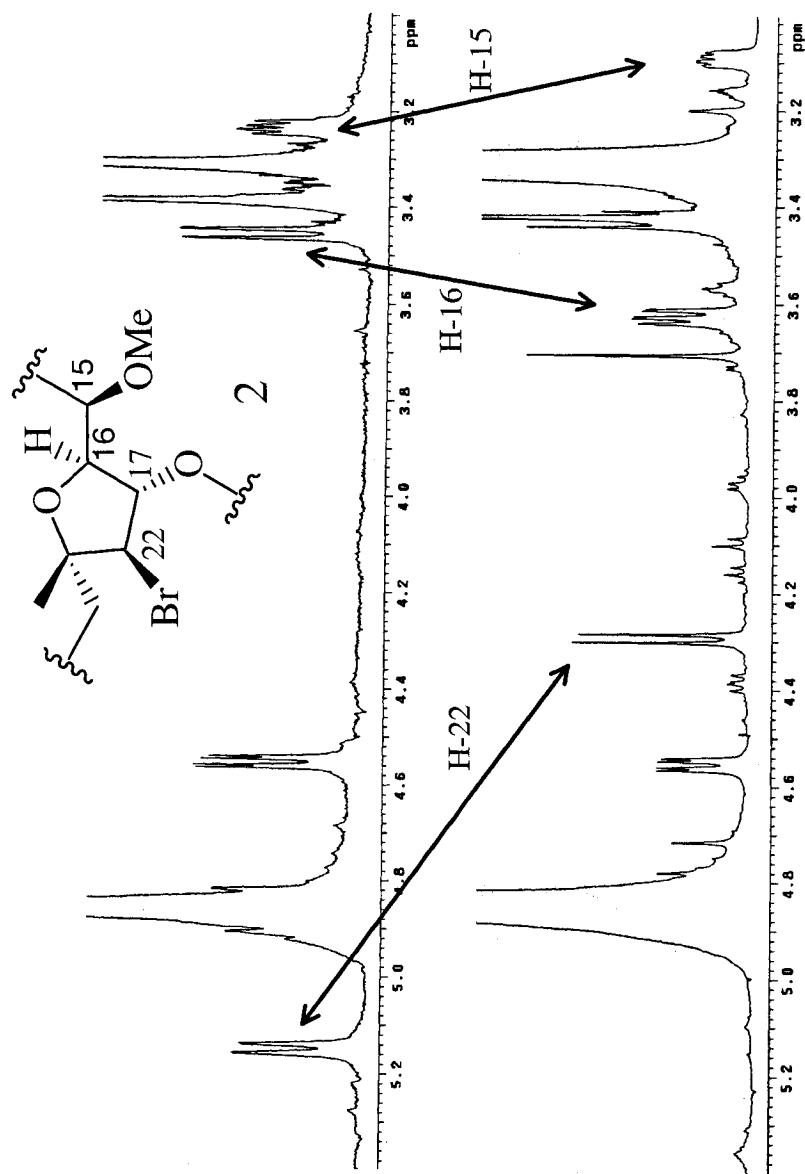
**Figure 4.11** Comparison of the midfield region of $^1$H NMR spectra for **1** (top) and **2** (bottom). Double-headed arrows indicate protons that are noticeably different between the two compounds. Trucated portion of compound **2** shown for clarity.
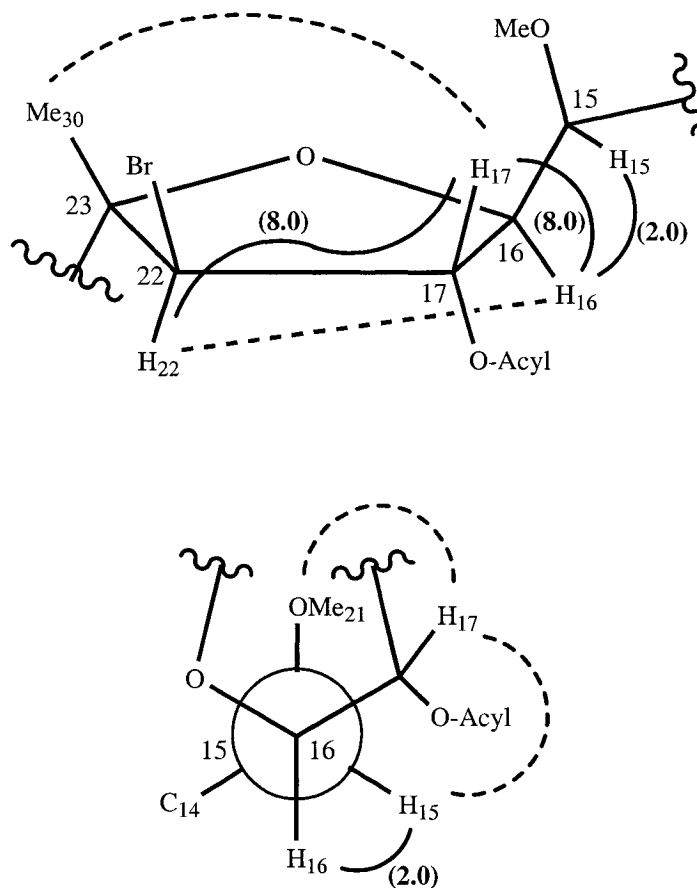
**Figure 4.12** Relative stereochemistry of C-15 to C-23 in leiodelide B (**2**). Important NOE's are illustrated with dashed lines. Vicinal proton-proton couplings ($^3J_{H,H}$) are indicated with solid lines (H—H). Coupling constants are shown in parenthesis and given in Hertz.
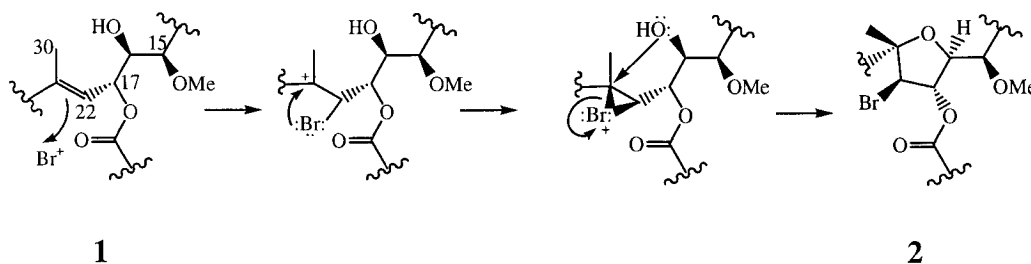
**Figure 4.13** Plausible mechanism for the formation of the tetrahydrofuran 16,23-ether bridge in **2** from **1**. Truncated portion of the molecule shown for clarity.

reactive bromonium intermediate. The nucleophilic hydroxyl oxygen at C-16 then attacks the more highly substituted C-23 to open the bromonium ring and create the tetrahyrdrofuran moiety. Assuming that **1** is the precursor of **2**, the relative configuration of C-15 to C-17 in **2** provides additional support for the proposed orientation of these centers in **1**. The rigid five-membered ring formed as a result of the 16,23-ether bridge in **2** validates the use of NOE enhancements and vicinal coupling to determine the relative configuration of C-16 and C-17 (Figure 4.12). It is encouraging that I observed the same relative orientation for these chiral centers in both **1** and **2**.

The leiodelides are the first members of an unprecedented class of polyketide natural products bearing several structural features of biogenetic interest. The oxazole unit could be derived from the amino acid serine, which would indicate a mixed biosynthetic origin for these compounds. The $\alpha,\alpha$-disubstituted carboxylic acid may be formed by a Baeyer-Villiger oxidation of an

intact acetate unit followed by a dehydrogenase-catalyzed oxidation to introduce the α-hydroxyl, as has been proposed for the biosynthesis of okadaic acid.[35] Although these compounds share some structural features with other lithistid metabolites such as theonezolide,[36] they do not appear to be closely related biochemically. Leiodelides A and B were found to be cytotoxic to HCT-116 human tumor cells at approximately 1.4 μg/mL (2.5 μM) and 3.8 μg/mL (5.6 μM), respectively, and their biological activity is currently undergoing further evaluation using the National Cancer Institute 60-cell line assay.

The text of this chapter is, in part, a reprint of the material that has been submitted for publication in the Journal of Organic Chemistry with co-authors Patrick Colin, Michelle Kelly, and William Fenical. I was the primary researcher and author, and the co-authors listed in this publication helped direct and supervise the research, which forms the basis of this chapter.

**Experimental**

**Sponge Collection and Identification:** The sponge was collected from the west side of Uchelbeluu Reef, Mutremdiu, Koror, Palau, Micronesia ($07°16.27'$N, $134°31.37'$E) by Patrick L. Colin using the manned submersible *Deep Worker 2000*, on 21 March 2001, on a sand and boulder slope at a depth of 240 m. The specimen forms a convoluted mass of thin flaring folded lamellae that may form tubes, with rounded incised margins, c. 500 mm diameter, wall 2.5 mm thick. The external surface has patches of tiny (<0.5 mm diameter) ostial pits, and the inner surface is completely covered in regularly and closely distributed oscules (<0.5 mm diameter). The lamellae margin is thick and rounded, sometimes indented or incised. The texture is stony, the surface smooth and granular with low irregular horizontal ridges, internal osculiferous surface is slightly furry with brishes of projecting diactines. The colour in life is tan. The skeleton consists of thorny rhizoclone desmas and fine diactinal spicules that may form a fringe. The sponge is a new species of the genus *Leiodermatium* ('Lithistid' Demospongiae: Family Azoriciidae) presently being described.[23] It was formerly known as *Leiodermatium pfeifferae* Carter, 1873 or *L. pfeifferae* Carter, 1873 *forma striata* Wilson, 1925. A voucher specimen has been deposited at the Natural History Museum, London, United Kingdom.

**HCT-116 Assay.** The HCT-116 cells were plated by Catherine Sincich in 96-well plates and incubated overnight at 37°C in 5% $CO_2$/air. Compounds were added to

the plate and serially diluted. The plate was then incubated for a further 72 h.

Cell viability was assessed at the end of this period through the use of a CellTiter

96 AQ$_{ueous}$ non-radioactive cell proliferation assay (Promega). Inhibition

concentration (IC$_{50}$) values are interpreted from the bioreduction of MTS/PMS by

living cells into a formazan product. The first step of the assay is the addition of

MTS/PMS to the sample wells followed by a 3 h incubation. The quantity of the

formazan product (proportional to the number of living cells) in each well was

then determined using a Molecular Devices Emax microplate reader that

measured the amount of 490 nm absorbance in each well, and the IC$_{50}$ value was

calculated by a SOFTMax analysis program. Etoposide (Sigma) and DMSO

(solvent) were used as positive and negative controls, respectively.

**Leiodelide A (1):** a pale yellow oil; CD (MeOH) [θ]$_{233}$ +11.9, [θ]$_{215}$ −11.0; UV

(MeOH) λ$_{max}$ (log ε) 224 (3.2); IR ν$_{max}$ (MeOH) 3400 (br), 2930, 1715, 1650,

1585, 1455, 1410, 1360, 1275, 1235, 1180, 1140, 1090, 1025, 990 cm$^{-1}$; for $^1$H

and $^{13}$C NMR data see Table 4.1; (+)-LREIMS $m/z$ (rel int) 350 (35), 508 (13),

526 (15), 551 (8), 558 (55), 576 (5), 598 (100), 599 (40), 600 (8); HRMALDIMS

[M + Na]$^+$ $m/z$ 598.2992 (calcd for C$_{31}$H$_{45}$NO$_9$Na, 598.2987).

**Leiodelide B (2):** a pale yellow oil; CD (MeOH) [θ]$_{234}$ +6.2, [θ]$_{212}$ −8.3; UV

(MeOH) λ$_{max}$ (log ε) 221 (2.8); IR ν$_{max}$ (MeOH) 3400 (br), 2935, 1715, 1655,

1460, 1415, 1360, 1270, 1225, 1200, 1140, 1095, 990, 655 cm$^{-1}$; for $^1$H and $^{13}$C

NMR data see Table 4.2; (+)-LREIMS $m/z$ (rel int) 557 (6), 577 (8), 598 (15), 654

(100), 655 (35), 656 (80), 657 (30), 658 (10), 676 (78), 677 (27), 678 (73), 679

(25), 680 (8); MALDIMS [M + Na]$^+$ $m/z$ 676.2074 (calcd for $C_{31}H_{44}{}^{79}BrNO_9Na$,

676.2092).

**Preparation of methyl ester 22:** KOH (40%, 7.5 ml) was added to 25 ml of

ether, and the mixture was stirred over an ice bath. While continuously stirring,

2.5 g of finely powdered nitrosomethylurea was added to the mixture in small

portions over a period of 1-2 minutes. After 30 minutes, the deep yellow

diazomethane-containing ether layer was removed by pipette. Water was

removed from the ethereal solution by drying over KOH pellets for 1 hour.

Several drops of the resulting diazomethane solution (~0.66M) were added to a

portion of compound **1** (5.1 mg) dissolved in 0.5 mL of MeOH, and the solution

was stirred overnight. The solution was dried down under $N_2$, and the purified

methyl ester (**22**) was obtained in roughly 20% yield by reverse-phased HPLC

(PRP-1 semi-prep; 25% to 100% acetonitrile/water; 2 mL/min.).

**22:** $^1$H NMR (CD$_3$OD) 0.97 (3H, d, H-20), 1.25 (3H, d, H-18), 1.35 (3H, s, H-

31), 1.60 (1H, m, H-12a), 1.61 (2H, m, H-14), 1.78, (3H, d, H-30), 1.92 (3H, d,

H-19), 2.04 (1H, m, H-12b), 2.30 (1H, m, H-27a), 2.39 (2H, m, H-4), 2.49 (1H,

m, H-27b), 2.71 (1H, m, H-11a), 2.77 (1H, m, H-24a), 2.81 (1H, m, H-24b), 2.83

(1H, m, H-11), 3.22 (1H, m, H-15), 3.38 (3H, s, H-21), 3.44 (1H, d, H-16), 3.68

(3H, s, CO$_2$Me), 4.54 (1H, dd, H-5), 5.15 (1H, d, H-22), 5.47 (1H, m, H-25), 5.54

(1H, m, H-26), 5.70 (1H, d, H-2), 5.75 (1H, t, H-17), 6.31 (1H, d, H-6), 6.89 (1H,

m, H-3), 7.67 (1H, s, H-9); (+)-EIMS $m/z$ 612 (M+Na)$^+$, (-)-EIMS $m/z$ 588 (M-H)$^-$

## References

1. Faulkner, D. J. (2002). Marine natural products. *Nat. Prod. Rep.* **19**, 1-48, and previous reports in this series.

2. Berquist, P. R., *Sponges.* 1978, Berkeley, CA: University of California Press. 140.

3. Bewley, C. A., Faulkner, D. J. (1998). Lithistid sponges: star performers or hosts to the stars. *Angew. Chem. Int. Ed.* **37**, 2162 - 2178.

4. Carmely, S., Kashman, Y. (1985). Structure of swinholide A, a new macrolide from the marine sponge *Theonella swinhoei. Tetrahedron Lett.* **26**, 511-514.

5. Kobayashi, M., Tanaka, J., Katori, T., Matsuura, M., Kitagawa, Isao (1989). Structure of swinholide A, a potent cytotoxic macrolide from the Okinawan marine sponge *Theonella swinhoei. Tetrahedron Lett.* **30**, 2963-2966.

6. Kitagawa, I., Kobayashi, M., Katori, T., Yamashita, M., Tanaka, J., Doi, M., Ishida, T. (1990). Absolute stereostructure of swinholide A, a potent cytotoxic macrolide from the Okinawan marine sponge *Theonella swinhoei. J. Am. Chem. Soc.* **112**, 3710 - 3712.

7. Bubb, M. R., Spector, I., Bershadsky, A. D., Korn, E. D. (1995). Swinholide A is a microfilament disrupting marine toxin that stabilizes actin dimers and severs actin filaments. *J. Biol. Chem.* **270**, 3463-3466.

8. Zampella, A., D'Auria, M. A., Minale, L., Debitus, C., Roussakis, C. (1996). Callipeltoside A: a cytotoxic aminodeoxy sugar-containing macrolide of a new type from the marine lithistida sponge *Callipelta* sp. *J. Am. Chem. Soc.* **118**, 11085-11088.

9. Kobayashi, J., Kondo, K., Shigemori, H., Ishibashi, M., Sasaki, T., Mikami, Y. (1992). Theoneberine: the first brominated benzyltetrahydroprotoberberine alkaloid from the Okinawan marine sponge *Theonella* sp. *J. Org. Chem.* **57**, 6680 - 6682.

10. Fusetani, N., Matsunaga, S., Matsumoto, H., Takebayashi, Y. (1990). Bioactive marine metabolites. 33. cyclotheonamides, potent thrombin inhibitors, from a marine sponge *Theonella* sp. *J. Am. Chem. Soc.* **112**, 7053-7074.

11. Matsunaga, S., Fusetani, N., Hashimoto, K., Walchli, M. R. (1989). Theonellamide F. A novel antifungal bicyclic peptide from a marine sponge *Theonella* sp. *J. Am. Chem. Soc.* **111**, 2582-2588.

12. Bewley, C. A., Faulkner, D. J. (1994). Theonegramide, an antifungal glycopeptide from the Philippine lithistid sponge *Theonella swinhoei*. *J. Org. Chem.* **59**, 4849-4852.

13. Schmidt, E. W., Bewley, C. A., Faulkner, D. J. (1998). Theopalauamide, a bicyclic glycopeptide from the filamentous bacterial symbionts of the lithistid sponge *Theonella swinhoei* from Palau and Mozambique. *J. Org. Chem.* **63**, 1254-1258.

14. Bewley, C. A., He, H., Williams, D. H., Faulkner, D. J. (1996). Aciculitins A-C: cytotoxic and antifungal cyclic peptides from the lithistid sponge *Aciculites orientalis*. *J. Am. Chem. Soc.* **118**, 4314 - 4321.

15. Gunasekera, S. P., Gunasekera, M., Longley, R. E., Gayle, K. S. (1990). Discodermolide: a new bioactive polyhydroxylated lactone from the marine sponge *Discodermia dissoluta*. *J. Org. Chem.* **55**, 4912 - 4915.

16. ter Haar, E., Kowalski, R. J., Hamel, E., Lin, C. M., Longley, R. E., Gunasekera, S. P., Rosenkranz, H. S., Day, B. W. (1996). Discodermolide, a cytotoxic marine agent that stabilizes microtubules more potently than taxol. *Biochemistry* **35**, 243-250.

17. Gunasekera, S. P., Pomponi, S. A., McCarthy, P. (1994). Discobahamins A and B, new peptides from the Bahamian deep water marine sponge *Discodermia* sp. *J. Nat. Prod.* **57**, 79-83.

18. Gulavita, N. K., Gunasekera, S. P., Pomponi, S. A., Robinson, E. V. (1992). Polydiscamide A: a new bioactive depsipeptide from the marine sponge *Discodermia* sp. *J. Org. Chem.* **57**, 1767 - 1772.

19. Bewley, C. A., Debitus, C., Faulkner, D. J. (1994). Microsclerodermins A and B. Antifungal cyclic peptides from the lithistid sponge *Microscleroderma* sp. *J. Am. Chem. Soc.* **116**, 7631 - 7636.

20. Schmidt, E. W., Faulkner, D. J. (1998). Microsclerodermins C-E, antifungal cyclic peptides from the lithistid marine sponges *Theonella* sp. and *Microscleroderma* sp. *Tetrahedron* **54**, 3043-3056.

21. Qureshi, A., Colin, P. L., Faulkner, D. J. (2000). Microsclerodermins F-I, antitumor and antifungal cyclic peptides from the lithistid sponge *Microscleroderma* sp. *Tetrahedron* **56**, 3679-3685.

22. D'Auria, M. A., Debitus, C., Paloma, L. G., Minale, L., Zampella, A. (1994). Superstolide A: a potent cytotoxic macrolide of a new type from the New Caledonian deep water marine sponge *Neosiphonia superstes*. *J. Am. Chem. Soc.* **116**, 6658-6663.

23. Kelly, M. (2006 (in press)). The marine fauna of new zealand: porifera: 'lithistid' demospongiae (rock sponges). *NIWA Biodiversity Memoir 120*.

24. Sandler, J. S., Forsburg, S. L., Faulkner, D. J. (2005). Bioactive steroidal glycosides from the marine sponge *Erylus lendenfeldi*. *Tetrahedron* **61**, 1199-1206.

25. Hiemstra, H., Houwing, H. A., Possel, O., van Leusen, A. M. (1979). Carbon-13 nuclear magnetic resonance spectra of oxazoles. *Can. J. Chem.* **57**, 3168-3170.

26. Yabuuchi, T., Kusumi, T. (2000). Phenylglycine methyl ester, a useful tool for absolute configuration determination of various chiral carboxylic acids. *J. Org. Chem.* **65**, 397 -404.

27. Norte, M., Gonzalez, R., Fernandez, J. J., Rico, M. (1991). Okadaic acid: A proton and carbon NMR study. *Tetrahedron* **47**, 7437-7446.

28. Pauli, G. F., Poetsch, F., Nahrstedt, A. (1998). Structure assignment of natural quinic acid derivatives using proton nuclear magnetic resonance techniques. *Phytochem. Anal.* **9**, 177-185.

29. Yasumoto, T., Murata, M., Oshima, Y., Sano, M., Matsumoto, G. K., Clardy, J. (1985). Diarrhetic shellfish toxins. *Tetrahedron* **41**, 1019-1025.

30. Kessler, H. (2003). Conformation and biological activity of cyclic peptides. *Angew. Chem. Int. Ed.* **21**, 512-523.

31. Eberstadt, M., Gemmecker, G., Mierke, D. F., Kessler, H. (1995). Scalar coupling constants - their analysis and their application for the elucidation of structures. *Angew. Chem., Int. Ed. Engl.* **34**, 1671-1695.

32. Matsumori, N., Kaneno, D., Murata, M., Nakamura, H., Tachibana, K. (1999). Stereochemical determination of acyclic structures based on

carbon-proton spin-coupling constants. a method of configuration analysis for natural products. *J. Org. Chem.* **64**, 866-876.

33. Williamson, R. T., Márquez, B. L., Gerwick, W. H., Kövér, K. E. (2000). One- and two-dimensional gradient-selected HSQMBC NMR experiments for the efficient analysis of long-range heteronuclear coupling constants. *Magn. Reson. Chem.* **38**, 265-273.

34. Darias, J., Rovirosa, J., Martin, A. S., Díaz, A. R., Dorta, E., Cueto, M. (2001). Furoplocamioids A-C, novel polyhalogenated furanoid monoterpenes from *Plocamium cartilagineum. J. Nat. Prod.* **64**, 1383 - 1387.

35. Murata, M., Izumikawa, M., Tachibana, K., Fujita, T., Naoki, H. (1998). Labeling pattern of okadaic acid from $^{18}O_2$ and $[^{18}O_2]$acetate elucidated by collision-induced dissociation tandem mass spectrometry. *J. Am. Chem. Soc.* **120**, 147 - 151.

36. Kobayashi, J., Kondo, K., Ishibashi, M., Walchli, M. R., Nakamura, T. (1993). Theonezolide A: a novel polyketide natural product from the Okinawan marine sponge *Theonella* sp. *J. Am. Chem. Soc.* **115**, 6661 - 6665.